TECHNICAL REPORT DOCUMENTATION PAGE

1. Report No.: TX -99/0-1860-1	2. Government Accession No.:	3. Recipient's Catalog No.:

4. Title and Subtitle: Subgrade Repair and Stabilization Using In-Situ Vitrification-Phase I: Final Report	5. Report Date: October 2001
	6. Performing Organization Code TechMRT
7. Author(s): Priyantha W. Jayawickrama, Umut Isler, Edgar A. O'Hair, and Douglas Gransberg	8. Performing Organization Report: No.0-1860-1
9. Performing Organization Name and Address: Texas Tech University Department of Civil Engineering Box 41023 Lubbock, Texas 79409-1023	10. Work Unit No.: (TRAIS)
	11. Contract or Grant No.: Project 0-1860
12. Sponsoring Agency Name and Address: Texas Department of Transportation Research and Technology P. O. Box 5080 Austin, TX 78763-5080	13. Type of Report and Period Cover: Final Report-Draft 1
	14. Sponsoring Agency Code

15. Supplementary Notes:
Study conducted in cooperation with the Texas Department of Transportation.
Research Project Title: "Subgrade Repair and Stabilization Using In-Situ Vitrification-Phase I: Final Report"

16. Abstract:

The technology embraced by the concentric graphite arc-melter (CGAM) promises to furnish a power tool to provide in-situ stabilization of unstable soils through vitrification. This ensures a new maintenance capability for a myriad of stabilization problems. The project will involve three phases. The first phase entails determination of the geotechnical properties of the resultant vitrified soils, a thorough constructability review and an economic analysis to verify the technology's potential for economic feasibility. Phase 2 will include the development of a prototypical CGAM that can be used in limited field trials to prove the concept under actual environmental conditions. Phase 3 will comprise detailed design and testing of a pre-commercial prototype CGAM system. Phase 3 will also include the development of the required construction techniques and safety systems as well as the design of the quality control instrumentation necessary to permit immediate implementation upon whether to continue onto the next phase based on the results of the completed phase.

17. Key Words: Vitrification, CGAM	18. Distribution Statement: No restrictions. This document is available to the public through the National Technical Information Service, Springfield, Virginia 22161

19. Security Classif.: (of this report) Unclassified	20. Security Classif.: (of this page) Unclassified	21. No. of Pages: 95 pages	22. Price:

Form DOT F 1700.7 (8-72)

SUBGRADE REPAIR AND STABILIZATION USING IN-SITU VITRIFICATION-PHASE I: FINAL REPORT

by

Priyantha W. Jayawickrama, Umut Isler
Edgar A. O'Hair and Douglas Gransberg

Research Report Number 0-1860

conducted for

Texas Department of Transportation

by the

CENTER FOR MULTICISIPLINARY RESEARCH IN TRANSPORTATION
TEXAS TECH UNIVERSITY

October 2001

IMPLEMENTATION STATEMENT

This report documents the findings from Phase I research activities of this project. In Phase I, the feasibility of using CGAM vitrification technology for stabilization of pavement soil subgrade was demonstrated in the laboratory. Phase II research will involve the design and manufacture of a soil vitrification system that could be demonstrated in the field. This system will not be fully self-contained but will be supported in the field by other support systems such as a portable generator and an air compressor. In Phase III, the above soil vitrification equipment will be used in a number of trial demonstrations in the field. Based on the findings from Phase III, an Implementation Project and Recommendation (IPR) will be developed and submitted to TxDOT for the implementation of the soil vitrification equipment on several, full-scale soil stabilization projects.

Prepared in cooperation with the Texas Department of Transportation and the U.S. Department of Transportation, Federal Highway Administration.

AUTHOR'S DISCLAIMER

The contents of this report reflect the views of the authors who are responsible for the facts and the accuracy of the data presented herein. The contents do not necessarily reflect the official view of policies of the Department of Transportation or the Federal Highway Administration. This report does not constitute a standard, specification, or regulation.

PATENT DISCLAIMER

There was no invention or discovery conceived or first actually reduced to practice in the course of or under this contract, including any art, method, process, machine, manufacture, design or composition of matter, or any new useful improvement thereof, or any variety of plant which is or may be patentable under the patent laws of the United States of America or any foreign country.

ENGINEERING DISCLAIMER

Not intended for construction, bidding, or permit purposes.

TRADE NAMES AND MANUFACTURERS' NAMES

The United States Government and the State of Texas do not endorse products or manufacturers. Trade or manufacturers' names appear herein solely because they are considered essential to the object of this report.

SI* (MODERN METRIC) CONVERSION FACTORS

APPROXIMATE CONVERSIONS TO SI UNITS

Symbol	When You Know	Multiply By	To Find	Symbol
		LENGTH		
in	inches	25.4	millimeters	mm
ft	feet	0.305	meters	m
yd	yards	0.914	meters	m
mi	miles	1.61	kilometers	km
		AREA		
in^2	square inches	645.2	square millimeters	mm^2
ft^2	square feet	0.093	square meters	m^2
yd^2	square yards	0.836	square meters	m^2
ac	acres	0.405	hectares	ha
mi^2	square miles	2.59	square kilometers	km^2
		VOLUME		
fl oz	fluid ounces	29.57	milliliters	mL
gal	gallons	3.785	liters	L
ft^3	cubic feet	0.028	cubic meters	m^3
yd^3	cubic yards	0.765	cubic meters	m^3
NOTE: Volumes greater than 1000 l shall be shown in m^3.				
		MASS		
oz	ounces	28.35	grams	g
lb	pounds	0.454	kilograms	kg
T	short tons (2000 lb)	0.907	megagrams (or "metric ton")	Mg (or "t")
		TEMPERATURE (exact)		
°F	Fahrenheit temperature	5(F-32)/9 or (F-32)/1.8	Celcius temperature	°C
		ILLUMINATION		
fc	foot-candles	10.76	lux	lx
fl	foot-Lamberts	3.426	candela/m^2	cd/m^2
		FORCE and PRESSURE or STRESS		
lbf	poundforce	4.45	newtons	N
lbf/in^2	poundforce per square inch	6.89	kilopascals	kPa

APPROXIMATE CONVERSIONS FROM SI UNITS

Symbol	When You Know	Multiply By	To Find	Symbol
		LENGTH		
mm	millimeters	0.039	inches	in
m	meters	3.28	feet	ft
m	meters	1.09	yards	yd
km	kilometers	0.621	miles	mi
		AREA		
mm^2	square millimeters	0.0016	square inches	in^2
m^2	square meters	10.764	square feet	ft^2
m^2	square meters	1.195	square yards	yd^2
ha	hectares	2.47	acres	ac
km^2	square kilometers	0.386	square miles	mi^2
		VOLUME		
mL	milliliters	0.034	fluid ounces	fl oz
L	liters	0.264	gallons	gal
m^3	cubic meters	35.71	cubic feet	ft^3
m^3	cubic meters	1.307	cubic yards	yd^3
		MASS		
g	grams	0.035	ounces	oz
kg	kilograms	2.202	pounds	lb
Mg (or "t")	megagrams (or "metric ton")	1.103	short tons (2000 lb)	T
		TEMPERATURE (exact)		
°C	Celcius temperature	1.8C + 32	Fahrenheit temperature	°F
		ILLUMINATION		
lx	lux	0.0929	foot-candles	fc
cd/m^2	candela/m^2	0.2919	foot-Lamberts	fl
		FORCE and PRESSURE or STRESS		
N	newtons	0.225	poundforce	lbf
kPa	kilopascals	0.145	poundforce per square inch	lbf/in^2

---

* SI is the symbol for the International System of Units. Appropriate

(Revised September 1993)

TABLE OF CONTENTS

LIST OF TABLES

LIST OF FIGURES

CHAPTER I
Introduction

1.1 Problem Statement

The problems arising from poor to marginal foundation and slope materials are endemic to the entire highway system in the State of Texas. Localized subgrade failure in both highway fill and around ancillary structures like bridges and culverts constitutes a major maintenance headache in every Texas Department of Transportation (TxDOT) district. These failures occur form a number of conditions ranging from the shrinking and swelling of cohesive soils to localized softening due to poor drainage conditions or the presence of organic materials. Current methods to repair localized failures are limited to excavation and replacement of unstable materials. Not only are these means to repair localized subgrade time consuming, but they are costly as well. TxDOT maintenance sections need a low cost alternative to excavation and backfill on routine maintenance, repair, and rehabilitation throughout a transportation facility's life cycle to achieve its design life.

This research involves the investigation of the feasibility of using a new soil stabilization technique that utilizes an emerging technology called Concentric Graphite Arc-Melter (CGAM), not only for repairing subgrade failures but also for stabilizing subgrades during construction of highways. The ability to stabilize soils in-situ will free operation and maintenance from unanticipated use in repairing defects caused by foundation and slope failures to other uses while enhancing TxDOT's overall effectiveness. The patent for this process is held by Montec Associates, Inc. who joined the Texas Tech University research team as a subcontractor to make this promising technology available for analysis and development.

1.2 In-situ Vitrification

Heating soils improve their quality as a foundation material. At a temperature range of 100°C to 250°C, absorbed molecular water is removed from the clayey soils. At 400°C to 600°C the structure of clay irreversibly changes, yielding a water resistant material. At about 1000°C the process of fusion starts, and higher temperatures result in complete melting.

Vitrification is melting soils and letting them cool down into a stable glass-like rock (similar to obsidian) suitable for structural support. The melting temperature is strongly dependent upon soil properties and for most soils of interest can range from 1,000°C to nearly 2,000°C.

In-situ vitrification would be a great help in the repair of differential roadway settlement around culverts and bridges. Unstable soils could be vitrified to extend existing footings by transforming the adjacent soil, via adding materials into the vitrification zone, to effectively spread the footing by distributing embankment load across a larger footprint. Emergency repairs of failed base course and subbase courses are other potential applications. If it can be shown that vitrification can reliably and permanently restore the integrity of a damaged structural fill, untold benefit is possible in virtually every season. Other applications include toe slope stabilization and riverbank stabilization (Lineberry, 1996).

Other needs are sited in areas with extremely poor foundation soil conditions where temporary stabilization is required during construction. Even though subgrade stabilization may be temporary and only required to perform for several weeks or months, the contractor must currently turn to expensive, time consuming conventional solutions such as driving piles or installing precast concrete foundations which are of an unnecessarily permanent nature. If soils could be temporarily stabilized in-situ, these measures would be unnecessary.

This report proposes the use of Concentric Graphite Arc Melter (CGAM) method for in-situ vitrification, as the latest and most promising one among a number of other in-situ vitrification methods. The innovative aspect for the proposed process is its use of a concentric graphite arc melter (CGAM) as the heat source. This device is robust, is not water-cooled (no heat losses), can operate in several modes (joule, submerged arc and non-transferred arc), and is simple and cheap. CGAM method and other main in-situ vitrification methods are presented in detail in Chapter II of this report.

1.3 Research Objectives

The primary objective of this research is to make an assessment of both the technical and economical feasibility of the proposed CGAM method for stabilization of various subgrades. The project also has the following specific objectives:

(a) To study the effect of vitrification on different types of soils (sands, silts, clays, etc.) by vitrifying them, determining qualities of vitrified soils as subgrade materials, and comparing them with each other.
(b) To studying the effect of water content of original soil on quality of vitrified product by vitrifying same soil both in saturated form and at natural water content, and comparing end products.
(c) To study the effect of density of original soil on quality of vitrified soil by vitrifying same soil both in loose form and in compacted form, and comparing end products.
(d) To estimate the cost of CGAM in-situ vitrification method as a subgrade stabilization application.
(e) To study the economical competitiveness of CGAM in-situ vitrification method with other common stabilization methods (lime, cement, and lime-fly ash stabilizations).

1.4 Research Approach

The research consisted of four primary tasks: (i) laboratory characterization of test soils before vitrification, (ii) vitrification experiments, (iii) testing of vitrified products, and (iv) economic analysis of the proposed soil stabilization process by CGAM method. Data obtained from the first three tasks was helpful in understanding the technical aspects of vitrification by CGAM method. The fourth task investigated the economical feasibility of the proposed process. These four tasks are further explained below.

As a first step, candidate soils were selected such that they represent a broad range of soil characteristics. Laboratory characterization of the seven soils that were selected for vitrification was accomplished at Texas Tech University laboratories. Laboratory characterization tests included x-ray diffraction and chemical analyses to determine their mineralogical compositions as well as geotechnical properties such as particle size distribution, and Atterberg limits.

Vitrification experiments were completed by Montec Assoc. laboratories in Butte, Montana. Each test soil was loaded into a test bin, brought to desired compaction and saturation conditions, and vitrified. A matrix of thermocouples was placed into the test bin at each experiment to monitor the soil heating and melting. Temperature and melt profiles in the soils during experiments were measured, power and material (graphite electrode) consumptions were recorded. These experiments were videotaped.

Once the vitrification experiments were complete, the vitrified melts obtained from all experiments were shipped back to Texas Tech University for further evaluation. Cylindrical core samples were obtained by drilling through the vitrified monoliths. The core samples were then subjected to a series of tests to determine unit weight, porosity, unconfined and modulus elasticity of each vitrified material. Susceptibility of vitrified materials to moisture intrusion was also tested by placing samples in water.

Economic analysis of the proposed soil stabilization process by CGAM method was done in order to assess economical feasibility of the proposed process. Possible stabilization applications by CGAM method were identified as: stabilization by CGAM vitrification of an entire area, stabilization by 5 feet spaced CGAM vitrified columns, stabilization by 10 ft spaced CGAM vitrified columns, and stabilization by 20 ft spaced CGAM vitrified columns. Cost estimates were made for each of these applications. Average compressive strengths to be expected at the end of each of these applications on sands, silts, and clays were calculated. Cost and strength data associated with other main conventional stabilization applications (lime, cement, and lime-fly ash stabilizations) were collected. Finally, CGAM vitrification method was compared to lime, cement, and lime-fly ash stabilization methods based upon the results from the above analysis.

This report documents the findings from review of literature review and the four tasks described above. Chapter II presents findings from the literature review. It provides a discussion of other thermal stabilization methods, with special emphasis on electrical vitrification methods such as Electric Joule Heating, Electric Plasma Torch, and the proposed CGAM Electric Arc Melter methods. Chapter III of this report presents laboratory characterization of test soils. A report from Montec Assoc. describing vitrification experiments is given in Appendix. Tests conducted to evaluate vitrified products and the results obtained are described in Chapter IV. Chapter V of this report presents details of economic analysis. Chapter VI includes the conclusions and recommendations from this research project.

CHAPTER II
Review of Background Literature

2.1 Thermal Treatment for Soil Stabilization; General Overview

Heating soils, especially clays, improves their quality as a base material. The greater the heat input per mass of soil being treated, the greater the improvement. The changes that take place within a clay soil as its temperature is increased include: 1) removal of absorbed molecular water, 2) irreversible changes in structure and properties such as decreases in swelling and compressibility, and increase in shear strength, 3) fusion that will form a brick-like material after cooling, and 4) melting that will form a glass-like rock (similar to obsidian) after cooling.

Heating soils has been studied and used as a means for soil treatment for over a century. Highways and railroad beds were constructed by the heat treatment of the soil prior to 1890 in the United States (Jankiewicz, 1972). Manufacturing bricks is done by heating clays. Early methods of heating soils included burning clays, in-situ heating soils via surface down, and in-situ heating soils via boreholes. Two main examples of these methods are as follows:

a) In 1930, an Australian engineer-inventor named Irvine reported the development and use of a machine to stabilize soils in-situ. The machine was mobile, wood-fired, and of the air-gas producer type to heat soils from surface-down (Jankiewicz, 1972).
b) In 1960, Litvinov reported the use of a method to stabilize soils in-situ via boreholes. The method involved burning various fuels in the soil being treated, the process of combustion taking place in sealed boreholes (Litvinov, 1960).

Although effective, the use of these early techniques were infrequent in the United States due to severe limitations in the temperature ranges, high operating costs (Mayne and Beaver, 1996), and the relative abundance of good aggregate in the country (Jankiewicz, 1972).

As described above, vitrification of soils consists of heating them up to their last 'melting' stage, and letting them cool down into a glass-like rock (similar to obsidian). The new focus for heat treatment for soil stabilization is on electrical vitrification methods. The electric joule heating method, the electric plasma torch method, and the proposed promising CGAM electric arc melter method are examined in following sections in detail as primary methods of electrical vitrification.

2.2 Electric Joule Heating Method

The first method developed and tried to electrically vitrify soils in-situ is Electric Joule Heating Method. Two graphite electrodes are inserted into the soil at a short depth. An electrically conductive path such as a metal or carbon material is used to initiate the flow of current between the graphite electrodes and eventually through the soil. This flow of electricity starts melting the conductive material and produces tremendous heat energy transmitting outwards. As the melting progresses, the soil becomes molten and forms an electrically conductive path as well as heat-transfer medium, allowing the process to continue (ASCE, 1997). This process is highly energy intensive, and provides relatively less control of melt geometry. Figure 2.1 shows the schematic diagram of electric joule heating method.

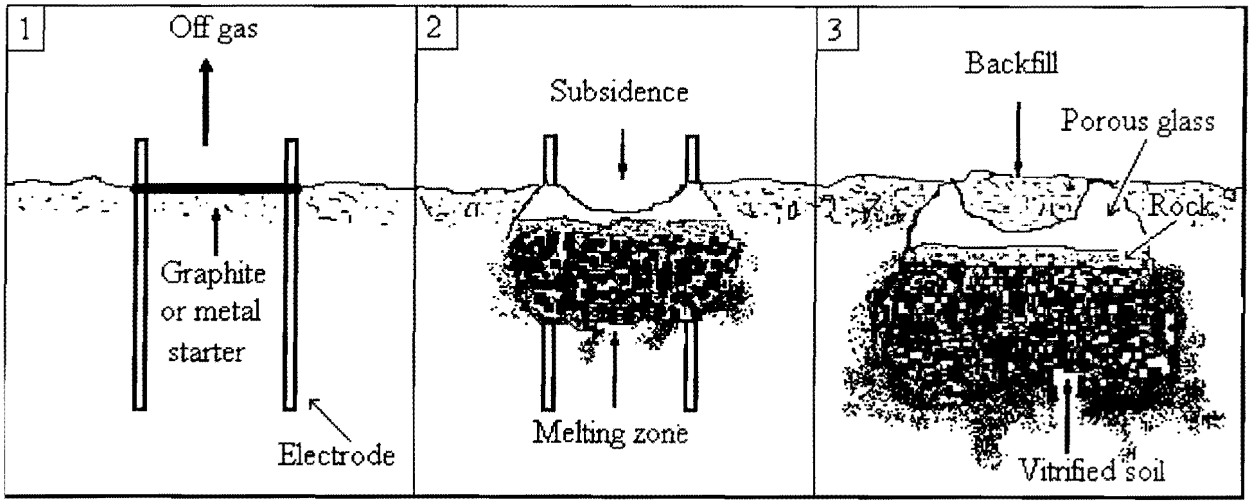

Figure 2.1: Electric Joule-Heating Vitrification Process (ASCE, 1997)

This method is generally applied from the ground surface downward; therefore it is also regarded as the top-down joule heating in-situ vitrification process. Once all the soil in the treatment zone becomes molten, the power to the electrodes is discontinued, and the molten soil is allowed to cool. The electrodes are cut near the surface and the pieces in the soil are left to settle into the molten soil to become a part of the vitrified mass (USEPA, 1994).

This primary method of vitrification was developed at Pacific Northwest Laboratory (PNL) for the US Department of Energy (DOE) in the early 1980s (Lowery et. al., 1994). A full-scale successful experiment was performed at the Hanford Nuclear Facility in Washington; however, another test on a waste site in the DOE complex at ORNL resulted in an incident. A subterranean vapor bubble formed below the melt and a 20-ton mass of molten magma was ejected, gases were released and damage to the equipment occurred (Montec associates, inc.).

2.2.1 Deficiencies for Electric Joule Heating Method

Some of the deficiencies related to this method are originated from its top-down application. This method's main issue of depth limitation is one of these. Currently, joule heating can treat soils, which are less than 20 ft. (6 m) deep only (Circeo et. al., 1994). And it has to treat all soil from surface down. It has no chance of treating only the required level of soil located at an intermediate stage.

Electric joule heating method is problematic for application at sites with volatiles, large voids, metals and combustible material in soil. Volatiles can cause melt disruption and ejection by pressure, as encountered at the incident at the DOE complex. Large voids in the soil create rooms for the molten soil to fit in, away from electrodes, consequently shutting down process by breaking the electrical circuit. Combustible material cause combustion, increase in pressure, and metals become part of the electrical circuit, making power control difficult (Circeo et al., 1994; Montec Associates, inc.).

In joule heating method, excess oxygen to the vitrification zone for in-situ combustion of soils is not supplied. Instead, the process must rely on in-situ pyrolysis, and external combustion. These deficiencies come out to be limitations to the use of the electrical joule heating method.

2.3 Electric Plasma Torch Method

This method is built upon so called 'plasma arc technology', which was originally developed by NASA in 1960's. Electric Plasma Torch Method is named after the employed basic tool 'plasma torch' (Circeo and Mayne, 1993).

The aim of the technology is to produce and spread high temperatures. Plasma is a name given to the ionized gas. It is accomplished by passing a flow of air through an electric arc. The atoms in the flowing air are ionized this way, and reach high enough temperatures to melt surrounding soils.

The method employs the use of a plasma torch to produce electric arc, and generate a plasma flame. The plasma torch utilizes a water-cooled barrel to prevent fast consumption of its components under high temperatures. The whole system consists of the following components: a plasma torch assembly, power supply and control panel, closed-loop water cooling system and heat exchanger, and a gas source (Circeo et al., 1994).

The torch is inserted into the bottom of a hole and ignited. A plasma emerges as a result of an injected gas passing through the arc formed between electrodes located at the end of the torch, and heats up the soil. As the soil melts, the torch is slowly withdrawn up. The standard non-transferred plasma torch must not be let come into contact with the melt, subsequently it must be kept at a certain safe distance from molten soil while operating. The borehole casing opposite the plasma flame is consumed. Once targeted melting levels are reached, the torch is extinguished, and at the end of the cooling period, a vertical column of stabilized mass is obtained. Plasma torch method application in-situ is illustrated in Figure 2.2.

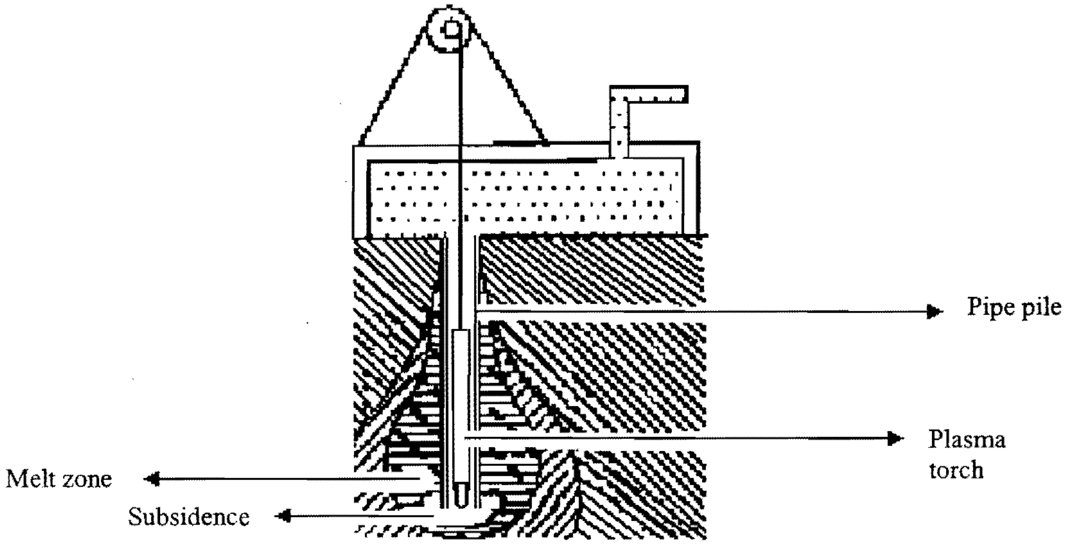

Figure 2.2: Vitrification by Plasma Torch (Circeo and Mayne, 1993)

2.3.1 Deficiencies for electric plasma torch method

Although the technology is convenient for melting soils, the selection of apparatus, plasma torch, leads to the inadequacy of the method. The findings of tests demonstrate a doubtful feasibility.

As the soil melts, due to the increase in its specific weight, its densification, it contracts and forms a cavity. This cavity often collapses from the top and put the torch in a danger of being immersed in the melt. Again as the soil melts, it also consumes the borehole casing, resulting in a quite active molten slag. The impingement of slag on the plasma torch electrodes and torch body accelerates wear, potentially causes catastrophic failure and/or lead to destruction of the electrodes. Therefore, the contact of the plasma torch with the molten media must be avoided. However, the splattering and frothing that is evident as a result of the described operating conditions makes the contact inevitable and inhibits the performance of a standard non-transferred plasma torch. Consequently, tests show that the plasma torch electrode life is about 20 hours, which is considered to be quite short for commercial operation (Blundy et al., 1996).

Automated instrumentation techniques applicable to such hot and dynamic environments are not available today. Therefore, the melt level is detected by manual probing and the plasma torch is kept away from the molten media only through visual observation. To avoid contacts as a result of this unhealthy determination of the distance between the torch and the media, one may maintain the torch's operation at a safer far distance from the melt. However in that case, relatively narrower columns are produced, or smaller amount of soil is vitrified (Blundy et al., 1996). Hence, lack of efficiency, loss of energy are faced. The plasma torch can either be operated at an efficient distance in productivity, but in that case risk of contact, shorter life, and failure would be undertaken, or it can be operated at a safer but less productive distance, significantly reducing the efficiency.

In addition to the energy losses mentioned above due to the operating distance, the employed water-cooling system itself possesses an energy loss of 30 – 40 % of the total energy given to the system. High amount of energy losses is present in this method. Moreover, the plasma torch is neither robust, nor versatile enough for the proposed application.

2.4 CGAM Electric Arc Melter Method

The process involved in this method is incorporated with the CGAM (concentric graphite arc-melter) technology. The initiative step is the installation of a borehole liner. The ResonantSonic^{TM} drilling system, as a technology allowing installations of casings without exhuming any material, may well be used for this operation. The borehole liner is kept empty by capping the bottom of it. As the successive step, a high-temperature concentric graphite arc-melter – CGAM is lowered through this empty liner, and the thermal operation is initiated by generating an electric arc.

The heat exerted melts the soil starting from the thermal source location, propagating radially outwards, even by consuming the liner. The density of the molten soil is higher than the original soil that has air voids among its particles. Hence, due to the densification the molten soil occupies less space and produces a cavity during the operation. Molten soils slough off cavity walls and accumulate at the bottom of the cavity. As the melt progresses, CGAM is withdrawn up gradually, resulting in a vitrified vertical column of alumina-silicate glass-ceramic material.

Depending on the size of the zone to be treated, repetitions of the process, each creating a column, are made. Multiple high-energy sources (CGAMs) may well be operated simultaneously. As a matter of fact, such an application provides the user with the option of using joule-heating between CGAMs, which will increase the effective melt zones and the process rates between the adjacent arc-melters.

It is not actually necessary to apply the process in a vertical shaft, since CGAM is suited for desired angled applications, too. Such an application may be of the interest in a situation where soil treatment is necessary below an existing structure without disturbing it. This angled operation may also be useful for placing the CGAM into a steep embankment.

Together with its flexibility of operation in a variety of modes (joule, submerged arc, or arc), advantageous allowances it provides in its use as a heat source, qualifies CGAM as the useful tool and the innovative aspect of the process.

2.4.1 Description of the Tool: CGAM

This handy tool simply consists of an outer concentric graphite electrode, covered by an electrode shroud, and an inner graphite rod electrode surrounded by the outer electrode. Initially, a direct-current arc is established between these two electrodes, while the plasma forming gas is being passed through this arc, into the media. Once this plasma forming gas converts the 'work piece' into an electrically conductive state, the arc transfers from the outer electrode to the conductive media, to the molten soils, or directly to the molten soils if electrodes are submerged, and then back up to the other electrode. Figure 2.3 below illustrates this process.

Besides its non-transferred arc start-up mode, the CGAM may also be started and operated in the Joule heating mode as mentioned above. When two CGAMs are used simultaneously, and once the molten soils formed in the adjacent boreholes make contact, power can be transferred between electrodes of the two adjacent CGAMs to provide Joule heating between the melts.

The graphite electrodes are off-the shelf components, which are nominally 8 feet in length. If longer graphite elements are needed for a specific melt, they are simply fit with a tapered thread (similar to that found on down-hole drill pipe, in the oil industry) and threaded together. The entire apparatus can be skid mounted and placed in the back of a typical dump truck, and powered by a portable 100-kilowatt generator.

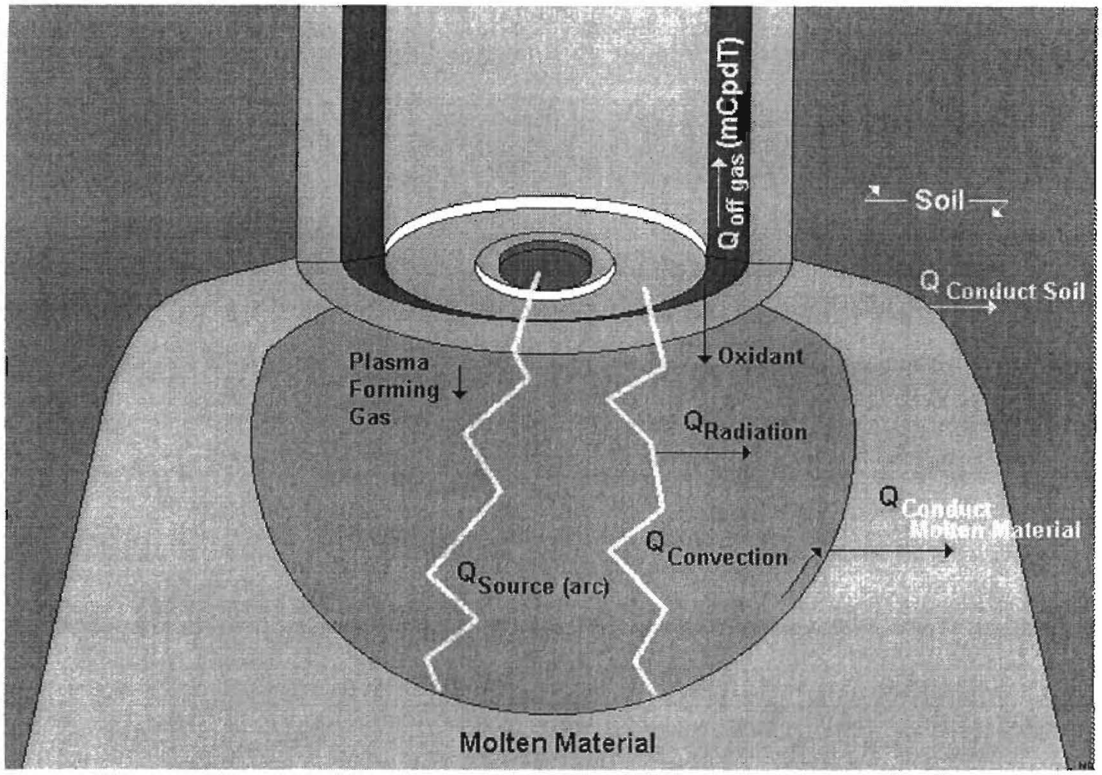

Figure 2.3: CGAM Details – Transfer of Arc and Heat Dissipation

2.4.2 Advantages

The advantages CGAM method presents are both related to qualifications of the employed innovative tool, CGAM itself, and its bottoms-up process of vitrification. Some of these advantages are as follows:

a) There is no depth limitation.
b) The zone to be treated can be located and vitrified with surgical precision.
c) The bottoms-up process allows the treatment zone to be limited only to the required levels of soil for vitrification. There is no need to treat all soils from surface down.
d) It is not necessary to apply the process in a vertical shaft. As mentioned earlier, CGAM can be operated at any angle without disturbing the superstructures.
e) Employing multiple CGAM sources, and operating them simultaneously, provides the option of using Joule-heating between CGAMs. Once the adjacent molten zones make contact, power may be transferred from one CGAM to another. Such an application increases process rates, as well as effective melt zones. Consequently, the pitches between adjacent boreholes may be left larger, and the total number of boreholes required smaller.

   It should be noted that only the general concept of 'transferring power between energy sources' is meant by the term "Joule-heating'. As a matter of fact, the application ways of joule-heatings mentioned in this method and 'electric joule heating method' mentioned at section 2.2 is quite different from each other. The 'electric joule heating method' requires an electrically conductive path for start-up, and it is a top-down process, while joule-heating by CGAM relies on the path formed by the contact of individually created molten zones by each CGAM, and it is a bottoms-up process. Moreover, the energy sources employed for both methods are different from each other.

f) The dynamic operating conditions will lead to the inevitable contacts of the molten media and the torch. As mentioned in the 'electric plasma torch method – deficiencies' section, these contacts caused failures and major problems with the performance of a plasma torch. For that reason a plasma torch needs to be operated at a safer far distance from the molten media to avoid contacts, and this distant-operation will significantly reduce operation efficiency. Those quite dynamic operating conditions, such as impingements and collapses of cavities, have not presented a problem to the CGAM, which makes submerged electrode operations possible.

g) The CGAM as a heat source is robust enough to operate reliably, safely, and efficiently in the subterranean environment. There is no power loss due to its operational techniques. Higher efficiency is obtained, since its insensitivity to the melt interface allows close operations. The lives of the graphite electrodes are longer.

h) Combustion gas, oxygen and/or air are supplied to the zone via borehole downcomer annulus, so that the process does not rely on in-situ pyrolysis only.

i) The tools of the CGAM process are easy to transport and convenient for rapid reaction. The entire apparatus can be skid mounted and placed in the back of a typical dump truck and powered by a portable 100-kilowatt generator. With the addition of a truck-mounted auger, the crew will be totally mobile and capable of reacting to a variety of both emergency and routine maintenance requirements.

2.5 Electrical Vitrification Methods; A Comparative Overview

Table 2.1 below shows a summary of differences between the three vitrification methods, and displays the offered improvements by CGAM method over the two other methods.

Having no depth limitations, or ability to limit the treatment zone only to the required vitrification levels are types of advantages the application process adopted by the CGAM method, bottoms-up application, offers. Electric Plasma Torch method also has these advantages associated with the bottoms-up application over Electric Joule Heating Method.

CGAM method's advantages over Electric Plasma Torch method come from its use of a concentric graphite arc-melter as a heat source. It's being energy-efficient, versatile – allows operations in a variety of modes (joule, submerged arc, or arc) and in angles -, and robust – keeps operating while submerged in the molten media – qualify CGAM as the useful tool and the innovative aspect of the process.

Table 2.1: Summary Comparison of Various Vitrification Methods' Parameters for Subterranean Soil Stabilization Process

Parameter	Electric Joule Heating	Electric Plasma Torch	CGAM Electric Arc Melter
Energy loss	No data available	30-40 % due to water-cooling	None
Electrode life	Consumable electrodes	About 20 hours	About 50 hours
Depth limitation	Less than 20 feet	None	None
Ability to limit the treatment zone only to the required vitrification levels	No, all soil from surface down must be treated	Possible	Possible
Oxygen supply by process, for in-situ combustion	No, must rely on in-situ pyrolysis	No	Yes, via borehole downcomer annulus
Suitability for operation while submerged in molten media	Suitable	Significant operation and durability problems	Suitable
Sensitivity to voids in the media	Yes, molten soil can flow away from electrodes, breaking the electrical circuit	Not sensitive	Not sensitive, melt may relocate, torch power is not affected
Versatility	None	Inadequate	Versatile enough, a variety of operations possible, including joule-heating
Implementability	Not practical	Problematic	Easy to transport and assemble, convenient for rapid reaction

CHAPTER III
Soil Characterization

3.1 Introduction

To investigate the effectiveness of Concentric Graphite Arc Melter (CGAM) technology as a soil stabilization technique, soil samples representing a broad range of soil conditions were obtained and subjected to vitrification. Among the parameters examined were: soil type, degree of saturation and initial density. This chapter describes the criteria and procedures used in the selection of candidate soils as well as the findings from a series of characterization tests performed on the soil material prior to vitrification.

3.2 Selection of Candidate Soils

The identification of candidate soils for this research project was accomplished as a joint effort between TxDOT Project Monitoring Committee (PMC) and Texas Tech University researchers. The criteria used in the selection of candidate soils were as follows:

(a) Selected soil samples should represent a broad range of soil categories including coarse-grained materials such as sand and fine-grained materials with varying degrees of plasticity.

(b) Soils should be selected such that various geographic and climatic regions within the state of Texas are represented.

(c) Special emphasis shall be placed on those soil types for which traditional methods of stabilization are not effective; e.g. high sulfate soils that are subject to sulfate heaving when lime stabilization is used.

(d) The wide range of moisture conditions and in-situ densities found in natural soil deposits should be represented.

The first phase research project budget allowed vitrification and testing of up to 10 soil samples. Large samples (i.e. two 55-gal drums) were obtained from seven different sources that were selected based on the criteria listed above. Seven of these samples were prepared at *in-situ* or *as-received* moisture content. Two samples were vitrified at saturation moisture contents to study the effectiveness of CGAM vitrification at fully saturated or near-saturated conditions. The effectiveness of CGAM vitrification under saturated conditions was of special interest because none of the existing stabilization methods can be used for soils that are either submerged or located below the water table. Additionally, one soil sample was prepared at loose state with density well below its in-situ density so that the effect of soil density on the efficiency of vitrification can be examined. The ten soil samples used in vitrification and testing are summarized in Table 3.1.

Table 3.1: Location, Type and Initial Density and Moisture Condition of Soil Samples

Source	Soil Type	Initial Density	Moisture Content
Lubbock district (Hockley Co.)	Low plastic clay	Compacted	Natural
Lubbock district (Hockley Co.)	Medium plastic clay	Compacted	Natural
Dallas district	Clay	Compacted	Natural
		Compacted	Saturated
El Paso district	High sulfate clay	Compacted	Saturated
		Compacted	Natural
Beaumont	Organic clay	Compacted	Natural
Childress district	Silt	Compacted	Natural
		Loose	Natural
Lubbock district (Turner pit at Stink Lake)	Sand	Compacted	Natural

3.3 Laboratory Test Program

The selected soil samples were tested in the laboratory before vitrification. The laboratory test program included the following types of tests:

(a) X-ray diffraction and chemical analyses to determine mineralogical compositions of the soils,
(b) In-situ or natural water content, and
(c) Soil index tests necessary for soil classification purposes.

The soil index test included particle size distribution and Atterberg limits tests. The following section describes each test method and the results obtained.

3.3.1 X-Ray Diffraction and Chemical Analysis

Samples from seven selected soil types were subjected to x-ray diffraction analyses to study their mineralogical composition. Table 3.2 summarizes the results of x-ray diffraction analysis. It identifies the percentage of different mineralogical constituents in each soil source. The following general observations could be made based on the data presented in Table 3.2.

(a) The percent of clay minerals in the soil samples generally varied from 15 to 45. The only exception was the El Paso district clay, which had an extremely high percent (65%) of clay minerals.

(b) The soils from Lubbock district (all three types: medium plastic clay, low plastic clay and sand), Beaumont district (clay), and Childress district (silt) have high percentages of quartz as being a part of their non-clay mineral compositions.

(c) The Dallas district clay has a significantly high percentage of calcite (60%).

Table 3.2: Results of Semi-Quantitative X-ray Diffraction Analysis

Soil Type	Non-Clay Minerals			Clay Minerals						
	Quartz	Plagioclase	K-feldspar	Calcite	Illite + Mica	I/S Mixed-layer	Smectite	Kaolinite	Amorphous *	% Clay Fraction
Lubbock (Hockley Co.) low plastic clay	60	2	2	1	15	15		5		35
Lubbock (Hockley Co.) medium plastic clay	50	2	3	-	15	10		5	15	45
Dallas clay	10		+	60	5		20	5		30
El Paso high sulfate clay	10	2	3	20	-		15	-	50	65
Beaumont organic clay	55	5	10	-	10		15	5		30
Childress silt	53	10	15	2	10		5	5		20
Lubbock (Turner pit at Stink Lake) sand	40	10	5	30			5		10	15

(*): Amorphous silicate amounts were estimated from the difference of total mineral phases from 100%.
(+): Present but below 1% level.
(-): Not detectable by X-ray diffraction.

For further verification of soil compositions, samples were subjected to chemical analyses in addition to x-ray diffraction analyses. The results are displayed in the Table 3.3. The results are in satisfactory agreement with X-ray diffraction data. One noteworthy observation is the high silica content in Lubbock soils, Beaumont clay, and Childress silt. These soils also showed high quartz content in x-ray diffraction analysis. Since the chemical composition of quartz is silica, this observation shows that the results of chemical and x-ray diffraction analyses are consistent.

3.3.2 Water Content

The water content of a material is the ratio of the mass of water to the mass of the solid material particles.

Water contents of undisturbed soil samples from seven sources were measured in accordance with the ASTM Standard Method – Designation No: D2216. The natural water contents are listed in the Table 3.4. Most soil samples have their natural water contents ranging from 13.0 % to 23.3 % with the extreme exceptions of Childress district silt having 3.5 %, and Beaumont district organic clay having 40.4 % water content. To study the effect of water content on vitrification process, the soil samples from Dallas district clay and El Paso district high sulfate clay were prepared at saturated water contents by adding water to soil samples.

3.3.3 Particle Size Distribution

Particle size distribution, quantitative determination of the distribution of particle sizes in soils, is one of the index tests required for soil classification. Initially it requires the amount of materials passing No.200 sieve, and may require further sieve analysis depending on the result.

A washed sieve analysis is performed to determine the percent finer than No. 200 materials in soils, according to the ASTM Standard Test Method – Designation No: D1140. The results are presented in the Table 3.4.

Only the Lubbock district soil from Turner pit at Stink Lake is subjected to further sieve analysis. The dry sieve analysis is performed according to the ASTM Standard Test Method – Designation No: D 422. The resulting particle-size graph is illustrated in Figure 3.1.

TABLE 3.3: Whole Rock ICP Analysis (Chemical Analysis) Results of Selected Soils

Mineral Constituent	Soil Source								
	Lubbock (Hockley Co.) low plastic clay	**Lubbock (Hockley Co.) medium plastic clay**	**Dallas clay**	**El Paso high sulfate clay**	**Beaumont organic clay**	**Childress silt**	**Lubbock (Turner pit at Stink Lake) sand**	***Lubbock (Turner pit at Stink Lake) sand**	**Standard SO-15/CSA**
SiO_2 %	77.61	73.81	23.81	47.31	73.81	73.11	59.81	59.41	49.21
Al_2O_3 %	9.05	7.46	6.66	11.78	10.97	8.19	1.51	1.5	12.83
Fe_2O_3 %	3	2.41	2.79	3.69	3.82	4.36	1.17	1.51	7.31
MgO %	0.68	0.59	0.78	1.58	1.12	1.87	2.87	2.87	7.27
CaO %	1.05	0.59	33.14	14.62	0.75	3.7	16.14	16.07	5.88
Na_2O %	0.46	0.44	0.16	2.43	1.27	1.35	0.55	0.55	2.41
K_2O %	1.6	1.34	0.78	2.15	1.94	2	0.45	0.49	1.85
TiO_2 %	0.49	0.42	0.39	0.5	0.57	0.46	0.13	0.12	1.66
P_2O_5 %	0.04	0.06	0.15	0.11	0.14	0.2	0.01	0.02	2.71
MnO %	0.04	0.03	0.13	0.06	0.03	0.05	0.01	0.02	1.39
Cr_2O_3 %	0.16	0.013	0.006	0.005	0.017	0.017	0.013	0.009	1.062
Ba ppm	378	359	160	348	481	366	1168	1158	2062
Ni ppm	24	20	24	35	24	29	< 20	< 20	62
Sr ppm	80	77	697	822	142	100	543	545	397
Zr ppm	352	308	101	232	255	251	225	117	712
Y ppm	19	15	12	24	25	16	< 10	< 10	21
Nb ppm	< 10	< 10	< 10	< 10	< 10	< 10	< 10	< 10	< 10
Sc ppm	4	3	4	5	5	3	<1	<1	8
LOI %	5.9	5.4	31.1	15.6	5.4	4.6	17	17.2	5.9
C/Tot %	0.85	0.5	7.22	2.74	0.01	0.4	3.57	3.71	3.86
S/Tot %	0.02	0.01	0.18	1.62	0.03	0.06	0.29	0.28	5.08
Sum %	100.04	92.66	100.01	100.01	99.95	100	99.89	99.98	99.87

(*): Rerun of Samples

Table 3.4: Water content, Minus 200, LL, PL and PI Values and USCS Classifications of 7 Selected Soil

Location of Soil	Water Content	% Passing No.200 Sieve	Liquid Limit	Plastic Limit	Plasticity Index	USCS Classification	AASHTO Classification
Lubbock district, Hockley County, medium plastic soil	16.2%	56.9%	31.5%	14.0%	17.5%	CL, sandy lean clay	A-6 (7)
Lubbock district, Hockley County, low plastic soil	14.7%	61.8%	29.0%	12.1%	16.9%	CL, sandy lean clay	A-6 (7)
Dallas district	23.3%	87.1%	54.5%	19.5%	35.0%	CH, fat clay	A-7-6 (32)
El Paso district	18.8%	87.3%	51.2%	18.2%	33.0%	CH, fat clay	A-7-6 (30)
Beaumont district	40.4%	82.8%	58.0%	16.3%	41.7%	OH, organic clay with sand	A-7-6 (35)
Childress district	3.5%	67.0%	Non-plastic	Non-plastic	NP	ML, sandy silt	A-4 (0)
Lubbock district (Turner pit at Stink Lake)	13.0%	0.1%	*	*	*	SP, poorly graded sand with gravel	A-1-b (1)

* The soil from Lubbock district - Turner pit at Stink Lake has values: Percent passing #4 sieve: 66 %, Cu = 17.11, and Cc = 0.267

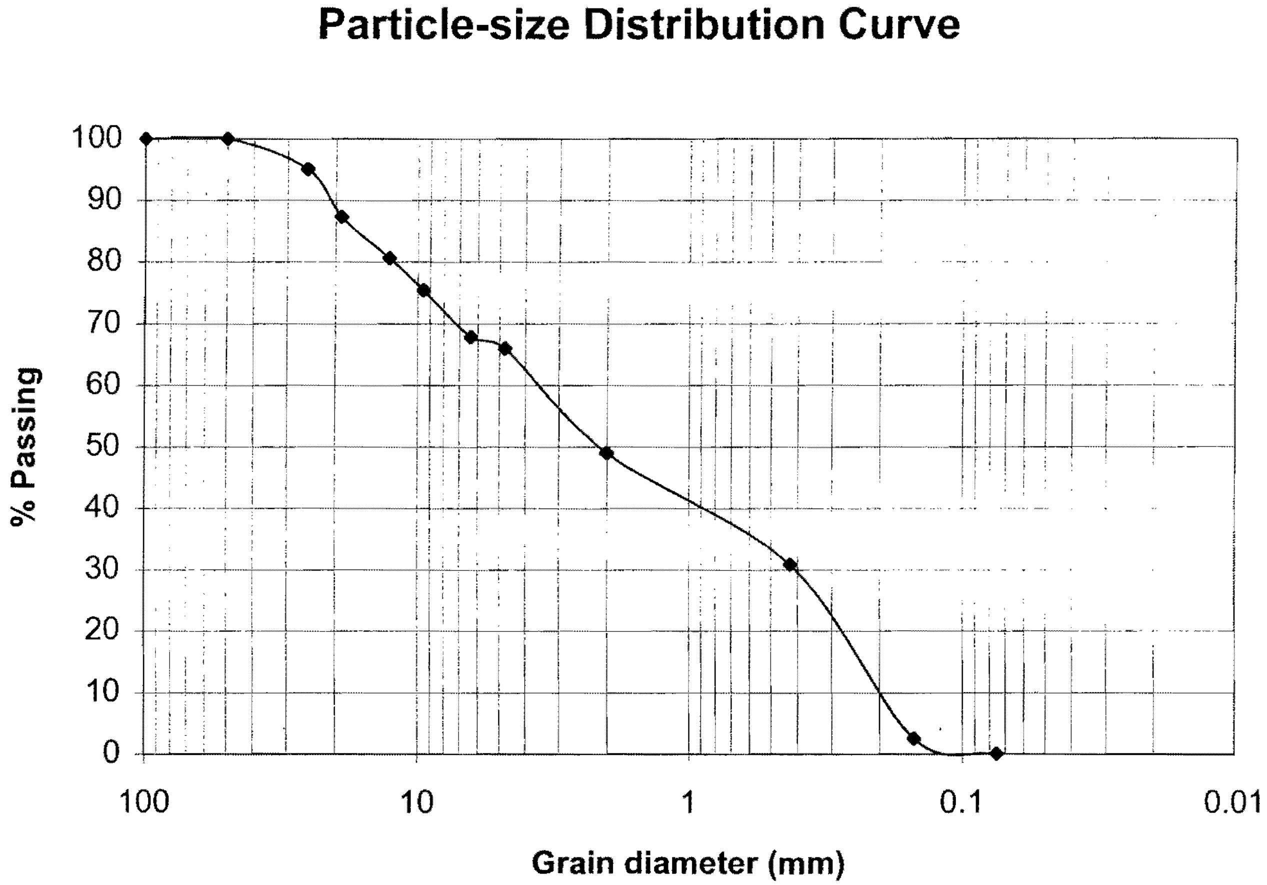

Figure 3.1: Particle-Size Distribution of Lubbock District soil From Turner Pit at Stink Lake

3.3.4 Atterberg Limit Analysis

The classification of fine-grained soils requires knowledge of plasticity of the soil. Soil plasticity is determined based on consistency limits proposed by the Swedish soil scientist, Atterberg. Atterberg, established four states of consistency for fine grained soils: liquid, plastic, semisolid, and solid. The dividing line between liquid and plastic states is the liquid limit (LL), and the dividing line between plastic and semisolid states is the plastic limit (PL). These limits are quantified in terms of water content. The difference between the liquid limit and plastic limit is the plasticity index (PI). Atterberg developed laboratory procedures for determining these limits and the index, which are useful numbers in classifying soils and making judgments in regard to their applications.

Liquid limit (LL), plastic limit (PL), plasticity index (PI) values of Lubbock - Hockley County soils, Dallas, El Paso, Childress and Beaumont district soils were determined in accordance with the ASTM Standard Test Method -- Designation no: D 4318. The plasticity characteristics of soil may influence the vitrification process. LL, PL, and PI values of these soils are listed in Table 3.4.

3.2.5 Classification of Soils

The selected sources of soils are classified according to the Unified Soil Classification System (USCS), ASTM – Designation No: D 2487. In this system, soils fall within one of three major categories: coarse-grained, fine-grained, and highly organic soils. These categories are further subdivided into 15 basic soil groups.

The results from soil classification conducted on the selected soils are presented in the Table 3.4. These classifications are based on the results from the index tests described above. According to the USCS classification the seven selected sources are grouped as follows:

(a) Sand with gravel; Lubbock district (Soil from Turner pit at Stink Lake)
(b) One sandy silt; Childress district Soil
(c) Sandy lean clay; Lubbock district, Hockley Co. (medium plastic soil) and Lubbock district, Hockley Co. (low plastic soil)
(d) Fat clay; Dallas district Soil and El Paso District Soil
(e) One organic clay with sand; Beaumont district Soil

The selected soils were also classified using the AASHTO Classification System, AASHTO-M145. AASHTO classification system rates soils according to their suitability for supporting highway pavements. The AASHTO system uses both grain-size distribution and Atterberg limits data to assign a *group classification* and a *group index* to the soil. The last column in Table 3.4 provides the AASHTO classification for the selected soil sources. The number shown outside the parenthesis is the group classification while the number shown inside is the group index

CHAPTER IV
Characterization of The Vitrified Soil

4.1 Introduction

After the selected soil materials were characterized at Texas Tech University for their geotechnical properties, sufficient quantities of soil from each source were shipped to Montec Associates, Inc. in Butte, Montana for vitrification. The vitrification of the soil material was accomplished by Montec under Subcontract No. 140G/0152-01. All the work completed under this subcontract is documented in a separate research report prepared by Montec Associates, Inc. This Montec report is attached as an Appendix to this report. It provides all the information related to soil preparation, equipment and methods used in soil vitrification, and data collected during the vitrification of soils.

Once the vitrification of the selected soil samples had been completed at Montec Associates, Inc. in Butte, Montana, the vitrified products were returned to Lubbock for further testing. The purpose of this testing program was to evaluate the vitrified material with respect to their mechanical properties such as unit weight, porosity, compressive strength, stiffness and susceptibility to moisture intrusion. This chapter describes the sampling methods and test procedures used in this evaluation and the results obtained.

Vitrified soils consisted of hard, dense, rock-like material that was black or very dark blue gray in color. The only exception was the vitrified melt obtained from Dallas sand, which had a light gray color. Some of the soils had smooth surface with glassy appearance similar that of obsidian. Others had rougher surface texture. It was also quite evident that vitrification has resulted in significant reduction in material volume. The extent of volume reduction and corresponding increase in density, however, varied significantly from one sample to another. The vitrified product consisted of three distinct zones of vitrification as shown in Figure 4.1. The inner core consisted of harder, monolithic material that was relatively free of fractures and voids. Surrounding the inner core was an approximately one inch thick outer shell that consisted of a more brick-like substance. This material was lighter in color and retained some of the original particle structure. The third and the outermost layer consisted of loose, unvitrified soil material.

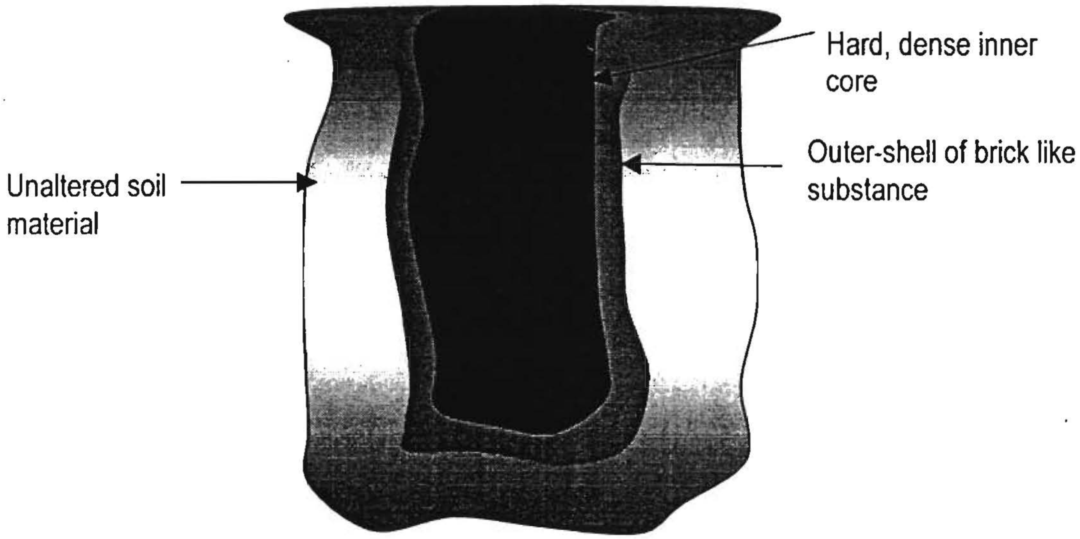

Figure 4.1 Schematic Cross-Section Through Vitrified Soil Showing Different Zones of Vitrification

4.2 Sample Preparation

As a first step, the vitrified mass was cleaned up by removing any loose soil material that was found on the outside. Secondly, pieces from outer shell were removed by using a hammer and a chisel. These chunks of material from the outer shell were tested for their stability against moisture intrusion by soaking in water. Unfortunately, owing to the limited thickness (approx. 1 inch) of the outer shell, it was not possible to obtain samples that are large enough for compression testing. As a result the mechanical properties such as Compressive strength and Modulus of elasticity of the outer shell material could not be determined.

The primary focus in this test program was on the evaluation of material from the inner core, which, in most cases, consisted of about 95% of the entire mass. To obtain samples of this material, the vitrified mass was clamped down firmly and drilled through using a concrete coring machine. A 2-inch diameter wet cutting diamond core bit was used for sample extraction. Figures 4.2 and 4.3 illustrate drilling operation.

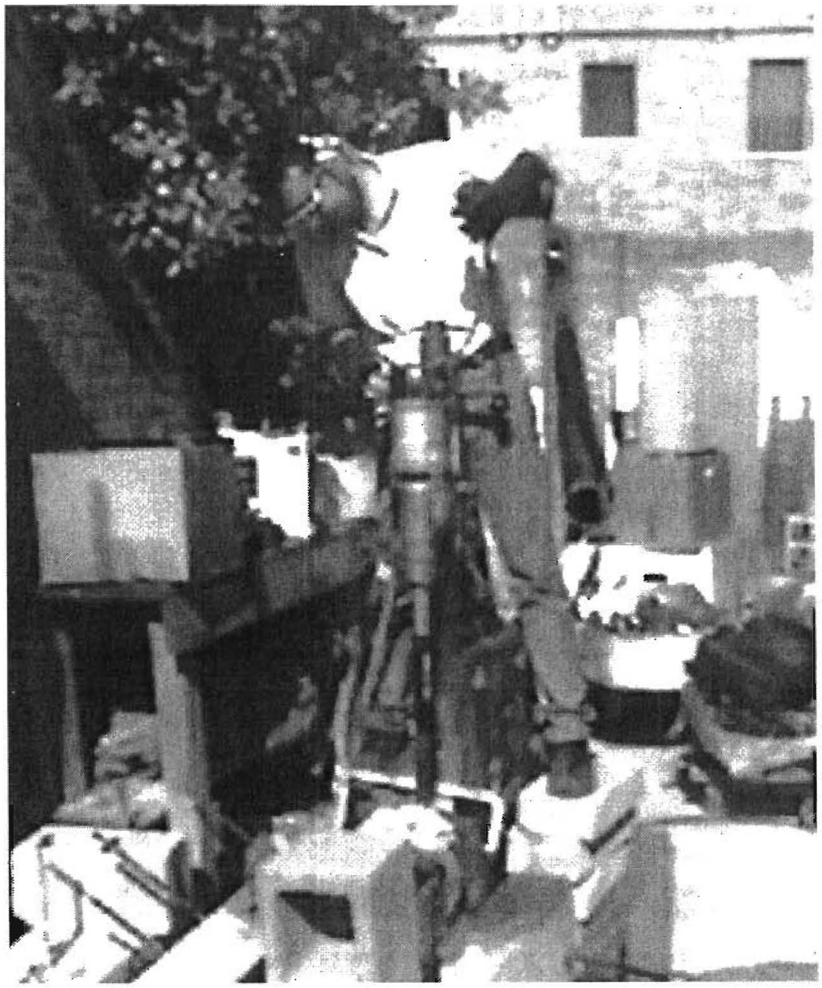

Figure 4.2 Drilling Operation

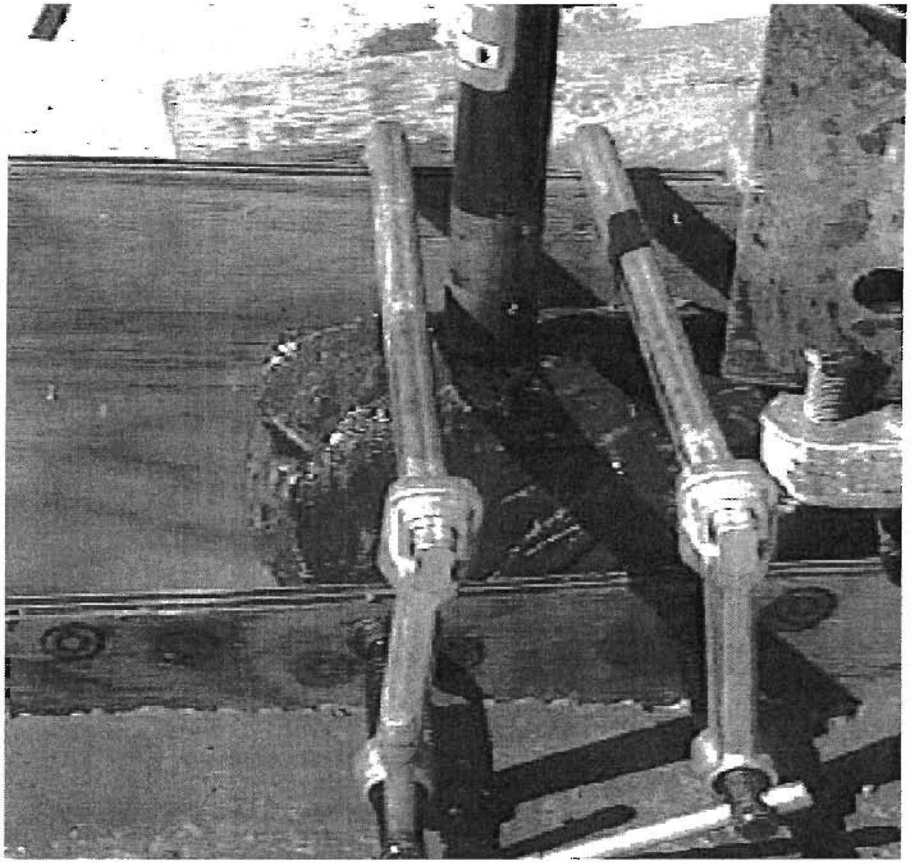

Figure 4.3 Clamped Vitrified Mass and Core Bit

Cores were intended to represent a wide range of materials found in the vitrified zone, and therefore, the samples were taken accordingly. Coring was a difficult and time-consuming process due to the high resistance offered by the material found within the vitrified masses. Furthermore, some of the vitrified products had numerous fractures that made it difficult to obtain a continuous, intact core. Once the cores were extracted, cylindrical specimens were prepared from the cores by sawing the cores at both ends at right angle to the axis of the core. Wherever possible, a diameter to height ratio of 1:2 was used in sample preparation.

As a representative sample, cores obtained from vitrified Beaumont organic clay (before their ends were sawed), vitrified Lubbock sand, and vitrified Dallas saturated clay are shown in Figures 4.4 to 4.6 in that order.

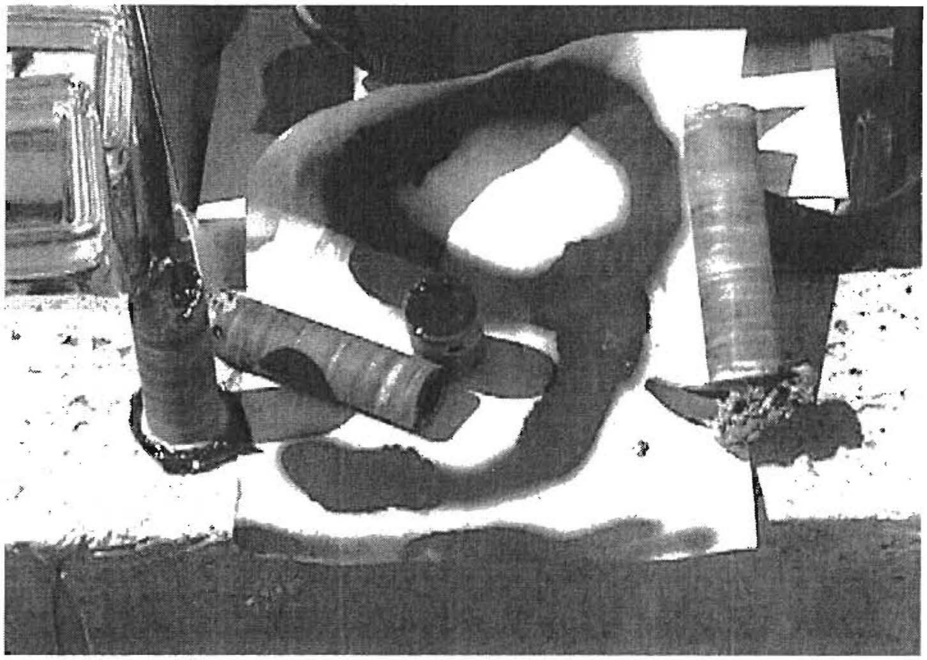

Figure 4.4 Cores Obtained From Beaumont Organic Clay Before Their Ends Were Sawed

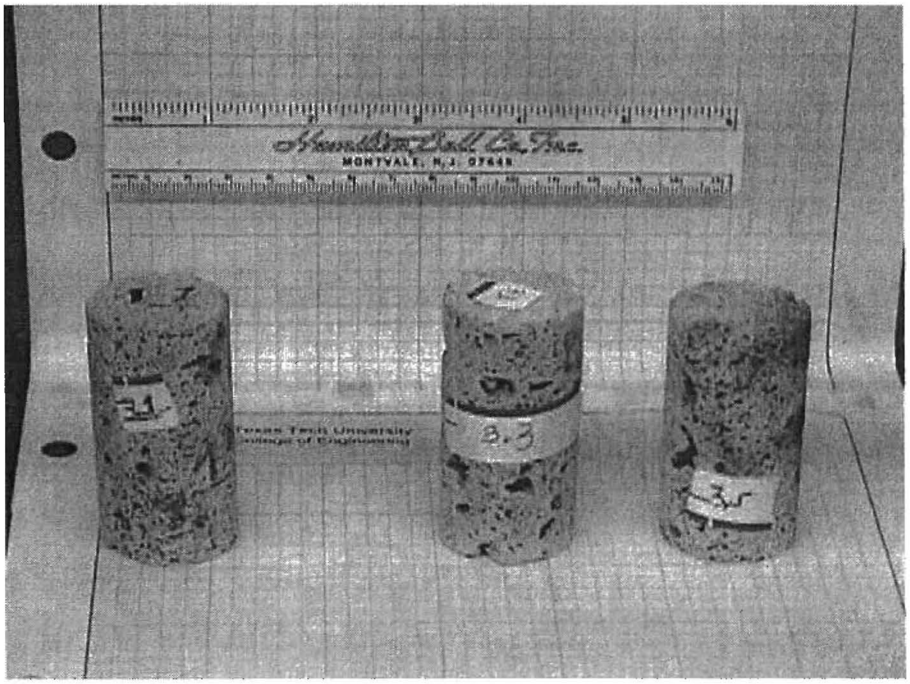

Figure 4.5 Cores Obtained From Lubbock Sand After Their Ends Were Sawed

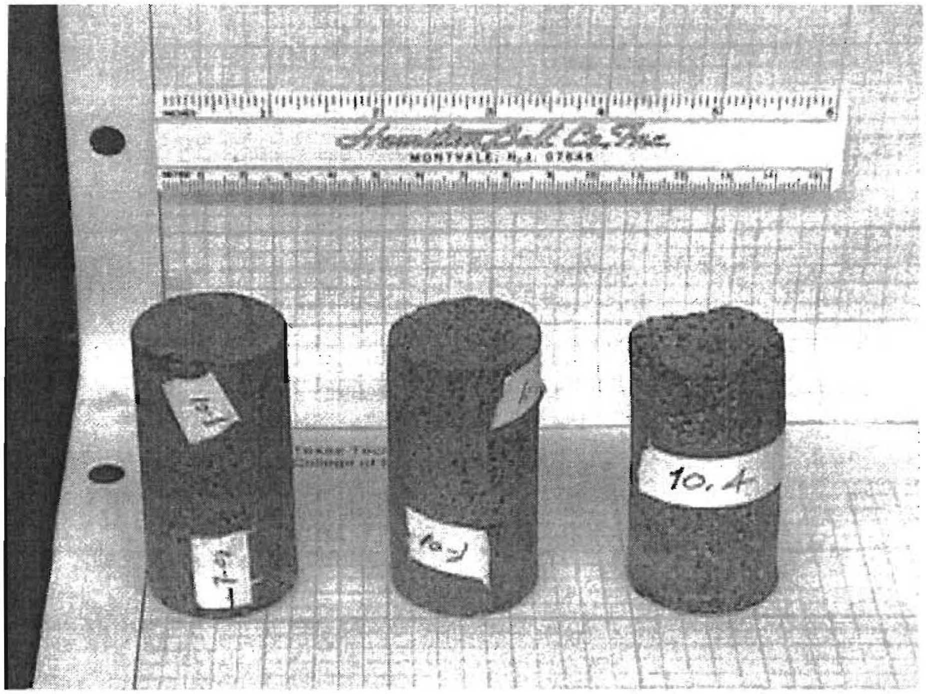

Figure 4.6 Cores Obtained From Dallas Saturated Clay After Their Ends Were Sawed

4.3 Laboratory Test Program

The primary objective of this laboratory test program was to evaluate the mechanical properties of the vitrified material. It is necessary to have such data on CGAM vitrified materials so that it can be compared with products obtained from other, more conventional stabilization methods. Such data is also needed to make comparisons between vitrification products obtained from different types of soils or between vitrification products obtained from the same soil but under different conditions (e.g. water content and initial density). The mechanical properties that were determined from these tests included the following: density, porosity, compressive strength, and elastic modulus. Among these, the compressive strength may be regarded as the primary criterion for comparison, since it is the main determinant for the effectiveness of the stabilization achieved. In addition to the mechanical properties mentioned above, the material from both inner and outer zones was also examined to determine their stability when soaked in water for prolonged period.

4.3.1 Material Density

The densities of the vitrified material varied significantly from one sample to another. The steps that were followed in the determination of material density were as follows:

(a) The average height and diameter of each cylindrical specimen were measured. The volume of the specimen was then calculated based on average height and diameter.

(b) The mass of each specimen was determined using an electronic balance with 8.0kg capacity and 0.01g precision.

(c) The densities of the material in each specimen was calculated by dividing the mass by volume.

(d) Four to seven core specimens were available for each vitrified sample. The density corresponding to each of these specimens was determined based on the procedure outlined above. Subsequently, the average of the four to seven densities was calculated and reported as the density for that vitrified sample.

The average density for each vitrified sample is given in Table 4.1. The standard deviation and coefficient of variation corresponding to each material are also shown. Figure 4.8 provides a graphical comparison between average densities.

Table 4.1 Density of Vitrified Materials

Soil Type	**Compaction/ Saturation Status of Material Before Vitrification**	**Average Density (g/cm^3)**	**Standard Deviation (g/cm^3)**	**Coeff. of Variation (%)**
Lubbock Hockley Co., low plastic - CL	Compacted	2.075	0.07	3.4
Lubbock Hockley Co., medium plastic - CL	Compacted	2.221	0.18	8.1
Dallas - CH	Compacted	1.685	0.26	15.4
	Compacted / Saturated	2.615	0.13	4.9
El Paso, High Sulfate - CH	Compacted	1.661	0.22	13.2
	Compacted / Saturated	2.443	0.11	4.5
Beaumont - OH	Compacted	2.466	0.04	1.6
Childress - ML	Compacted	2.049	0.06	2.9
	Loose	2.387	0.005	0.2
Lubbock district (Turner pit at Stink Lake) - SP	Compacted	1.523	0.03	2.0.

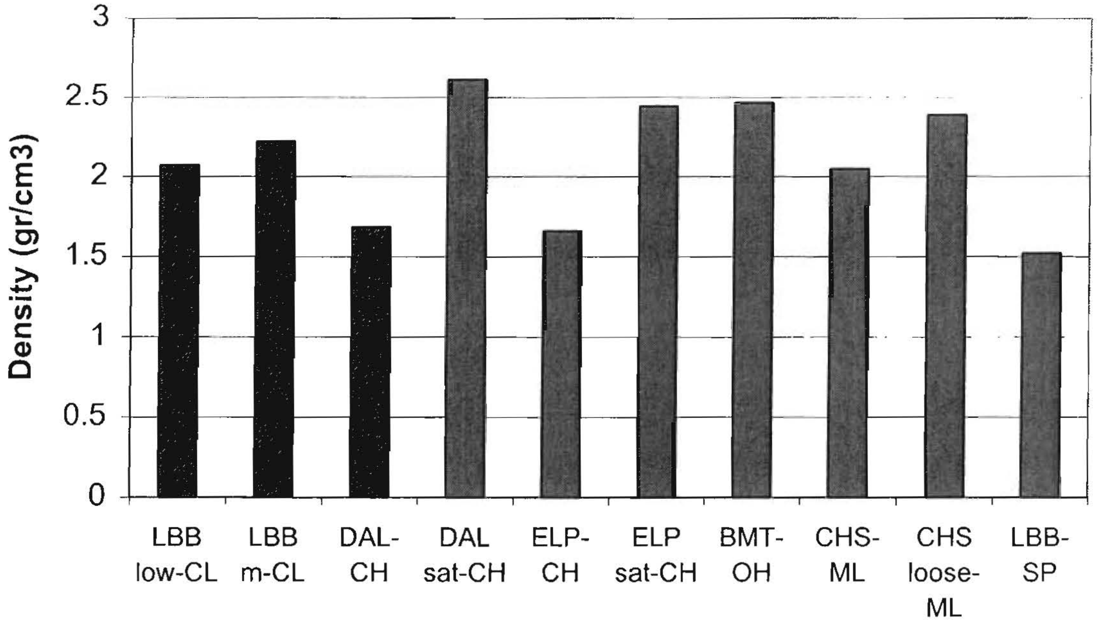

Figure 4.7 Densities of Vitrified Soils

4.3.2 Porosity

Porosity is the ratio of volume of voids in a material to the total volume of that material expressed as a percentage. Porosity of the vitrified material could be determined based on measured densities if the specific gravities of the solid minerals were known. To determine the specific gravity of the solid mineral, the vitrified product should be crushed into small enough particles such that individual particles would not contain any occluded air voids. Unfortunately, crushing vitrified materials into small enough fragments that are free of occlusions was not found to be practical for many of the vitrified materials. This was especially true for those materials with high crushing strength and extremely small voids. Therefore, as an alternative to this approach, the porosity values were *estimated* using an assumed average specific gravity value of 2.65. Once again, the cylindrical specimens were used for the above porosity calculations. The procedure used in the determination of porosity is as follows:

(a) In the estimation of porosity, a specific gravity of 2.65 was assumed for the solid vitrified material. Accordingly, the mass of each specimen, M_s was divided by 2.65 g/cm^3, to obtain the volume of solids in the specimen.

$$\text{Volume of solids, } V_s = M_s/2.65$$

(b) The volume of voids, V_v is the difference between total volume, V and volumes of solids, V_s

$$V_v = V - V_s$$

(c) Porosity, n is then as expressed as follows:

$$n = \left(\frac{V_v}{V} \right) .100\%$$

The porosity was calculated for each specimen using the above procedure and average porosity estimated based on these values. The average value corresponding to each vitrified sample is presented in Table 4.2. The same information is also shown graphically in Figure 4.8.

Table 4.2 Estimated Porosity of Vitrified Materials

Soil Type	**Compaction /saturation Status of Material before Vitrification**	**Estimated Porosity (%)**[1]
Lubbock Hockley Co., low plastic - CL	Compacted	21.7
Lubbock Hockley Co., medium plastic - CL	Compacted	16.2
Dallas - CH	Compacted	36.4
	Compacted /saturated	1.3
El Paso, High Sulfate - CH	Compacted	37.3
	Compacted /saturated	7.8
Beaumont - OH	Compacted	6.9
Childress - ML	Compacted	22.7
	Loose	9.9
Lubbock district (Turner pit at Stink Lake) - SP	Compacted	42.5

[1] Porosity values reported in this table have been estimated based on an assumed specific gravity of 2.65.

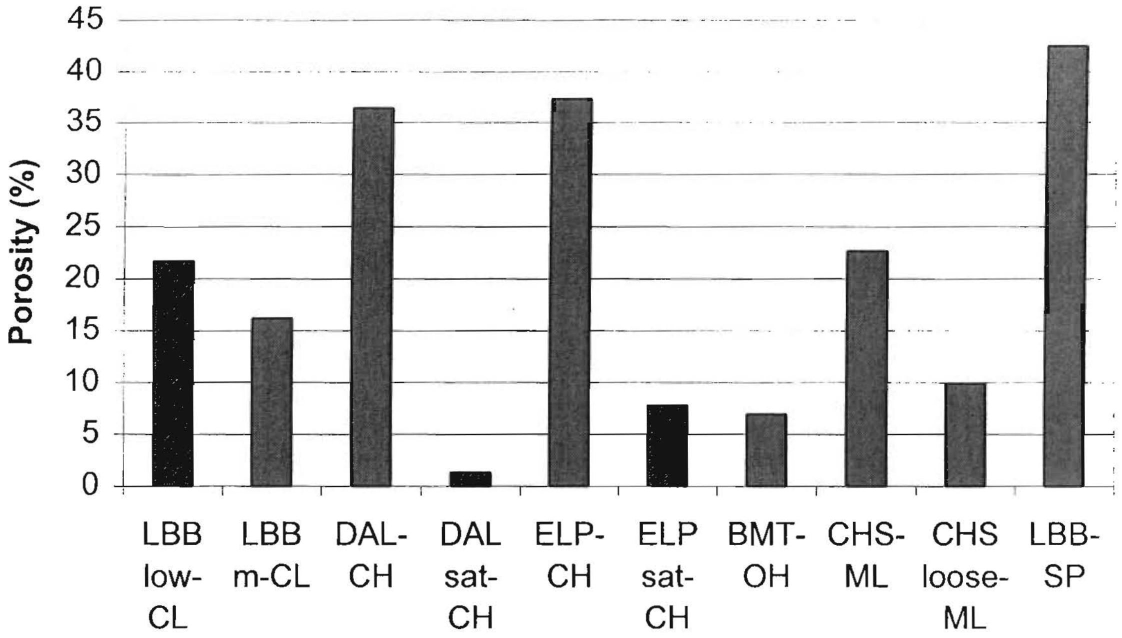

Figure 4.8 Porosities of Vitrified Soils

Two significant observations can be made in the data reported in Tables 4.1 and 4.2.

(a) First, in both cases where sample saturation was used (i.e. Dallas, CH soil and El Paso, High Sulfate soil), the saturated condition resulted in higher density and lower porosity than those samples that were prepared at natural water content.

(b) Second, the initial compaction did not necessarily result in higher density and lower porosity of the final vitrified product. In fact the exact opposite trend can be seen in the data obtained for the Childress-ML material. This data shows that the sample prepared in loose condition yielded higher density and lower porosity when compared with the sample that was initially compacted.

4.3.3 Unconfined Compressive Strength Test

Unconfined compressive strength is commonly used in the evaluation of material that has been stabilized by conventional methods such as lime and cement stabilization. In this test, a cylindrical specimen of the stabilized material is subjected to uniaxial compression load while no lateral confining pressure is applied on the test specimen.

Tests were performed in the Texas Tech Civil Engineering Material Testing Laboratory. A Model 880 MTS testing machine consisting of a 55-kip capacity load frame, a servo-controlled hydraulic actuator and a computer control station was used to perform the tests. Samples were loaded using compression platens. The samples were not capped during the compression tests. A container was attached to the testing machine to capture debris from the fractured samples. A photograph of the testing machine is given in Figure 4.9. Compression loads and deflections were measured during the testing. Stress-strain relationships for the samples were calculated from the sample dimensions, load values and position of the loading actuator during the testing

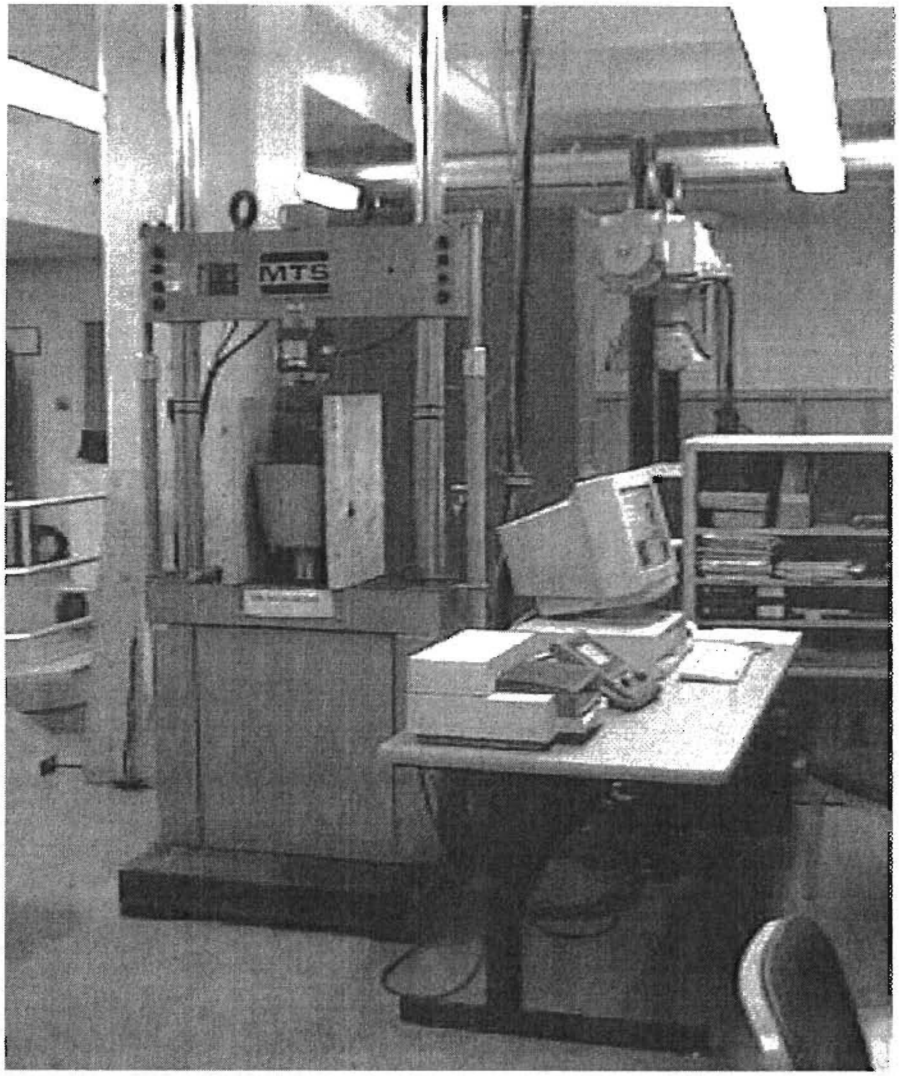

Figure 4.9 Compressive Strength Testing Setup

For each vitrified samples several specimens were subjected to compression testing. Loading was applied to the samples monotonically in stroke control at a rate of 2 x 10^{-4} in/sec. The change in length at any loading during the testing is the difference between the initial actuator position and the actuator position at the given load value. Time, actuator position and load value were automatically recorded at 5-sec intervals during loading. Loading was continued until failure of the sample.

The general failure mode of the vitrified soil samples is due to diametrical expansion of the samples when loaded along the axis of the cylinder. Porous samples absorbed loading, but are not capable of sustaining high load values. Denser samples also fail by diametrical expansion, but are more brittle and can sustain much higher loads.

The unconfined compressive strength of the sample was calculated by dividing the ultimate load by the measured cross section area of the core. Average of compressive strengths calculated for multiple samples obtained from a given vitrified sample was recorded as the average compressive strength of that vitrified sample. The average compressive strengths, standard deviations and coefficients of variation are given in Table 4.3. Average compressive strengths are also shown in Figure 4.10 for easy comparison.

Table 4.3 Data on Compressive Strength of Vitrified Materials

Soil Type	**Compaction / saturation**	**Compressive Strength (psi)**	**Standard Deviation (psi)**	**Coeff. of Variation (%)**
Lubbock Hockley Co., low plastic - CL	Compacted	2,527	614.1	24.3
Lubbock Hockley Co., medium plastic - CL	Compacted	3,588	667.4	18.6
Dallas - CH	Compacted	2,526	874.0	34.6
	Compacted / saturated	6,312	1041.5	16.5
El Paso, High Sulfate - CH	Compacted	1,392	393.9	28.3
	Compacted / saturated	2,800	907.2	32.4
Beaumont - OH	Compacted	2,582	692.0	26.8
Childress - ML	Compacted	2,301	230.1	10.0
	Loose	4,861	831.2	17.1
Lubbock district (Turner pit at Stink Lake) - SP	Compacted	1,653	424.8	25.7

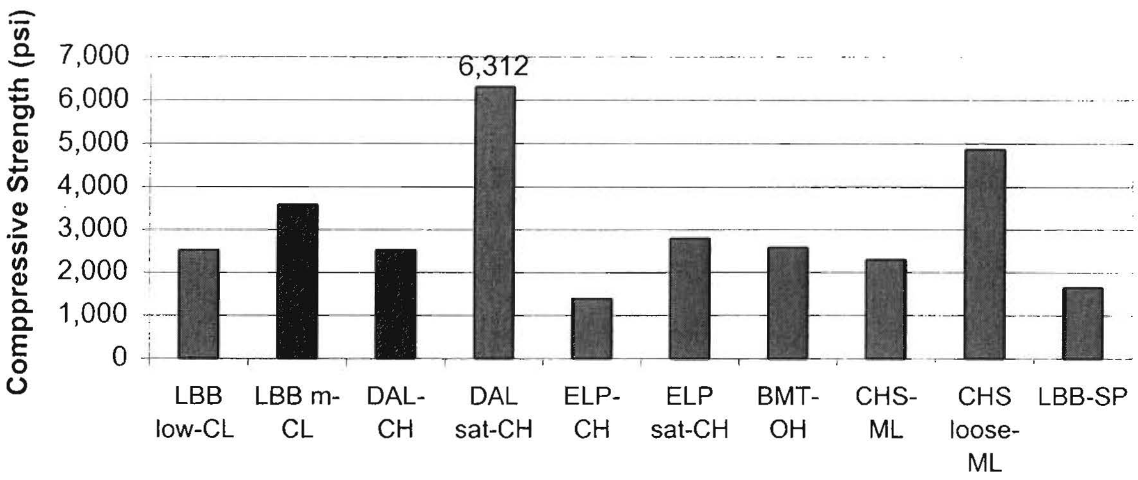

Figure 4.10 Compressive Strengths of Vitrified Soils

4.3.4 Modulus of Elasticity:

Modulus of elasticity of a material provides a measure of its stiffness or resistance to deformation. Elastic moduli of the vitrified materials were calculated using the load-deflection characteristics obtained from unconfined compression strength tests. The steps involved in this calculation are as follows:

(a) The stress applied on the sample was calculated by dividing the load by the initial cross section area of the specimen.

(b) Similarly, the strain was calculated as the ratio of the axial compression of the sample and initial sample length. The axial compression of the sample is equal to the travel of the loading platen. This could be easily obtained as the difference between the current and initial positions of the actuator.

(c) The stress and strain values calculated were plotted to obtain stress-strain diagrams for specimen being tested.

(d) Subsequently, the modulus of elasticity of the material was calculated as the slope of the straight-line portion of the stress-strain curve. An example of a stress-strain diagram including illustration of this calculation is given in Figure 4.11.

(e) Finally, the average of the elastic module determined for all specimens from a given vitrified sample was recorded as the average modulus of elasticity of that vitrified sample.

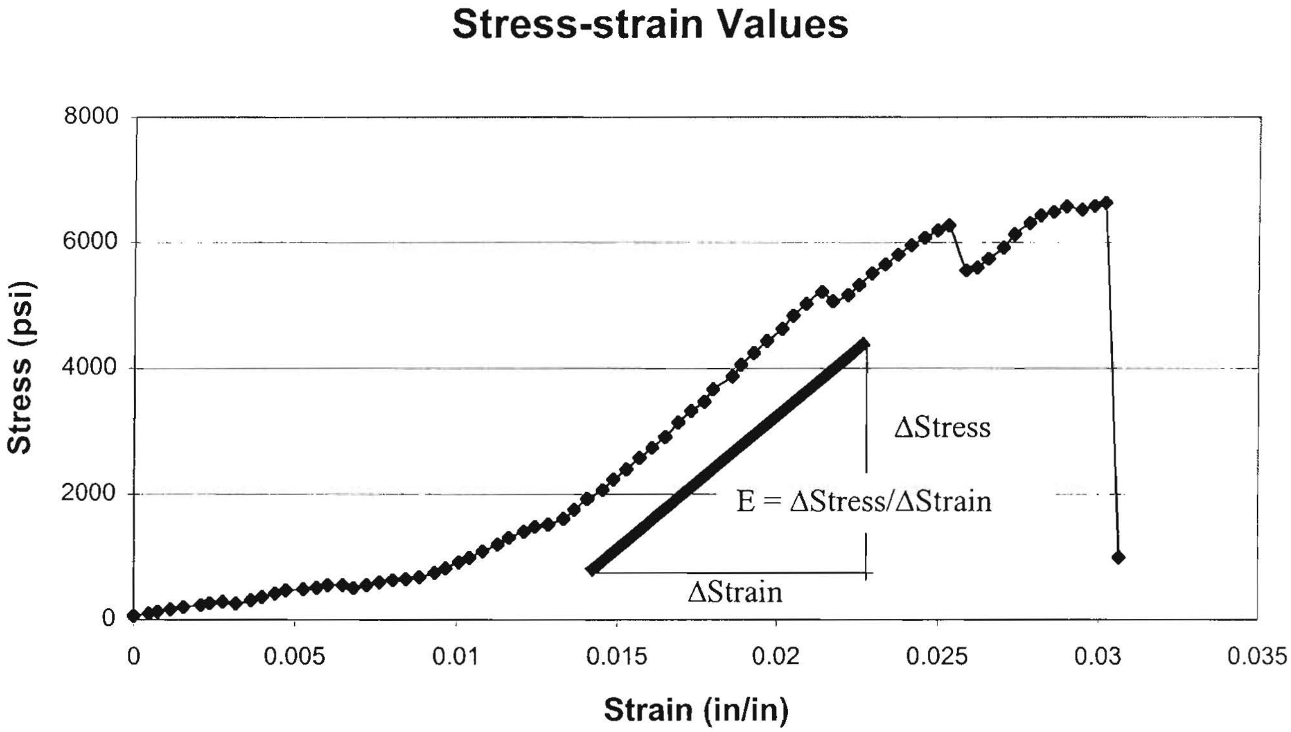

Figure 4.11 Stress-Strain Diagram and Modulus of Elasticity (E) Finding of a Vitrified Dallas Saturated Clay Specimen

The data from modulus of elasticity calculations for vitrified samples are given in Table 4.4. The average modulus of elasticity values are also compared graphically in Figure 4.12.

4.3.5 Moisture Susceptibility of Vitrified Materials

One of the primary drawbacks in conventional methods of soil stabilization is their inability to retain the stabilization effect against exposure to water. Previous research has shown that water, as it percolates through the stabilized material, removes the stabilizing agent from the soil gradually transforming the material back to its original condition. Unlike conventional methods of stabilization, soil vitrification does not rely on chemical interaction to achieve stabilization effect. It achieves strength gain through more fundamental transformation of the material. Therefore, it can be anticipated that the vitrified soils will be less susceptible to moisture attack. To verify this fact, material obtained from both outer and inner zones of vitrified samples were placed in glass jars filled with water and allowed to soak for several months. Figure 4.13 shows the vitrified material being soaked in water as described. After several months, the soaked material was examined to find out whether there were any signs of softening, volume expansion or disintegration.

Table 4.4 Average Modulus of Elasticity of Vitrified Materials

il Type	ompaction / aturation	Average Modulus of Elasticity (psi)	Standard Deviation (psi)	Coeff. of Variation (%)
ubbock Hockley o., low plastic - CL	Compacted	196,783	44,473	22.6
ubbock Hockley o., medium plastic - L	Compacted	202,631	41,336	20.4
allas – CH	Compacted	249,528	66,873	26.8
	Compacted / saturated	445,004	52,510	11.8
l Paso, High Sulfate CH	Compacted	108,685	31,301	28.8
	Compacted / saturated	234,193	50,586	21.6
Beaumont - OH	Compacted	245,901	42,541	17.3
Childress - ML	Compacted	262,209	35,660	13.6
	Loose	242,165	19,615	8.1
Lubbock district (Turner pit at Stink Lake) - SP	Compacted	150,203	36,049	24.0

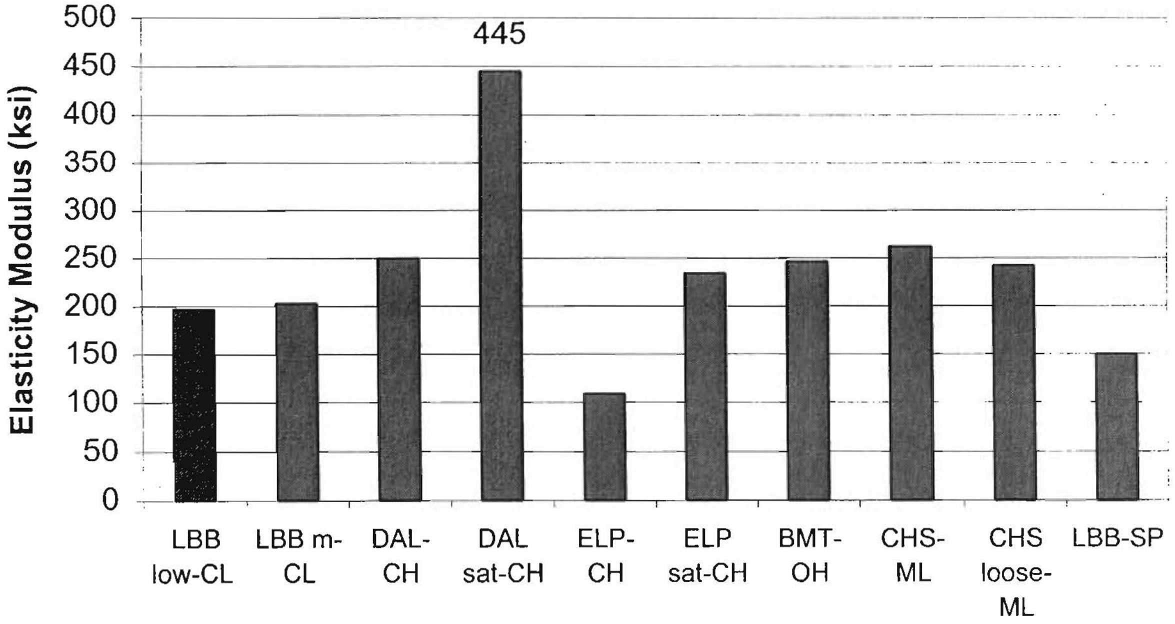

Figure 4.12 Elacticity Moduli of Vitrified Soils

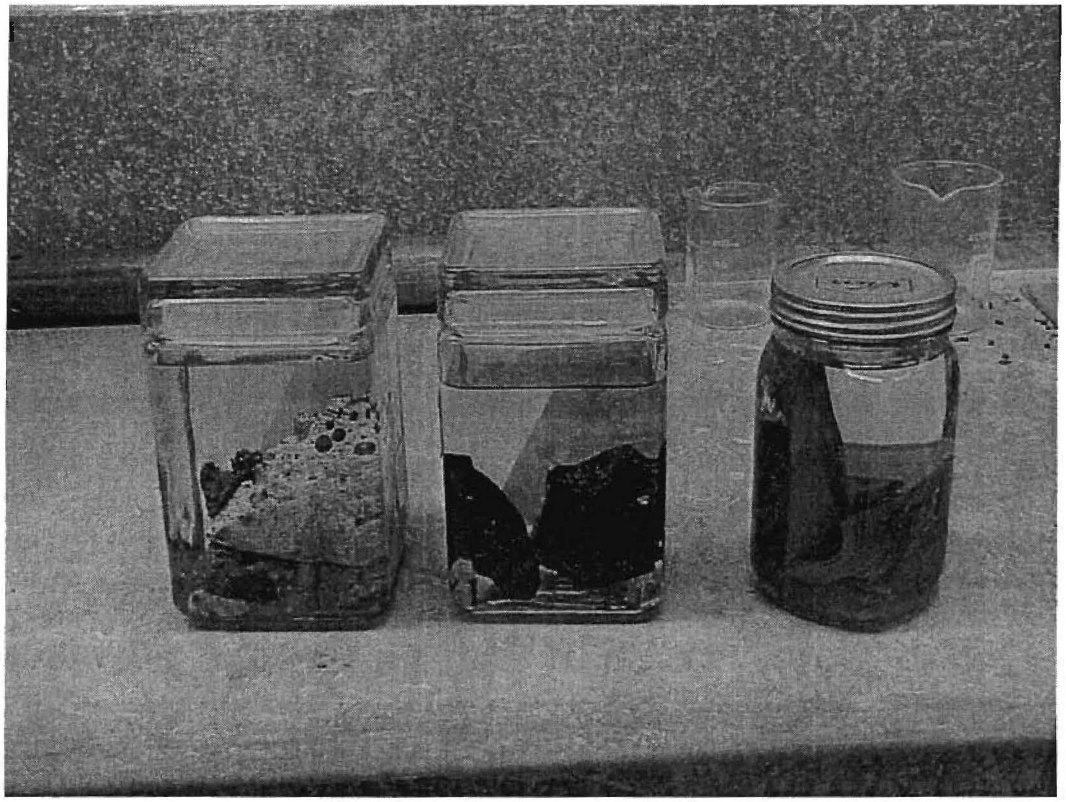

Figure 4.13 Outer and Inner Zone of Vitrified Material in Water

4.4 Conclusions

Following observations are made based on review of data collected on vitrified material:

a) Test results on density, porosity, compressive strength and modulus of elasticity are in general agreement with each other. Those vitrified soils with higher densities also have lower porosities, higher compressive strengths and higher elasticity moduli. Dallas saturated clay and Childress loose silt were among the soils that produced highest strengths while El Paso clay and Lubbock sand produced lowest strengths.

b) Test results obtained from vitrified forms of saturated soils differ greatly from vitrified forms of same soils with natural water contents. Saturated samples from both Dallas clay and El Paso clay yielded higher unit weights, lower porosities, higher compressive strengths and higher elasticity moduli (less elastic) than their unsaturated counterparts. The porosity, density, strength and moduli differences were more pronounced for the Dallas clay. The vitrified Dallas clay with natural water content can be rated as an average to low strength material compared to the general population. The vitrified form of saturated Dallas clay, on the other hand, had the highest strength.

c) Comparison between compacted and loose samples from Childress silt reveals that the differences in vitrified material properties are much smaller that those observed between saturated – natural water content states. The vitrified loose Childress silt had lower porosity and higher density than vitrified compacted Childress silt. Also, vitrified loose Childress silt had much more compressive strength but almost the same modulus of elasticity. However, it must be pointed out that only one soil, Childress silt, was vitrified in both compacted and loose states and therefore, these results cannot be used to draw general conclusions with respect to effect of initial density on the properties of vitrified product.

d) Vitrified sand produced lower unit weight, higher porosity, and less strength than clays and silts. Other than this observation, no other relationship between the quality of the vitrified product and the type of parent soil material was established.
e) A comparison between the vitrified products obtained from five clay samples at natural water contents revealed that they yielded similar mechanical properties except for vitrified El Paso clay. It has lower unit weight, higher porosity, and less strength than other four (Dallas, Lubbock low plastic, Lubbock medium plastic, and Beaumont) vitrified clay samples.

The following conclusions can be drawn from the results of tests and measurements by the help of above observations:

a) Vitrified soils are strong. Data about other conventional stabilization methods, which was collected in order to assess competitiveness of vitrification process and given in Chapter V, gives the highest amount of strength that has been reached by lime, cement, or lime-fly ash stabilizations to be 1,050 psi. It is shown that the compressive strength of materials coming out of vitrification process range between 1,392 to 6,312 psi, which is far above ranges of other conventional stabilization methods. On average vitrified materials have close strengths to that of typical concrete's.
b) Vitrified materials in general can be rated as elastic. Average levels of elastic moduli of vitrified materials are less than concrete's.
c) Mechanical properties vary among vitrified materials. They even vary among the specimens from the same vitrified soil. Type of soil, condition of soil (saturation, compaction), amount of power application, type of power application (high voltage-low current, or vice versa), and temperature profile (stronger material at the inner core where the highest temperatures were reached) might be considered as determinants of this variability.
d) Less porous vitrified material with higher unit weights are stronger and less elastic.
e) Better quality material is obtained by vitrifying saturated soils. This might also be due to the fact that testers in Montec Associates had to increase voltage while vitrifying saturated soil to which high current could not be applied. Thus, they had been able to keep power consumption in constant levels. High voltage might also be responsible for stronger vitrified material.
f) Dallas and El Paso clays are the soils that were saturated and then vitrified. They are both fat clays (CH) with small particle sizes. Their percentages passing no.200 sieve are 87.1 and 87.3, respectively. If saturation is the reason for high quality end product, but not the high voltage, whether saturation is good for all soils, or good for only fat clays with small particles should be studied.
g) Compaction prior to vitrification might be a useless effort to obtain stronger material as displayed in the case of Childress silt. Further research is required to verify better performance of material obtained by vitrifying loose state soils than material obtained by compacting, and then vitrifying soils.
h) Saturation might only be effective on compacted soils. It should be studied whether it is possible to obtain even better material by vitrifying loose and saturated soils, or whether the soils should be vitrified either in their loose states or in their compacted and saturated states.

i) When vitrified, clays and silts display better performances than sands. Studying more silt and sand samples should further test this fact.
j) Vitrified El Paso clay's poorer performance compared to vitrified forms of other clay samples with natural water contents is likely to be due to the soil's high sulfate content. Saturating the soil prior to vitrification leads to a better quality material, though.
k) Brick-like material forms in the outer vitrification zones, which also can be useful.
l) Water does not cause softening or disintegration of either vitrified material or brick-like material from outer vitrification zones.

CHAPTER V
Economic Analysis

5.1 Introduction

Cost associated with stabilization is a primary consideration in the selection of a suitable stabilization method for a given pavement subgrade improvement project. Therefore, in this chapter, the costs associated with subgrade soil stabilization using in-situ vitrification are examined. The cost of soil stabilization by vitrification method is then compared with those for conventional methods. The conventional methods of soil stabilization that are examined in this report are: lime stabilization, cement stabilization, and lime-fly ash stabilization. It must be noted that the strength gain that is achieved for a given soil varies with the particular stabilization agent or the stabilization technique used. Therefore, the economic comparison between different methods of stabilization is performed on the basis of strength gain per unit cost of stabilization. The same parameter is also used as the basis for determining the conditions under which the new technique is found to be most cost effective.

Costs associated with these conventional methods of soil stabilization were determined based on data collected from previous TxDOT projects. Wherever possible, pavement subgrade stabilization projects involving the same soils that were vitrified and tested in this research project were selected. When data for the same subgrade soils were not available, data on similar soils were used in the analysis.

5.2 Assumptions Used in Economic Analysis

One of the significant differences between in-situ vitrification method and other conventional methods mentioned above is that, in vitrification method, soil is treated at selected points on a grid pattern rather than uniformly over the entire area. In this sense, the treatment process is more similar to lime slurry injection method or soil stabilization with mini-piers or stone columns. Therefore, the gain in subgrade soil strength with this method will not be uniform over the entire treatment area. Therefore, to perform this comparison, one must know not only the soil strength gained *at* treatment points but also how it varies *between* treatment points. Unfortunately, the data necessary to determine strength gain between treatment points is not available at this time. On the other hand, one cannot proceed with the economic analysis without any information on variation of soil strength with radial distance from the treatment point. Therefore, the strength gain between treatment points were estimated based on the following assumptions:

(a) The variation of soil strength with radial distance from the point of treatment follows the same pattern as the variation of the maximum soil temperature reached at a particular point with radial distance. In other words, if the temperature variation follows a cubical polynomial, it is assumed that the same functional form could be used to describe the variation of soil strength with radial distance.

(b) The coefficients in the selected functional form could be obtained by matching the average strength measured for each vitrified material with the average strength calculated based on the assumed functional form. The specific procedures used are described more completely in Section 5.6.3.

Until now, all of the vitrification experiments conducted in the research project have been performed on soils contained in 55-gal drums. As a result, the available data cannot be used to validate the above assumptions. Therefore, it will be necessary to collect necessary strength data during future field vitrification experiments and hence validate these assumptions.

5.3 Lime Stabilization

5.3.1 Collected Raw Compressive Strength Data for Lime Stabilization

The data obtained related to unconfined compressive strength improvement of soils after lime-stabilization is as follows.

5.3.1.1 From TxDOT Dallas District

The data obtained from TxDOT Dallas district is based on tests made on 3 soil types in the years 1971 and 1972 as shown in Table 5.1.

Table 5.1 Compressive Strengths of Dallas Sites

Location	**Soil type**	**UCCS w 0% lime**	**UCCS w 2% lime**	**UCCS w 4% lime**	**UCCS w 6% lime**	**UCCS w 8% lime**
A - Dallas County, Loop-9	Reddish orange clayey sand	14.7 psi	105.7 psi	147.8 psi	109.5 psi	105.1 psi
B - Dallas County, Loop-9	Brown-tan, gray, and orange silty sandy clay with granular caliche.	7.1 psi	192.7 psi	262.0 psi	224.7 psi	199.5 psi
Location	**Soil type**	**UCCS w 0% lime**	**UCCS w 2% lime**	**UCCS w 3% lime**	**UCCS w 4% lime**	**UCCS w 5% lime**
C Kaufman County, F.M. 3039	Tan w/gray and orange silty clay w/fine caliche	3.9 psi	138.0 psi	195.8 psi	233.6 psi	247.0 psi

5.3.1.2 From TxDOT Childress District (Construction/Lab – Ronald Hatcher)

The data obtained from the Childress District is not about the soil type that has been previously collected from Childress for vitrification (Childress silt).

Amount of lime added = 3%

UCCS of the natural soil = 25 psi

UCCS of the lime-stabilized soil = 50 psi

Lime stabilization does not lead to a significant increase in UCCS, and lime stabilization is preferred in order to lower the PI rather than to increase the strength.

5.3.1.3 From TxDOT Beaumont District (Lab supervisor – Ronnie van Pelt)

The shear strength ranges represent Beaumont clay, including soil type that has been vitrified.

Amount of lime added = 4-6 %

Shear strength of natural soil = 0.5 tsf – 3 tsf

UCCS of natural soil (2 × shear strength) = 1 tsf – 6 tsf = 13.9 psi – 83.3 psi.

There is no data available on the strength of soil after lime stabilization as indicated by Ronnie Van Pelt.

5.3.1.4 From the Book: "Handbook for Stabilization of Pavement Subgrades and Base Courses with Lime" (Little, 1995)

Compressive strengths for lime-treated soils from different regions have varying values as shown in Table 5.2 (Little, 1995).

5.3.2 Average UCCS of Natural Soils

Existing data of natural soil-UCCS from 5 Texas locations (Dallas A, Dallas B, Dallas C, Childress, Beaumont) is used to estimate an average value for UCCS of clays. An example is shown in the equation below.

$$(14.7 + 7.1 + 3.9 + 25 + 48.6) / 5 = 19.86 = \underline{20 \text{ psi}}$$

This value also falls into 250-2000 psf range for undrained shear strength of soft-medium-stiff consistency soils (ASTM D2488-90), which would represent average soils (UCCS equivalent of this range is 3.5 – 27.8 psi).

5.3.3 Compressive Strength of Lime-Stabilized Soils

Avg. Values for Lime-Stabilized Clays with 3-5-7% Lime

Compressive strengths of 20 clay types following lime-stabilization with 3% lime by weight are indicated in Tables 5.1 and 5.2 and the section concerning the Childress District. These clay types are: Dallas B (3%-value is read from its '% lime vs. compressive strength curve'), Dallas C, Childress, Arlington, Beaumont, Burleson, Victoria, Denver, Bryce B, Cisne B, Drummer B, Fayette B, Fayette C, Accretion-Gley, Huey B, Huey D, Illinoian Till, Greenville B, Cecil B, St. Ann Bauxite. An average of these values will be the value for compressive strength of clay after 3% lime stabilization, and it is 185 psi.

Compressive strength values after lime stabilization with 5% lime addition belonging to same clay types (except Childress) are shown in Tables 5.1 and 5.2. A reasonable compressive strength value for clay stabilized with 5% lime addition would be an average of these values, which is 232 psi.

A compressive strength value for clay after lime-stabilization by 7% lime addition is found by taking the average of clay types, except Childress and Dallas C clays, found in Tables 5.1 and 5.2. Compressive strength value taken for clays after 7% lime-stabilization is 270 psi.

Average Values for Lime Stabilized Silts with 3%, 5%, and 7% Lime

Compressive strength data belonging to 7 silt types are used to estimate average compressive strength values for lime-stabilized silts with 3%, 5%, and 7% lime additions. These silt types are: Bryce A, Drummer A, Fayette A, Loam Till, Davidson B, Clalitos B, Nipe B.

Compressive strength of silt after 3% lime-stabilization = 97 psi.
Compressive strength of silt after 5% lime-stabilization = 137 psi.
Compressive strength of silt after 7% lime-stabilization = 154 psi.

Table 5.2 Data of 28-Day Compressive Strengths for Lime Treated Soils (Little, 1995)

Location	Unified Soil Classification	Compressive Str.(psi)–3%	Compressive Str.(psi)–5%	Compressive Str.(psi)–7%
Arlington, TX	CH	250	350	650
Beaumont, TX	CH	70	100	200
Burleson, TX	CH	150	220	310
Victoria, TX	CH	100	190	260
Denver, CO	CL	300	400	350
Bryce A, IL	MH	43	58	53
Bryce B, IL	CH	201	212	193
Cisne B, IL	CH	107	190	189
Drummer A, IL	ML	29	49	32
Drummer B, IL	CH	186	152	146
Fayette A, IL	ML	37	46	49
Fayette B, IL	CL	109	114	113
Fayette C, IL	CL	137	185	125
Accretion-Gley, IL	CL	263	247	283
Huey B, IL	CL	223	216	233
Huey D, IL	CL	222	179	197
Illinoian Till, IL	CL	150	186	143
Loam Till, IL	MH	172	184	174
Davidson B, IL	MH	198	268	324
Greenville B, IL	CL	455	517	551
Norfolk B, IL	SC	347	421	332
Clalitos B, IL	MH	114	133	132
Nipe B, IL	ML	87	220	311
Cecil B, IL	CH	168	163	224
St. Ann Bauxite, IL	CH	104	292	495

Avg. Values for Lime-Stabilized Sands with 3-5-7% Lime

Compressive strength values of 3%, 5%, and 7% lime added Dallas A sand are read from a curve that was drawn utilizing compressive strength data of Dallas A sand with different percentages of lime addition from Table 5.1. These values and compressive strength values of Norfolk B sand from Table 5.2 are averaged to estimate compressive strength values for lime-stabilized sands with 3-5-7% lime additions.

Compressive strength of sand after 3% lime-stabilization = 240 psi.
Compressive strength of sand after 5% lime-stabilization = 274 psi.
Compressive strength of sand after 7% lime-stabilization = 219 psi.

5.3.3 Unit Costs of Lime-Stabilization Applications

A twelve-month report on the average, low-bid unit prices on jobs contracted by the Texas Department of Transportation (TxDOT, 1999) is utilized to calculate a unit cost for unit volume of subgrade stabilization with lime. Item numbers 260-0505, 260-0508, 260-0510, 260-0512, and 260-0515 from this report give unit price and application quantity data about lime treatments of subgrades with 6", 8", 9", 10", and 12" depths, respectively.

To find a unit cost for lime stabilization, first unit prices for these treatments that are given in the form of unit price per area ($\$/y^2$) are converted into unit prices per volume ($\$/y^3$), and then a weight factor associated with each treatment is found based upon their application quantities. Finally, sum of unit prices per volume of these treatments multiplied with their weight factors is recorded as the unit cost for lime stabilization. Table 5.3 shows finding unit prices per volume and weight factors of 6", 8", 9", 10", and 12" depth lime treatments.

Table 5.3 Unit Prices and Weight Factors Associated with Lime Treatment Applications

Type of Lime Treatment	**Unit Price per Area² ($\$/y^2$)**	**Unit Price per Volume ($\$/y^3$)***	**Area Treated² (y^2)**	**Volume Treated (y^3)****	**Weight Factor*****
6" depth	0.98703	5.92218	3,291,365	549,658	0.385
8" depth	1.19053	5.35738	2,575,684	571,802	0.4
9" depth	1.41685	5.6674	299,969	74,992	0.053
10" depth	1.1086	3.99096	500,001	139,000	0.097
12" depth	0.89167	2.67501	278,622	92,781	0.065

* Unit Price per Volume ($\$/y^3$) = Unit Price per Area ($\$/y^2$) / depth of treatment (y)
** Volume Treated (y^3) = Area Treated (y^2) * depth of treatment (y)
*** Weight Factor = Volume Treated / 1,428,233 y^3 (total volume treated by all treatments)

Unit cost per y^3 of subgrade stabilization with lime = $\sum$ (Unit Price per Volume × Weight Factor) = $\$5.92218/y^3 \times 0.385 + \$5.35738/y^3 \times 0.4 + \$5.6674/y^3 \times 0.053 + \$3.99096/y^3 \times 0.097 + \$2.67501/y^3 \times 0.065 = \underline{\$\ 5.285}$

Most soils require between 2% and 5 % lime (ASTM C-977). Based on this assumption, a 3% lime addition can be assumed as a most common application. Consequently, the estimated unit cost of lime stabilization above is assumed to represent an average of 3% lime addition.

A former study on equipment cost of lime and cement stabilization showed that increase in equipment cost of stabilization with admixtures is approximately half the increase in admixture quantity (e.g. when the admixture quantity is increased from a to 3a, equipment cost increases from b to 2b).

However, the cost of lime which is $88.37702/ton as shown in item 20-503 of the twelve-month study on the average, low-bid unit prices of jobs contracted by the Texas Department of Transportation (TxDOT, 1999) is more than four times the equipment cost estimated in the mentioned study. With the inclusion of cost for water, ratio of equipment cost in total cost becomes even smaller. As a result of this, the amount that equipment cost increases less with the increasing lime amount becomes negligible. Therefore, an estimation of lime stabilization cost-increase proportional to the added lime-increase is made as follows.

Estimated cost of 1cy subgrade lime-stabilization by adding 3% lime = $5.285.
Estimated cost of 1cy subgrade lime-stabilization by adding 5% lime = (5/3) × $5.285 = $8.808.
Estimated cost of 1cy subgrade lime-stabilization by adding 7% lime = (7/3) × $5.285 = $12.332.

5.4 Cement Stabilization

5.4.1 Data and Compressive Strength of Cement-Stabilized Soils

Mitchell (1976) presented a very comprehensive review of the strength properties of cement-stabilized soils. He concluded that the unconfined compressive strength is generally described as increasing linearly with the cement content percent. The following table (Table 5.4) modified from the Air Force Manual (1982) presents the compressive strength values for different types of soils and the usual range of cement percents.

Table 5.4 Compressive Strength Ranges of Cement Stabilized Soils

Soil Type	Usual Range in Cement Requirement (%)	Compressive Strength (psi)
Sandy and gravelly soils	3 – 11	400 – 1000
Silty soils	7 – 13	300 – 900
Clayey soils	9 – 16	250 – 600

Assuming compressive strength will increase linearly with percentage of cements, the values within the usual range can be estimated by interpolations shown in Table 5.5.

Table 5.5 Average Compressive Strengths of Cement Stabilized Soils

Soil Type	Usual Range in Cement Requirement (%)	Wet Compressive Strength (psi)
Sandy and gravelly soils	3	400
	7	700
	11	1000
Silty soils	7	300
	10	600
	13	900
Clayey soils	9	250
	13	450
	16	600

5.4.2 Unit Costs of Cement Stabilization Applications

The typical requirements after cement-stabilization application are estimated to be in the range of 300-500 psi. Based upon the fact that cement-stabilization works best with sands and that 300-500 psi range is shown in Table 4 to be reached at 3% cement addition, average of costs shown in certain related items from the twelve-month study on the average, low-bid unit prices on jobs contracted by the Texas Department of Transportation (TxDOT, 1999) is assumed to represent an average of 3% cement addition. These items: 275-0509, 275-0510, 275-0523, 275-0534, and 275-0541, which are cement treatments with 6", 7", 8", 10", and 12" depths, respectively are utilized for unit prices and quantities. Weighted average of costs shown at these items are taken, and a final average cost value for 3% cement addition per cy is estimated in the same way as above for lime-stabilization. The resulting average unit cost per y^3 of stabilization with cement by 3% is $ 4.695.

The cost of cement is more than the cost of lime, holding a larger ratio in total cost of cement stabilization. Therefore, it is realistic to assume a cement stabilization cost-increase proportional to the added cement-increase. As a result of that assumption, the following costs per y^3 for different percentages of cement addition are estimated.

For 7% cement addition = (7/3) * $4.695 = $10.955.
For 9% cement addition = (9/3) * $4.695 = $14.085.
For 10% cement addition = (10/3) * $4.695 = $15.65.
For 11% cement addition = (11/3) * $4.695 = $17.215.
For 13% cement addition = (13/3) * $4.695 = $20.345.
For 16% cement addition = (16/3) * $4.695 = $25.04.

5.5 Lime-Fly Ash Stabilization

5.5.1 Collected Raw Compressive Strength Data for Lime-Fly Ash Stabilization

Table 5.6 is prepared utilizing data collected about lime-fly ash applications to: a typical Texas clay (Chu et al, 1955), a Lubbock clay (Dozier, 1999), a North Dakota clay, and a Plainfield sand (Dobie at al, 1975).

5.5.2 Compressive Strength of Lime-Fly Ash Stabilized Soils

Using data from Table 5.6, the average compressive strength values for clays and sands are estimated. Three different percentage values for clays are used for three different locations. The percentages that are used are % 9, 15, 20. The data suggests the following average values:

Average Estimated Compressive Strength for Clays
By adding 9 % lime-fly ash = 308 psi
By adding 15 % lime-fly ash = 463 psi
By adding 20 % lime-fly ash = 549 psi

Average Estimated Compressive Strength for Sands
By adding 15 % lime-fly ash = 400 psi
By adding 20 % lime-fly ash = 750 psi

Table 5.6 Compressive Strength of Lime Fly Ash Stabilized Clays and Sands

Location	Soil Type	Total Admixture Ratio *	Compressive Strength of Stabilized Soil
Lubbock	Clay	9 %	100 psi
Texas **	Clay	9 %	600 psi
North Dakota **	Clay	9 %	226 psi
Lubbock **	Clay	15 %	150 psi
Texas	Clay	15 %	900 psi
North Dakota **	Clay	15 %	338 psi
Lubbock **	Clay	20 %	200 psi
Texas **	Clay	20 %	1050 psi
North Dakota	Clay	20 %	396 psi
Plainfield	Sand	15 %	400 psi
Plainfield	Sand	20 %	750 psi

* A 1 to 4 mixture application of lime to fly ash is the ratio, which is encountered the most in literature, case histories. Hence, this ratio of 1:4 is assumed to be the most common lime to fly ash ratio applied.

** Compressive strength vs. total mixture percentage curve for a typical Texas clay is given by Chu et al (1955). Compressive strength values of other clays (North Dakota and Lubbock) for different percentages than their given percentages are estimated based on the assumption that, similar curves for those clays are also going to show the same trend as of Texas clay's used by Chu et al.

5.5.3 Unit Costs of Lime-Fly Ash Stabilization Applications

Besides the 1 to 4 ratio of lime to fly ash, a 15% total mixture percentage is also a value that is encountered the most in literature, case histories. Therefore, cost given in the twelve-month study on the average, low-bid unit prices of jobs contracted by the Texas Department of Transportation (TxDOT, 1999) is assumed to represent a 15% total mixture addition. The related item number is 265 – 5014, and the estimated cost for 1-cy treatment is calculated as follows.

Cost given for a 600mm deep subgrade treatment = \$7.2/m^2.
Cost of treatment per volume (15% lime-fly ash added) = \$7.2 / 0.6 m^3 = \$12 / m^3 = <u>\$9.175/cy.</u>

The same assumption of cost-increase being proportional to the added lime-fly ash increase is made. Costs per cy for different percentages of lime-fly ash addition are estimated below.

For 9% lime-fly ash addition = (9/15) * \$9.175 = <u>\$5.505.</u>
For 20% lime-fly ash addition = (20/15) * \$9.175 = <u>\$12.233.</u>

5.6 In-situ Vitrification

5.6.1 Data From Experiments

Following information in Table 5.7 has been obtained after vitrification testing of Texas soils, performed in Montana by Montec (Appendix - Farrar and Haack, 1999):

Table 5.7 Vitrification Testing Parameters for TX Soils

Barrel No	Soil origin and type	Compaction/ Saturation	Test Dur. (min)	Total Power (kW-hr)	Avg. power (kW)	Cathode (outer electrode) loss (lbm)	Anode (inner electrode) loss (lbm) **
1	Lubbock, Hockley Co. medium plastic soil – CL, sandy lean clay	Compacted	65	104.6	95	8.5	<1.4
2	Lubbock, Hockley Co. low plastic soil – CL, sandy lean clay	Compacted	130	62	97.1	8.1	<1.6
3	Lubbock district (Turner pit at Stink Lake) - SP, poorly graded sand with gravel	Compacted	90	118.4	93	9.3	<1.6
4	El Paso, high sulfate - CH, fat clay	Compacted	105	124.2	84	8.0	<2.3
5	El Paso, high sulfate - CH, fat clay	Compacted - saturated	100	137.2	91	8.9	<1.8
6	Childress - ML, sandy silt	Compacted	90	127.5	99	5.6	<1.8
7	Childress - ML, sandy silt	Loose	110	120.7	89	11.9 *	<2.5
8	Beaumont - OH, organic clay with sand	Compacted	80	122.2	106		
9	Dallas - CH, fat clay	Compacted	85	124.4	104		
10	Dallas - CH, fat clay	Compacted - saturated	80	129.8	114		

* Measurements were not made for each test and the loss is an average over these four tests.

** The anode loss during testing was less than the cathode and its length was typically trimmed between tests to match the cathode length – the mass shown reflects the trimmed length.

5.6.2 Compressive Strength of Vitrified Soils

Compression strength tests applied to vitrified samples so far have given the following results in Table 5.8.

Table 5.8 Compressive Strengths of Vitrified Soils

Barrel No.	Soil Origin and Type	PI	Compaction/ Saturation	Compressive Strength (psi)
1	Lubbock, Hockley Co. medium plastic soil – CL, sandy lean clay	17.5%	Compacted	3,588
2	Lubbock, Hockley Co. low plastic soil – CL, sandy lean clay	16.9%	Compacted	2,527
3	Lubbock district (Turner pit at Stink Lake) - SP, poorly graded sand with gravel	-	Compacted	1,653
4	El Paso, high sulfate - CH, fat clay	33.0%	Compacted	1,392
5	El Paso, high sulfate - CH, fat clay		Compacted - Saturated	2,800
6	Childress - ML, sandy silt	NP	Compacted	2,301
7	Childress - ML, sandy silt		Loose	4,861
8	Beaumont - OH, organic clay with sand	41.7%	Compacted	2,582
9	Dallas - CH, fat clay	35.0%	Compacted	2,526
10	Dallas - CH, fat clay		Compacted - Saturated	6,312

From Table 5.8 it is concluded that vitrified clay, silt and sand strength values, and an average compressive strength value for all soils are found as follows.

Vitrified clay compressive strength (average of barrel numbers 1,2,4,5,8,9,and 10) = 3,104 psi.
Vitrified silt compressive strength (average of barrel numbers 6 and 7) = 3,581 psi.
Vitrified sand compressive strength (barrel number-3 soil) = 1,653 psi.
Average compressive strength value for all soils = 3,054 psi.

5.6.3 Soil Stabilization by Vitrifying Columns with Certain Spacings

Rather than a pure-vitrification application, adequate soil-stabilization might be achieved by forming vitrified columns in soil with certain spacings in between.

LSPI (lime slurry pressure injection) is another method for stabilization, in which lime slurry is injected in soil with typically 5-ft spaced centers (Little, 1995).

Taking that spacing as a reference point, in an application of forming 22" diameter vitrified columns that are 5 feet apart from center to center in a grid format, an average final strength of stabilized area is estimated.

5.6.3.1 Estimation of Compressive Strength in an Area Stabilized by 5-Feet Spaced Vitrified Columns:

Temperature distribution data at the conclusion of each barrel's testing is given in vitrifying-test report of Montec(Appendix - Farrar and Haack, 1999), as well. An approach assuming that stress-distribution is going to be proportional to temperature distribution over the area is adopted to estimate stress distribution and average strength between columns. An average approximate temperature distribution curve is shown in Figure 5.1.

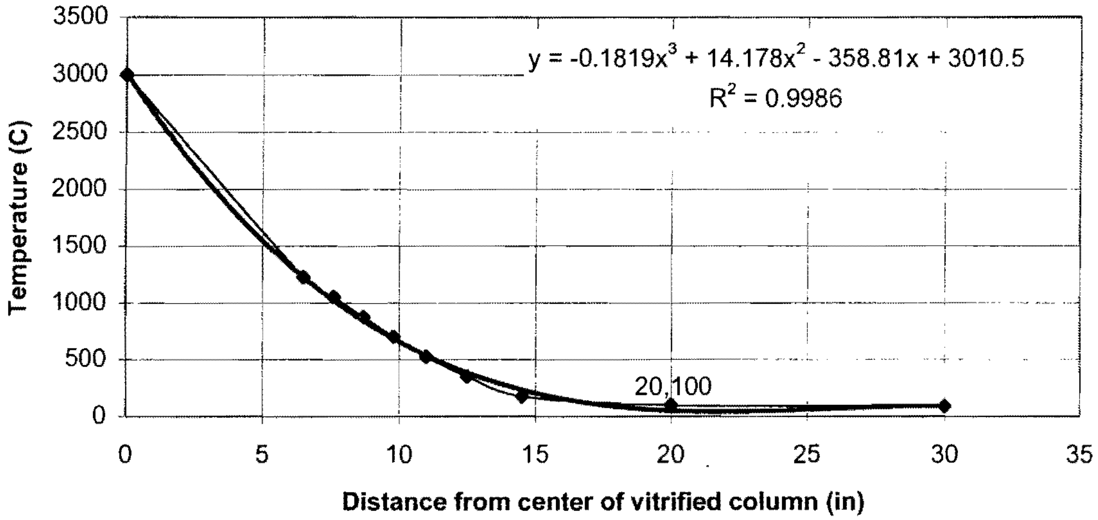

Figure 5.1 Average Temperature Distribution Curve of Tested Soils (The thicker line indicates a third degree polynomial curve added as a trendline to the curve obtained by joining temperature data, its equation is also displayed.)

Soil inside the barrel had an estimated average compressive strength of 3,054 psi. During testing, the barrel wall was located 11 inches apart from the center (radius of column is 11 inches). Hence, the ratio of compressive strength values to temperature values is determined from the average compressive strength inside the barrel at 3,054 psi. The following curve of compressive strength distribution between centers of vitrified columns results (Figure 5.2).

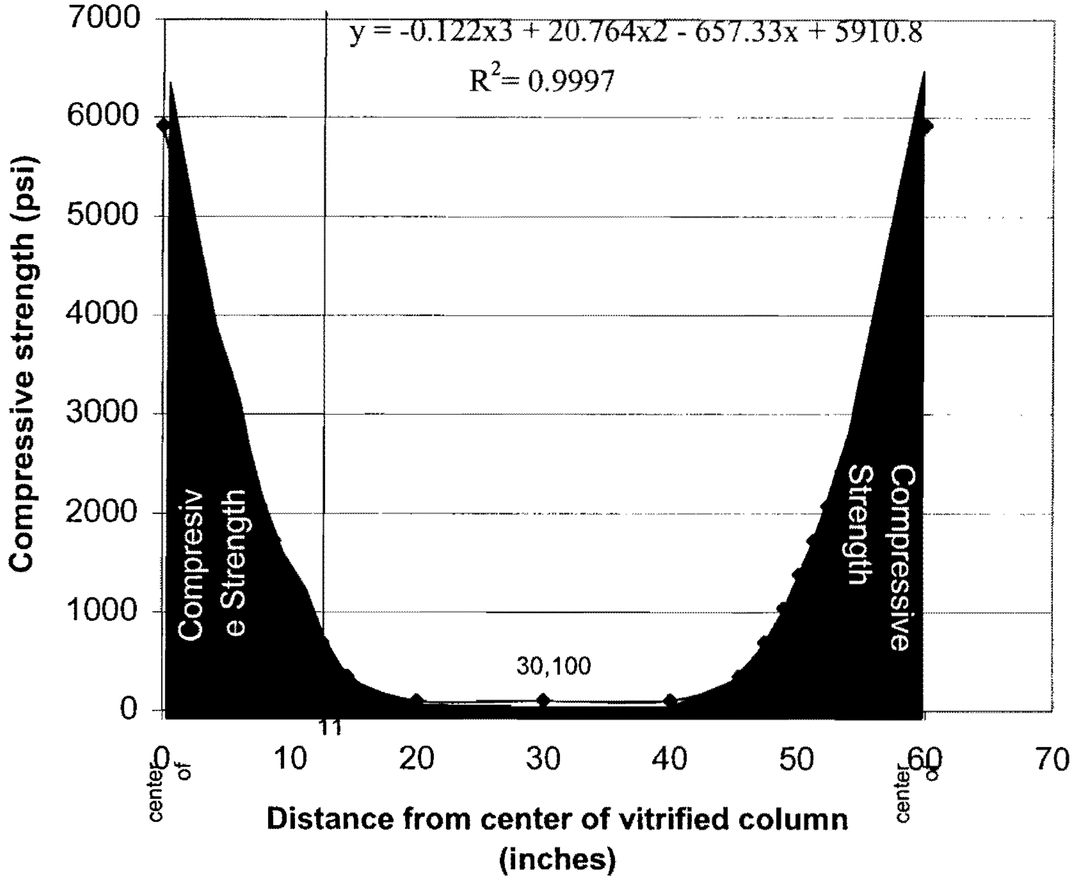

Figure 5.2 Estimated Compressive Strength Distribution Curve in Between 5 Feet Spaced Vitrified Columns (Compressive strength value is estimated to reach a constant value of 100psi after 20 inches away from a core. Equation displayed represents a third degree polynomial curve as a trendline to the first half of (0-30) compressive strength curve drawn by joining data points)

When the distance from the center of the vitrified columns is 30”, the compressive strength is assumed to be a constant value of 100 psi. Although it may not seem reasonable to obtain a strength of 100 psi at a temperature of 100 C as shown in Figures 1 and 2, it is strongly possible that the actual strength level at that region is even going to be far over 100 psi level due to the following three factors.

a) There are going to be no barrels on site. During the testing process, soils were vitrified inside barrels, which actually act as barriers in front of dynamic molten media, preventing it from spreading. On the site, molten soil and ionized - melting gas would diffuse more into the soil through voids, heating a larger zone, and causing a more uniform temperature, and consequently more strength distribution.
b) Shear strength, and subsequently compressive strength of soils between columns, will increase due to the soil arching effect.
c) If two pieces of vitrification equipment are operated simultaneously in Joule-heating mode, current would be transferred from one CGAM to another, heating and melting soils in between, and increasing their strengths.

To calculate the average compressive strength value between the two vitrified column centers, the total area under the above curve must be calculated and then divided by the total length of 60 inches.

The area under the curve consists of two symmetrically equal areas on the sides, and a rectangle under 100 psi value in the center between 20-40 inches.

For the best approximation of the value of each symmetrical area, integral of trendline's equation from 0 to 20 inches is shown in the following equation.

$$\int_0^{20} -0.122x^3 + 20.764x^2 - 657.33x + 5910.8\, dx$$

$$= -0.122x^4/4 + 20.764x^3/3 - 657.33x^2/2 + 5910.8x \Big|_0^{20}$$

The rectangular area in the center = (40 inches – 20 inches) × 100 psi = 2,000 inches-psi.

Total area under the curve = 37,241 + 2,000 + 37,241 = 76,482 inches-psi

Average compressive strength in a stabilized area by 5-feet spaced vitrified columns = 76,482 inches-psi / 60 inches = 1,275 psi.

5.6.3.2 Compressive Strength in Grids of Soil and 10-Ft Spaced Vitrified Colums

The same strength distribution curve in Figure 2 is estimated with an addition of 5 feet more distance with a 100 psi constant strength value. Simply taking the average estimated strength value for 5-ft spacings, and 100 psi strength value of additional 5-f t will give us the average value for 10-ft spacings.

Average compressive strength in a stabilized area by 10-feet spaced vitrified columns = 688 psi.

5.6.3.3 Compressive Strength in Grids of Soil and 20-Ft Spaced Vitrified Colums

This time an average of estimated strength value for 10-ft spacings, and the 100 psi strength value of additional 10-ft is going to give us the average value for 20-ft spacings.

Average compressive strength in a stabilized area by 20-feet spaced vitrified columns = 394 psi.

5.6.3.4 Compressive Strength in Clays Stabilized by Spaced Vitrified Columns

Approximation for average compressive strength estimation in a grid area with vitrified columns can also be applied to clays. The average compressive strength of vitrified clays has been estimated to 3,104 psi. The ratio of this strength to the overall estimated average strength of 3,054 psi is also valid for strengths for 5-ft spaced vitrified columns. Based upon that, compressive strength values of clays with vitrified columns are calculated as follows.

Estimated Strength of Clays with 5, 10, and 20-Ft Vitrified Columns

5-ft spaced vitrified columns = (3,104/3,054) * 1,275 = 1,296 psi.
10-ft spaced vitrified columns = (1,296 + 100) / 2 = 698 psi.
20-ft spaced vitrified columns = (698 + 100) / 2 = 399 psi.

5.6.3.5 Compressive Strength in Silts Stabilized by Spaced Vitrified Columns

Applying the ratio of above estimated compressive strength of silts (3,581 psi) to the general average estimation of 3,054 psi results in the following.

Estimated strength of silts with 5-ft spaced vitrified columns = (3,581/3,054) × 1,275= 1,495 psi.
Estimated strength of silts with 10-ft spaced vitrified columns = (1,495 + 100) / 2 = 798 psi.
Estimated strength of silts with 20-ft spaced vitrified columns = (798 + 100) / 2 = 449 psi.

5.6.3.6 Compressive Strength in Sands Stabilized by Spaced Vitrified Columns

Applying the ratio of above estimated compressive strength of sands (1,653psi) to the general average estimation of 3,054 psi results in the following.

Estimated strength of sands with 5-ft spaced vitrified columns = (1,653/3,054) × 1,275 = 690 psi.
Estimated strength of sands with 10-ft spaced vitrified columns = (690 + 100) / 2 = 395 psi.
Estimated strength of sands with 20-ft spaced vitrified columns = (395 + 100) / 2 = 248 psi.

5.6.4 Unit Cost of Vitrification

In order to do a unit cost estimation of an on-site vitrification operation, cost of consumable sources such as energy, fuel, graphite electrode and steel casing are taken into account as well as appropriate rental rates for labor and equipment.

Using the vitrification test data from Montana as shown in Table 6, an average duration to vitrify an one barrel amount of soil is estimated as follows

Volume of vitrified soil in a barrel with 33" length, 22" diameter (cy) = (π× 11" ×11" × 33") / 46,656 in^3/y^3 = 0.269 cy. ⇒ 0.25 cy of vitrified mass is assumed considering outer partially vitrified zones.

If 1 foot deep columns are vitrified in practice, the vitrified volume at the end of 1 operation yields 0.25 × 12 / 33 = 0.091 cy.

Average duration of 10 tested barrels for one operation of vitrifying 0.25 cy = 93.5 min.

The duration estimated to vitrify a 1-foot deep column (0.091 cy) in 1 operation = 93.5 × 12 / 33 = 34 min. Together with the setting up time, 45 min. of duration is estimated for each operation of vitrifying 0.091 cy soil.

With regard to these numbers, in an 8-hour day:

480 min / 45 min/oper. ≅ 11 operations, and 11 operations * 0.091 cy/operation = 1 cy
⇒ 1 cy/day of soil is estimated to be vitrified.

An item-by-item cost estimation for 1 cy of vitrification in an 8 hour-day is as follows:

5.6.4.1 Cost of Vitrification Equipment and Carrier

The proposed vitrification technology incorporates the use of a concentric graphite arc melter (CGAM). Rental rate of a truck mounted CGAM with its related equipment such as a manipulator arm is assumed to be equivalent to the rental rate of a truck mounted auger equipment.

--Auger equipment - hydraulic powered 3-point hitch ⇒ \$15.44/day - from K-III blue book (K-III Directory Corporation, 1997), section – 'Drilling', pg. 8-2 – Texas adjustment factor applied.
--Carrier –diesel powered 4*2 truck with max GVW of 35,000 lbs, and engine-power of 265 HP ⇒ \$155.38/day (K-III blue book, section - 'Trucks', pg. 20-6 – Texas adjustment factor applied).

Total estimated daily cost of truck-mounted vitrification equipment = \$170.82.

5.6.4.2 Cost of Power Supplier

Montec As. employs a 1.0 MW Rapid Electric SCR controlled unit and a 0.5 MW Robicon frequency modulated unit.
--Estimated purchase price of an average power supplier is \$25,000. 7 years of life at a 2000 hrs/year usage is also estimated.
--Estimated daily ownership-cost of power-supplier = [\$25,000 / (7 yr * 2000 hr/yr)] * 8hr/day = \$14.29.

5.6.4.3 Cost of Portable Generator

--From the vitrifying-test data average power utilization for vitrification is as follows.
(95 + 97.1 + 93 + 84 + 91 + 99 + 89 + 106 + 104 + 114) / 10 = 97.2 kW
--Therefore, a 110 kW generator is suitable for this application is \$60.62/day (K-III blue book, section – 'Motors & Generators', pg. 11-8 – Texas adjustment factor applied).

5.6.4.4 Cost of Operator

--An operator hired to operate the equipment is estimated at \$7.5/hr.
--Daily estimated cost to hire an operator = 7.5 * 8 = \$60.

5.6.4.5 Cost of Energy Consumption

--Estimated price of commercial electricity is \$0.05/kW-hr, while the estimated price of electricity from generator is \$0.1/kW-hr.
--From the vitrifying-test data, average energy usage for vitrification of 0.25 cy = (104.6 + 62 + 118.4 + 124.2 + 137.2 + 127.5 + 120.7 + 122.2 + 124.4 + 129.8) / 10 = 117.1 kW-hr
--Average energy consumption for 1 cy of vitrification = 4 * 117.1 = 468.4 kW-hr
If commercial electricity were used, the estimated daily energy cost would be: 468.4 kW-hr × \$0.05/kW-hr = \$23.42.
--By usage of electricity from generator, the estimated daily energy cost is = 468.4 kW-hr * \$0.1/kW-hr = \$46.84.

5.6.4.6 Cost of Fuel Consumption

Caterpillar Performance Handbook shows that hourly fuel consumption of construction equipment with the same engine of a 110 kW generator is 1.5 – 2.5 gallons (Caterpillar Inc., 1998). A generator is estimated to consume less diesel than construction equipment, therefore the lower limit of 1.5 gallons/hour of that range is estimated to be the fuel consumption rate of the generator.

--Estimated price of diesel = \$1.1 / gallon.
--Estimated daily cost of fuel consumption = \$1.1/gallon × 1.5 gallon/hr × 8 hr = \$13.2

5.6.4.7 Cost of Graphite Electrode and Steel Casing Consumption

Following information has been obtained from Farrar at Montec As. (1999):

--Outer diameter of the outer electrode = 8"

--Inner diameter of the outer electrode = 5".

--Diameter of inner electrode (rod) = 3".

--Density of graphite = 2,2 gr/cm^3 = 0.07948 lb/in^3.

--Estimated price of a 72" long pair = $650.

--Based upon the above information, estimated price of graphite electrode per weight is found as follows:

-Volume of 72" long outer electrode = 2205.4 in^3.

-Volume of 72" long inner electrode = 508.9 in^3.

-Total volume of a 72" long pair of electrodes = 2714.3 in^3.

-Weight of a pair = 2714.3in^3 * 0.07948 lb/in^3 = 215.7 lbs.

-Price of electrode per lb = $650 / 215.7lbs = $3.01/lb.

--Average weight of graphite electrode consumption is calculated from the test results in Montana as follows.

Average graphite electrode consumption in an operation of vitrifying 33" depth (both outer and inner electrodes - an average of 0.2 lb deducted from trimmed inner electrode weights) = (8.5 + 8.1 + 9.3 + 8 + 8.9 + 5.6 + 11.9 * 4 + 1.2 + 1.4 + 1.4 + 2.1 + 1.6 + 1.6 + 2.3 × 4) / 20 = 5.725 lbs

Avg. estimated graphite electrode consumption in a proposed 1-ft operation = (12 / 33) × 5.725 = 2.08 lbs.

If 11 operations/day is proposed, daily estimated graphite consumption = 2.08 × 11 = 22.88 lbs.

Estimated cost of daily graphite electrode consumption = 22.88lbs × $3.01/lb = $68.87.

Based upon information from Montec As., the estimated price of steel casing is $10/ft. If it is assumed that at 25% of the cases steel casing won't be necessary due to the characteristics of the soil to be vitrified, the average cost of steel casing comes up to be: 75% of $10/ft = $7.5/ft.

At 11 operations of 1-ft deep, 11 feet of steel casing will be consumed.

Estimated cost of daily steel casing consumption = $7.5/ft × 11ft = $82.5.

Total estimated daily cost of graphite electrode and steel casing consumption = 82.5 + 68.87 = $151.37.

5.6.4.8 Total Cost of Vitrifying 1-cu.yd. Zone

Sum of the costs found will give the cost of purely vitrifying a 1-cy zone.
The estimated cost of purely vitrifying a 1-cy zone = 170.82 + 14.29 + 60.62 + 60 + 46.84 + 13.2 + 151.37 = $517.14.

Unit Cost of Soil Stabilization by 5-ft Spaced Vitrified Columns

By forming a grid area with 5-ft spaced, 1-foot deep vitrified columns, the volume of stabilized zone at the end of each day with an estimated operation of 11 columns will yield the following.

$11 \times 5 \text{ ft} \times 5 \text{ ft} \times 1 \text{ ft} = 275 \text{ ft}^3 = 10.18 \text{ yd}^3$

The estimated cost of stabilizing 1-cy zone by 5-ft spaced, 1-ft deep vitrified columns = $517.14 / 10.18 = $50.8.

Unit Cost of Soil Stabilization by 10-ft Spaced Vitrified Columns

Forming a grid area with 10-ft spaced, 1-foot deep vitrified columns, at the end of each day with an estimated operation of 11 columns, stabilizes a zone with a volume of:

$11 \times 10 \text{ ft} \times 10 \text{ ft} \times 1 \text{ ft} = 1100 \text{ ft}^3 = 40.74 \text{ yd}^3$.

The estimated cost of stabilizing 1-cy zone by 10-ft spaced, 1-ft deep vitrified columns = $517.14 / 40.74 = $12.694.

Unit Cost of Soil Stabilization by 20-ft Spaced Vitrified Columns

If the same process of forming grid is done with 20-ft apart columns this time, the stabilized volume at the end of a day with 11 operations will yield the following.

$11 \times 20 \text{ ft} \times 20 \text{ ft} \times 1 \text{ ft} = 4400 \text{ ft}^3 = 162.96 \text{ yd}^3$.

Estimated cost of stabilizing 1-cy zone by 20-ft spaced, 1-ft deep vitrified columns = $517.14 / 162.96 = $3.173.

5.7 Comparison Between Different Stabilization Alternatives

5.7.1 Comparison Analysis I: Defender-Challenger Analysis Utilizing Cost Index Numbers (CIN) of Stabilization Methods

5.7.1.1 Cost Index Number (CIN) Calculations

CIN (cost index number) is a concept used to display relative cost values of each method. The most common applications of each method are chosen while comparing their costs for clays, silts and sands. These common and reasonable applications assumed, and costs of stabilization methods using them are detailed in the following paragraphs.

Lime stabilization with a 3% lime addition for all clays, silts and sands is assumed to be the most common application. Unit cost for all clays, silts and soils with this application is $5.285/cy of stabilization.

Cement stabilization with a 13% cement addition for clays, 10% cement addition for silts, and 3% addition for sands are assumed to be the most common applications. Related unit cost for sands, silts, and clays respectively are $4.695/cy, $15.65/cy, and $20.345/cy.

Lime-fly ash stabilization with a 15% total admixture addition is assumed to be the common application. Related cost is $9.175/cy.

Stabilization by 10-ft spaced, 1-ft deep vitrified columns is taken to be the most reasonable application. Related cost is $12.694.

Cost Index Numbers for Stabilization of Sands

The least amount among costs for sand-stabilization is the cost of cement stabilization ⇒

CIN for cement stabilization of sands = 1

CIN for lime stabilization of sands = 5.285 / 4.695 = 1.126

CIN for lime-fly ash stabilization of sands = 9.175 / 4.695 = 1.954

CIN for stabilization of sands by vitrification = 12.694 / 4.695 = 2.704

Cost Index Numbers for Stabilization of Silts

The least amount among costs for silt-stabilization is the cost of lime stabilization ⇒ CIN for lime stabilization of silts = 1

CIN for cement stabilization of silts = 15.65 / 5.285 = 2.961

CIN for stabilization of silts by vitrification = 12.694 / 5.285 = 2.402

Cost Index Numbers for Stabilization of Clays

The least amount among costs for clay-stabilization is the cost of lime stabilization ⇒

CIN for lime stabilization of clays = 1

CIN for cement stabilization of clays = 20.345 / 5.285 = 3.85

CIN for lime-fly ash stabilization of clays = 9.175 / 5.285 = 1.736

CIN for stabilization of clays by vitrification = 12.694 / 5.285 = 2.402

5.7.1.2 Defender-Challenger Analysis

Defender-challenger analysis is a method used to compare various stabilization alternatives considering both relative costs and quality gains. This method enables comparing alternatives in terms of cost and increase in quality. Its aim is making a healthy decision based on both quantitative and qualitative aspects of alternatives. The defender- challenger method is performed by comparing cost index numbers and compressive strength gains of alternatives to one another incrementally, and utilizing the best one in terms of cost and strengths.

Decision of Best Alternative Among Sand-Stabilization Methods by Defender-Challenger Analysis

Started by comparing cement and lime stabilization of sands – cement stabilization is the defender and lime is the challenger.

Table 5.9 Defender- Challenger Analysis For Sands: Cement vs. Lime

Stabilization	CIN	Psi	ΔCIN	ΔPsi
Cement	1	380 *		
Lime	1.126	220	12.6%	- 42.1%

*** Compressive strength increase is taken by subtracting the average value of 20 psi estimated for compressive strength of natural soils, from the compressive strength values estimated after stabilization.**

Cement stabilization remains the defender since despite a 12.6% cost increase, lime stabilization still supplies 42.1% less strength. Cement stabilization is the defender, and lime-fly ash is now the challenger.

Table 5.10 Defender- Challenger Analysis For Sands: Cement vs. Lime Fly-Ash

Stabilization	CIN	Psi	ΔCIN	ΔPsi
Cement	1	380		
Lime-Fly Ash	1.954	380	95.4%	0%

Cement stabilization still remains the defender since lime-fly ash stabilization displays no additional strength gain despite the 95.4% cost increase. Vitrification is now the challenger.

Table 5.11 Defender-Challenger Analysis For Sands: Cement vs. Vitrification0

Stabilization	CIN	Psi	ΔCIN	ΔPsi
Cement	1	380		
Vitrification	2.704	375	170%	- 1.3%

Vitrification is not good enough to replace cement stabilization for stabilizing sands since cost increases and strength decreases.

Cement Stabilization is decided to be the best alternative for stabilization of sands because it proposes the maximum amount of compressive strength increase for unit cost.

Decision of Best Alternative Among Clay-Stabilization Methods by Defender-Challenger Analysis

The method begins by comparing lime and cement stabilization of clays – lime stabilization is the defender, and cement is the challenger.

Table 5.12 Defender-Challenger Analysis For Clays: Lime vs. Cement

Stabilization	CIN	Psi	ΔCIN	ΔPsi
Lime	1	165 *		
Cement	3.85	430	285%	161%

*** Compressive strength <u>increase</u> is taken by subtracting the average value of 20 psi estimated for com pressive strength of natural soils, from the compressive strength values estimated after stabilization.**

Lime stabilization is still the defender. Despite a 285% cost increase, cement stabilization displayed only a 161% strength increase over lime stabilization. Lime stabilization remains the defender, and lime-fly ash is the challenger.

Table 5.13 Defender-Challenger Analysis For Clays: Lime vs. Lime-Fly Ash

Stabilization	CIN	Psi	ΔCIN	ΔPsi
Lime	1	165		
Lime-Fly Ash	1.736	443	73.6%	168%

The lime-fly ash stabilization becomes the defender because it has a higher strength increase. Vitrification is now the challenger.

Table 5.14 Defender-Challenger Analysis For Clays: Lime- Fly Ash vs. Vitrification

Stabilization	CIN	Psi	ΔCIN	ΔPsi
Lime – Fly Ash	1.736	443		
Vitrification	2.402	678	38.4%	53.1%

Vitrification is better since it increases the strength by 53.1% with a 38.4% cost increase. Vitrification is decided to be the best alternative for stabilization of clays, because it proposes the maximum amount of compressive strength increase for unit cost.

Decision of Best Alternative Among Silt-Stabilization Methods by Defender-Challenger Analysis

Again, the method begins by comparing lime and cement stabilization of clays. Lime stabilization is the defender, and cement is the challenger.

Table 5.15 Defender-Challenger Analysis For Silts: Lime vs. Cement

Stabilization	**CIN**	**Psi**	**ΔCIN**	**ΔPsi**
Lime	1	77		
Cement	2.961	580	196.1%	653.2%

*** Compressive strength increase is taken by subtracting the average value of 20 psi estimated for compressive strength of natural soils, from the compressive strength values estimated after stabilization.**

Cement stabilization is still the defender because there is a 196.1% cost increase. It displayed a huge 653.2% strength increase over lime stabilization. Cement stabilization is defender, and vitrification is the challenger (no data available for lime-fly ash stabilization of silts).

Table 5.16 Defender-Challenger Analysis For Silts: Cement vs. Vitrification

Stabilization	**CIN**	**Psi**	**ΔCIN**	**ΔPsi**
Cement	2.961	580		
Vitrification	2.402	778	-18.9%	34.1%

Vitrification is a far better alternative than cement-stabilization because it supplies 34.1% more strength for less cost.

Vitrification is decided to be significantly the best alternative for stabilization of silts, as because it proposes the maximum amount of compressive strength increase for unit cost.

5.7.2 Comparison Analysis II: Comparison of 'Cost vs. Strength Gain' Curves of Stabilization Methods

Costs of different applications of stabilization methods, and strengths obtained by them are determined in above sections 5.1 to 5.4. These data are utilized to draw cost vs. strength gain curves for each type of soil (sand, silt, and clay) for visual comparison of stabilization methods. The economically efficient methods for stabilizing each type of soil are seen from these curves.

5.7.2.1 Cost vs. Compressive Strength Curves for Sands

Costs and strengths after treatment of sands associated with different applications of stabilization methods were determined in above sections 5.1 to 5.4. These applications were: 3%, 5% and 7% lime additions for lime stabilization; 3%, 7%, and 11% cement additions for cement stabilization; 15%, and 20% lime-fly ash additions (lime to fly ash ratio of 1 to 4) for lime-fly ash stabilization; and complete vitrification, 5-ft spaced, 10-ft spaced and 20-ft spaced

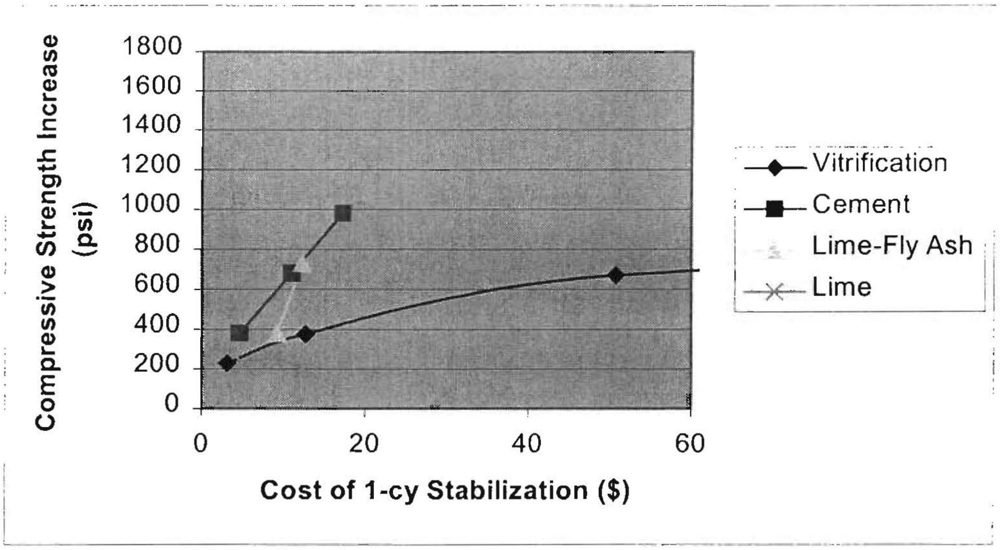

* Compressive strength increase is taken by subtracting the average value of 20 psi estimated for compressive strength of natural soils, from the compressive strength values estimated after stabilization.

Figure 5.3 Cost vs. Strength Curves of Stabilization Methods for Sands.

Cost and strength data associated with: 3%, 5% and 7% lime additions for lime stabilization; 9%, 13%, and 16% cement additions for cement stabilization; 9%, 15% and 20% lime-fly ash additions (lime to fly ash ratio of 1 to 4) for lime-fly ash stabilization; and complete vitrification, 5-ft spaced, 10-ft spaced and 20-ft spaced vitrified columns for in-situ vitrification were utilized for locating points and drawing 'cost vs. compressive strength' curves of stabilization methods for clays.

5.7.2.2 Cost vs. Compressive Strength Curves for Clays

This time the vitrification curve is seen on top of other curves in Figure 5.4, meaning in-situ vitrification is the stabilization method that gives highest strength for same costs.

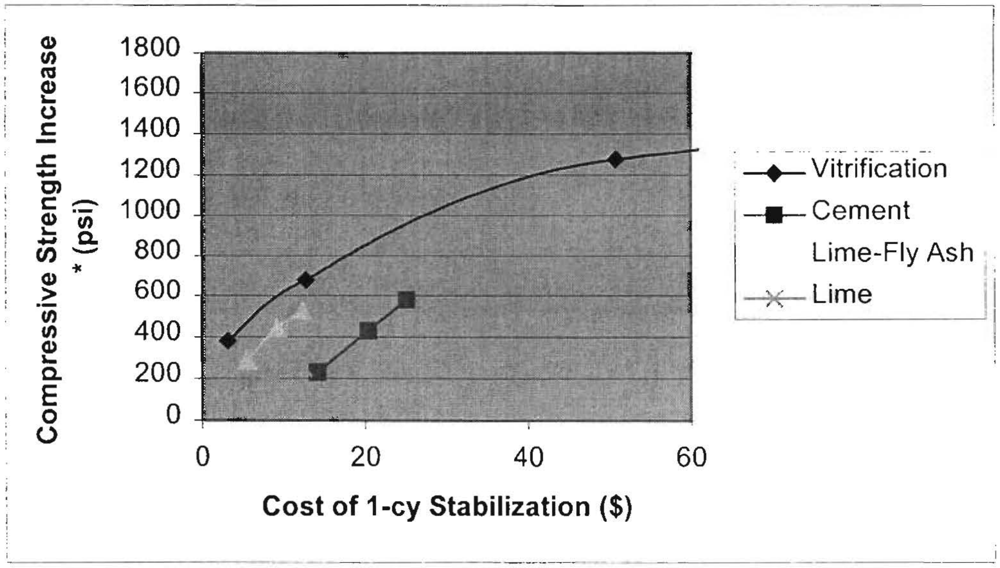

Figure 5.4 Cost vs. Strength Curves of Stabilization Methods for Clays.

5.7.2.3 Cost vs. Compressive Strength Curves for Silts

Points used drawing these 'cost vs. compressive strength' curves for stabilizing silts were determined by strengths and costs of: 3%, 5% and 7% lime additions for lime stabilization; 7%, 10%, and 13% cement additions for cement stabilization; and complete vitrification, 5-ft spaced, 10-ft spaced and 20-ft spaced vitrified columns for in-situ vitrification (no data were available for stabilizing silts with lime-fly ash stabilization).

Again, vitrification curve is seen on top of other curves in Figure 5.5, showing that in-situ vitrification is the most economically efficient method for stabilizing silts over lime and cement stabilizations.

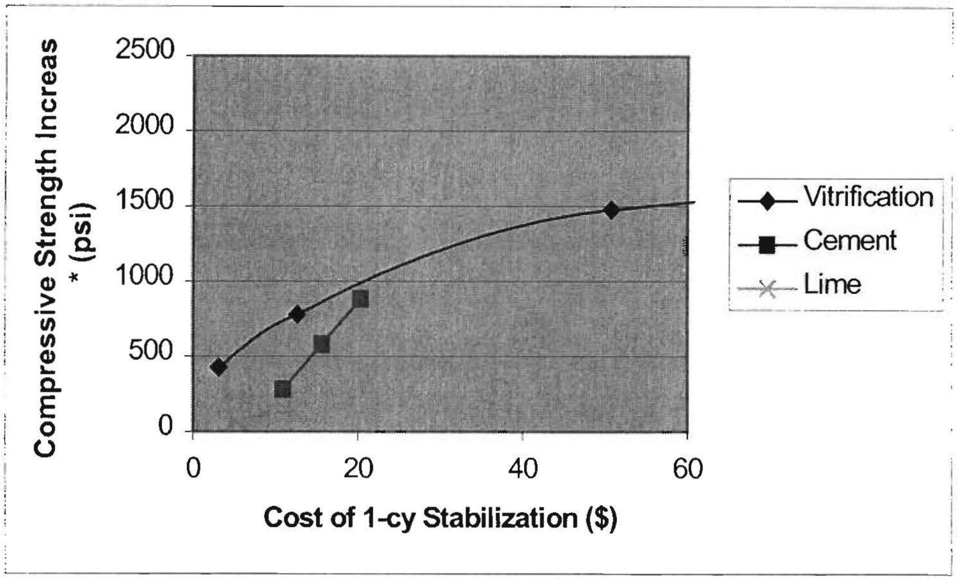

Figure 5.5 Cost vs. Strength Curves of Stabilization Methods for Silts.

5.8 Conclusion

Both comparison analyses in section 5.5 pointed in-situ vitrification as an economically superior method for stabilizing clays and sands. As for the sand stabilization, vitrification did not seem to be a better method than cement and lime-fly ash stabilizations.

It has to be kept in mind that, only one sand sample, and only two states (compacted and loose) of one silt sample was vitrified and tested. The average stabilization performance of vitrification on sands and silts might differ with the increasing number of sand and silt testings.

Forming a grid of vitrified columns using CGAM method could be a feasible means of subgrade stabilization. First comparison analysis, defender-challenger analysis, showed that although it is somewhat more expensive ($\$12.694/y^3$), stabilizing silts or clays by 10-ft spaced vitrified columns provide much more strength (678 psi for clays, and 778 psi for sands) than common applications of other methods. In other words, more strength is estimated to be gained per unit cost of stabilization by forming a grid of 10-ft spaced vitrified columns, than common applications of other conventional stabilization methods. Stabilization by 20-ft spaced vitrified columns is estimated to be cheaper ($\$3.173/y^3$) and still resulting in competitive strengths (399 psi for clays, 449 psi for silts, and 248 psi for sands) of the stabilized region. These two in-situ vitrification applications, forming 10-ft and 20-ft spaced vitrified columns, are estimated to give adequate levels of strength to subgrades for reasonable costs, and might be feasible means of subgrade stabilization.

Another important point is that the average estimated strength values of stabilized soils by vitrified columns with varying intervals (5,10 and 20 ft.) are theoretical values, and are not very much dependable. The true strength values are to be determined by field-testing. There are several reasons to be optimistic about the actual performance of vitrified columns, such as:

- soil arching effect between vitrified columns,
- chances of better diffusion of melt on field than in the lab,
- chances of obtaining better stabilization quality by operating CGAM in 'joule heating' mode.

To what extent above factors are going to be effective on the final stabilization quality are to be better understood after the field testing.

CHAPTER VI
Conclusions and Recommendations

6.1 Conclusions

The primary objective of the first phase of this research project was to perform a preliminary evaluation of CGAM vitrification technology as a viable tool for use in subgrade repair and stabilization. The results obtained show that the method can be used effectively for a broad range of soils conditions. Vitrification was successfully achieved for sands, silts and clays with varying degrees of plasticity. Results also demonstrated that vitrification can be achieved under relatively dry as well as saturation conditions. Furthermore, the vitrified products proved to be extremely stable against water intrusion. None of the vitrified products showed any signs of softening, disintegration, swelling/shrinking even after prolonged soaking in water.

The specific conclusions drawn from this research are listed below.

a) Vitrified soils are strong and elastic. Their strength range is far above strength ranges of end products of other conventional stabilization methods. On the average, their strengths are around a typical concrete's strength, and their elastic moduli are less than a typical concrete's modulus of elasticity, which means they can absorb much more energy than concrete. The following figure (6.1) showing stress and strain values of a typical concrete (Mindess and Young, 1981), a vitrified El Paso high sulfate clay sample, and a vitrified Dallas clay demonstrates strength, elasticity (slopes of straight line portions), and energy absorption (areas under curves) level differences of vitrified soils from concrete. It also demonstrates variability in between vitrified soils.

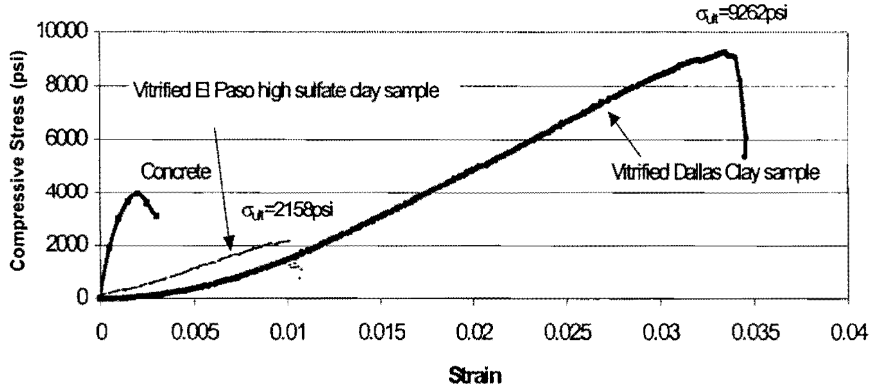

Figure 6.1 Stress-Strain Comparisons of a Typical Concrete and Two Vitrified Soil Samples

b) Mechanical properties vary among vitrified materials. They even vary among the specimens from the same vitrified soil. Type of soil, condition of soil (saturation, compaction), amount of power application, type of power application (high voltage-low current, or vice versa), and temperature profile (stronger material at the inner core where the highest temperatures were reached) might be considered as determinants of this variability.

c) Mechanical properties of vitrified clay samples and vitrified silt sample (Childress silt) are close. On the other hand, vitrified sand sample (Lubbock sand) has lower unit weight, higher porosity, and less strength. Vitrification might be more effective on improving clays and silts, and less effective on improving sands.

d) Vitrification caused less improvement of El Paso clay compared to other clay samples. This fact might be due to El Paso clay's high sulfate content. If El Paso clay is saturated and then vitrified, a better quality material (stronger, denser) is obtained, though. Vitrification might be less effective on improving high-sulfate content soils.

e) Both saturated Dallas clay and saturated El Paso clay samples showed a better improvement after vitrification than Dallas and El Paso clay samples with natural water contents. Saturation might be a way of obtaining stronger material. On the other hand, this might also be due to the fact that testers in Montec Ass. had to increase voltage while vitrifying saturated soil to which high current could not be applied. Thus, they had been able to keep power consumption in constant levels. High voltage might also be responsible for stronger vitrified material.

f) Loose Childress silt sample showed a better improvement after vitrification than compacted Childress silt sample. Vitrification might be less effective on improving compacted soils.

g) Surrounding the inner vitrified cores were outer shells that consisted of brick-like materials. These brick-like materials are also improved forms of soils and are useful subgrade material.

h) Water does not cause softening or disintegration of either vitrified material or brick-like material from outer shells.

i) Complete vitrification of an area is not a feasible means of subgrade stabilization as it would be expensive and giving too much higher quality of subgrade than required. It can be a perfect solution to repairing certain localized subgrade failures, though. Forming a grid of vitrified columns using CGAM method could be a more feasible means of subgrade stabilization. Cost and quality of stabilization would depend on length of spacings between these columns. Stabilization by 10 ft spaced vitrified columns is estimated to result in a much more stronger subgrade than other conventional stabilization methods (lime, cement, and lime-fly ash stabilizations), but it is also estimated to be more expensive than them. On the other hand, stabilization by 20 ft spaced vitrified columns is estimated to be cheaper and still resulting in competitive strengths. These two in-situ vitrification applications, forming 10-ft and 20-ft spaced vitrified columns, are estimated to give adequate levels of strength to subgrades for reasonable costs.

j) As illustrated in Figures 5.4 and 5.5 of Chapter V, for stabilizing silts and clays, strength obtained per unit amount of money spent is estimated to be more for all stabilization applications using CGAM method (complete vitrification, 5 ft, 10 ft, and 20 ft columns) than other conventional methods. However, as illustrated in Figure 6.4 of Chapter VI, the situation is reverse for stabilizing sands. In other words, stabilizing silts and stabilizing clays by in-situ vitrification using CGAM method are more economic than other conventional stabilization methods. On the other hand, stabilizing sands by in-situ vitrification using CGAM method is less economic.

k) The true strength values of subgrades stabilized by vitrified column grids using CGAM method might come out to be more than what was calculated in Chapter V. There are several reasons for being optimistic about actual stabilization performance of vitrified column grids by CGAM, such as: 1) soil arching effect between vitrified columns, 2) chances of better diffusion of melt on field than in the lab, 3) chances of obtaining better stabilization quality by operating CGAM in 'joule heating' mode. To what extent these factors are going to be effective on the final stabilization quality are going to be understood after the field testing of proposed CGAM in-situ vitrification process.

6.2 Recommendations for Future Research

This research shows that the innovative in-situ vitrification process by CGAM method is a promising means of repairing and stabilizing subgrades, and it is worth conducting further research on. Areas of future research can be decided in light of findings from this research. Effect of vitrification on different soil types, effect of vitrification on soils with different saturation and compaction conditions, and availability and use of brick-like material found on the outer shells of vitrified material are recommended topics for future research.

Only one sand sample (Lubbock sand), and only two states (compacted and loose forms of Childress silt) of one silt sample have been vitrified and tested. More silt and sand samples should be studied to better question effect of vitrification on improvement of sands and silts.

Again, only two samples of the same kind (El Paso and Dallas fat clays) were tested to study the effect of saturation, and only one sample (Childress silt) was tested to study the effect of compaction on vitrification. More samples have to be studied to further verify current findings, especially the surprising finding about compaction's reverse effect on vitrification quality.

Brick-like materials that were obtained on the outer shells of vitrification materials can be satisfactory subgrade materials alone. Cost of obtaining brick-like materials rather than vitrified materials by CGAM method, and their qualities as subgrade materials should also be studied.

APPENDIX

Test Data Report

TEST DATA REPORT

Prepared for:

TEXAS TECH UNIVERSITY

SUBCONTRACT NUMBER 140G/0152-01

SUBGRADE REPAIR AND STABILIZATION USING IN-SITU VITRIFICATION

Prepared by:

Montec Associates, Inc.
P.O. Box 4182
Butte, Montana 59702-4182
(406) 494-5555

Lawrence C. Farrar, P.E.
Principal

David P. Haack
Senior Engineer

February 1999

Introduction

This report provides a summary of the test results and a description of methods used to evaluate the effect of robust in-situ vitrification process on densifying soils. The process has application for subgrade repair and stabilization of roadbeds and footings that underpin structures. An increase in soil density is achieved by melting indigenous soils into a rock-like mass using a high temperature energy source.

Results from 10 tests conducted on a range of Texas soil types, with varying moisture and density values, are presented. These data include process power and soil temperature measurements as it is heated then melted. Figures and pictures of the test assembly and of the resultant product are presented. Representative plots of time versus temperature during heat-up and cool-down are also included.

Technology Description

Montec's concept for subterranean stabilization incorporates the use of a concentric graphite arc melter (CGAM), which can be mounted as a mobile high-temperature heat source as shown in Figure 1. A key element that contributes to the effectiveness of this process is use of the CGAM as a high-temperature heat source. The CGAM consists of an inner graphite rod and an outer graphite annulus. Gas is flowed in the gap between these electrodes and an arc is struck between them, resulting in the formation of hot plasma-gas. The CGAM is essentially a non-transferred plasma torch which does not require cooling water and is fabricated from off-the-shelf graphite electrode materials. Because of its simplicity and robustness, the CGAM can be operated in a subterranean environment without concerns for excessive wear or damage to the electrodes in this harsh environment.

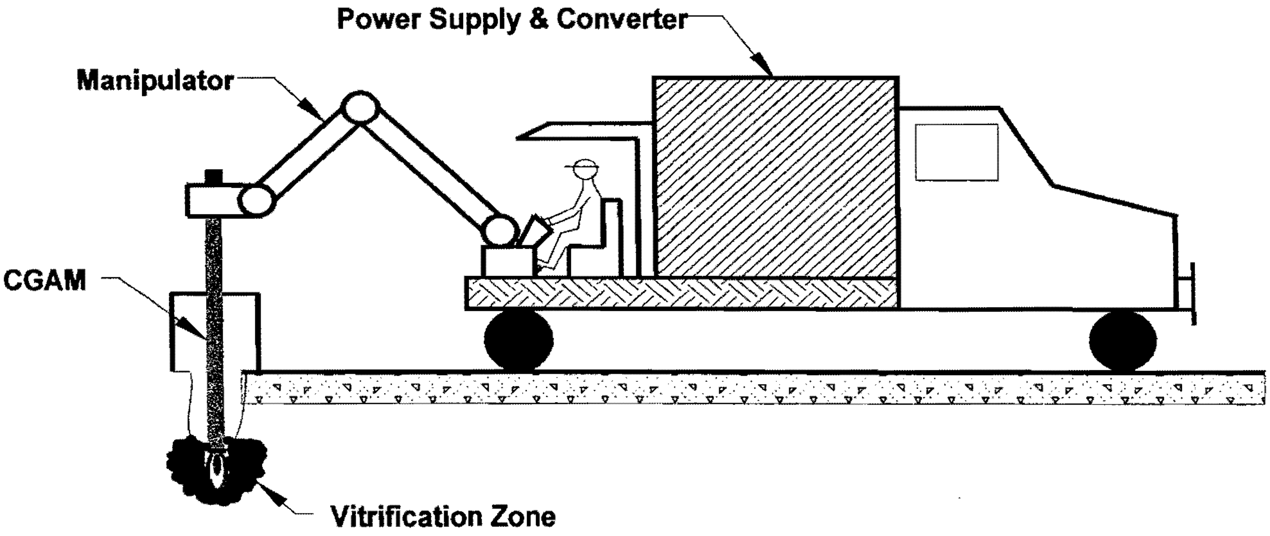

Figure 1. Conceptual diagram of CGAM mounted on field deployable subgrade repair and stabilization apparatus.

Subcontract Objectives

Montec's work statement specified the use of this technology to vitrify ten different samples and compositions of Texas soils. The work included instrumenting the process to measure soil temperature distribution, process power, process pressure and gas flows as a function of time. Our tasks include establishing soil melt development as a function of these process operating variables and soil conditions such as composition and moisture.

Pretest activities conducted at Montec included determining the soil moisture content, loading and compacting the soils into the test barrel and measuring the compacted soil density using the ASTM D1556 - 90, Standard Test Method for Density and Unit Weight of Soil in Place by the Sand-Cone Method as a guide.

Post-test activities include documentation of the results and presentation of the test data and analysis of the results.

Description of Soils

Table 1 summaries the soil properties (as tested moisture and density). Water was added to Barrel #'s 5 and 10 to saturate the soils and the soil was loaded in Barrel #7 as a loose file, without compaction.

Table 1. Summary of soils test matrix.

Barrel Number	Soil Origin and Type	Test Variables			Wet Density (lbm/ft^3)	Dry Density (lbm/ft^3)
		Soil Type	Moisture (%)	Compaction		
1	Hockley County High Plastic	√	13.47	Compacted	108.1	93.1
2	Hockley County Low Plastic	√	14.71	Compacted	110.9	92.4
3	Lynn County High Fragment Calicihe	√	11.26	Compacted	103.3	90.1
4	Brewster High Sulfate	√	16.14	Compacted	99.4	80.8
5	Brewster High Sulfate		37.91 (saturated)	Compacted	95.5	70.8
6	Childress	√	5.28	Compacted	99.1	78.1
7	Childress		5.59	Loose	71.6	67.0
8	Beaumont	√	33.56	Compacted	104.0	69.3
9	Dallas	√	23.45	Compacted	106.0	82.2
10	Dallas		47.99 (saturated)	Compacted	92.2	65.0

Soils Preparation Method

Figure 2 shows the test configuration, which included the placement of a 10 inch diameter schedule 10 pipe in the barrel and compacting the soil in the annular space between the pipe and barrel in 3 inch lifts using a pneumatic soil compactor. A matrix of thermocouples was placed in each barrel to monitor the soil heating and melting in the radial and axial position. The matrix thermocouple measurements, shown in Figure 2, provided a method to monitor the melt growth rate and shape during the test operation heat-up monitor the cool-down rate subsequent to the test operations.

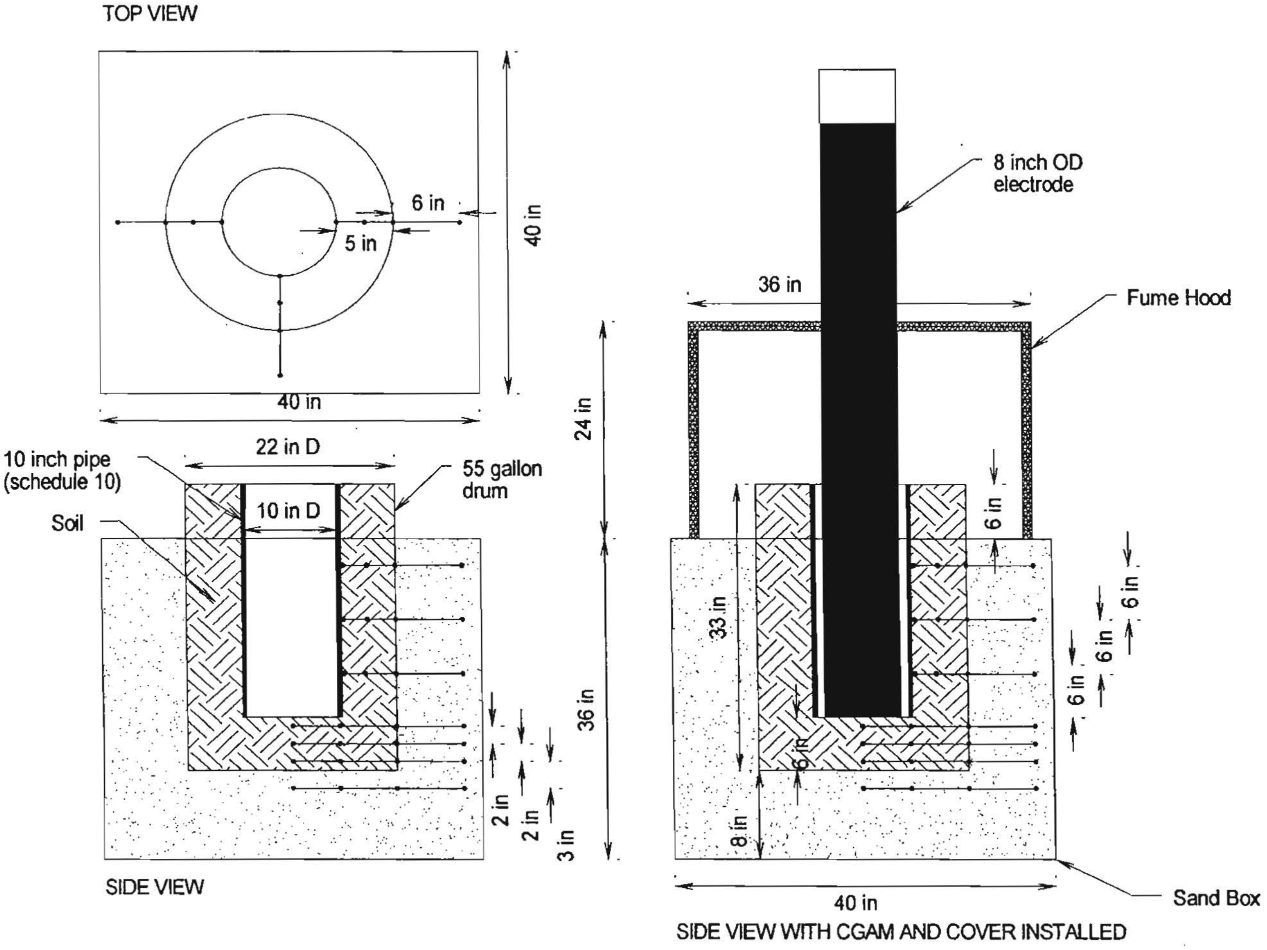

Figure 2. Schematic showing placement of test barrel in sand box, location of pipe for placement of CGAM into the barrel, configuration of CGAM, off gas cover and layout of thermocouple measurements.

Vitrification Equipment Description

Figure 3 shows a block diagram of the system used. A photograph of the test apparatus is provided in Figure 4. A light gauge metal hood, lined with a common ceramic insulation, was placed over the barrel to gather exhaust (water vapor and gases from organic material in the soil). The blue box in Figure 4 is the hood. The 8 inch diameter rod extending vertically out of the top of the hood is the CGAM electrode.

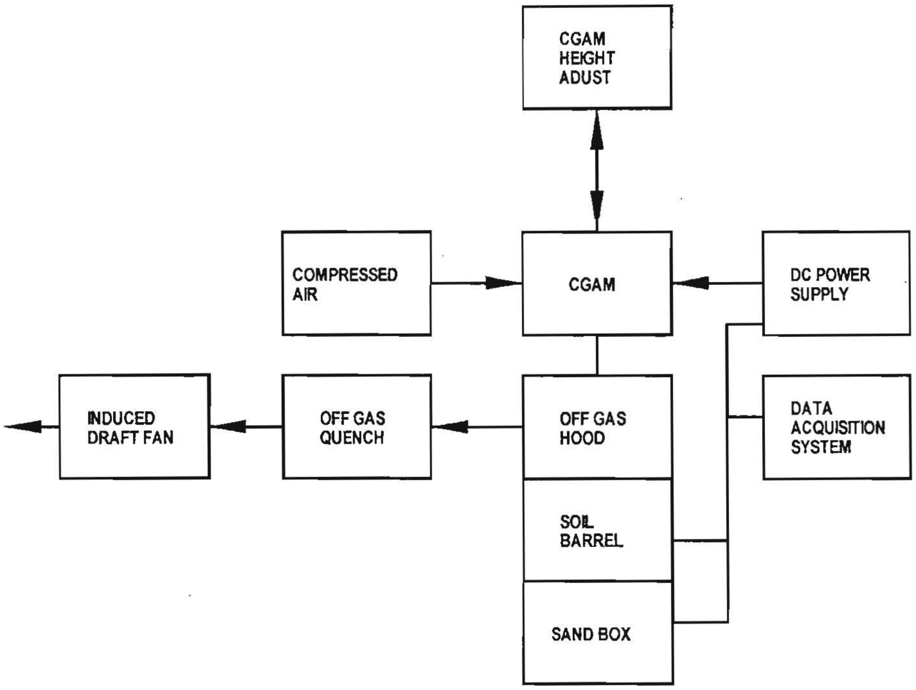

Figure 3. Block diagram of test configuration.

As shown in Figure 2 the prepared barrel was placed in a 40 inch the square box. The box was filled with sand to sustain a soil-like boundary around the barrel to provide a natural (slow) cooling rate for the vitrified material. The rate of the cooling affects the mechanical nature and integrity of the vitrified mass as it cools. Therefore, it is important to provide a thermal interface to the cooling melt close to its natural

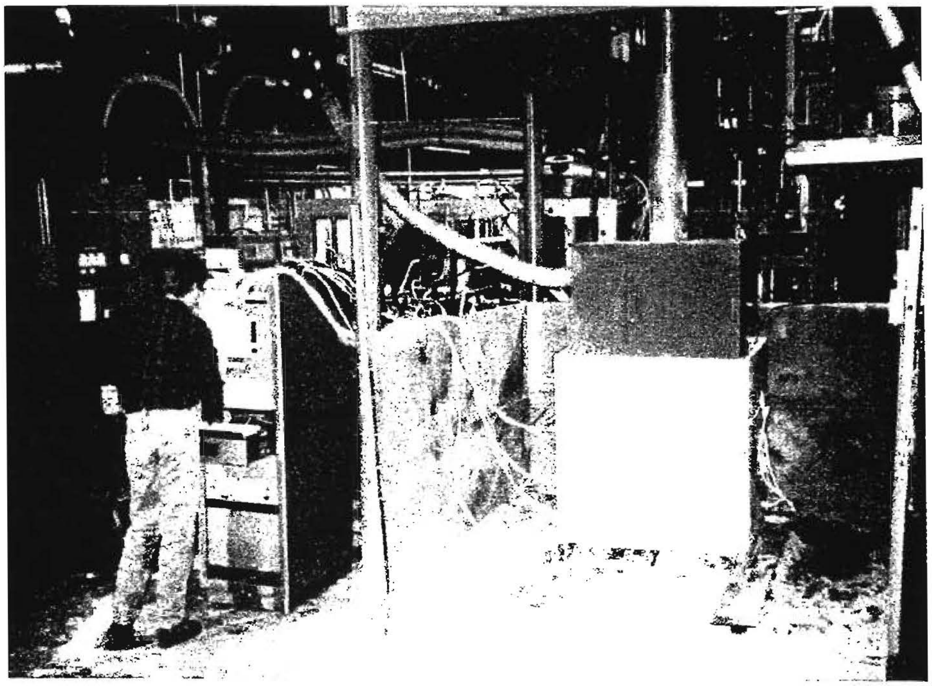

Figure 4. Photograph showing test configuration.

environment. Thermo-couples were placed in the box to monitor temperature of the sand surrounding the can during heat-up and cool-down. Subsequent to the melt cycle (typically lasting 1.5 hours), the barrel remained in the sandbox for 24 hours, where the barrel contents were typically near room temperature. The photograph in Figure 5 provides a view of the barrel placed in the sand box.

The electrode axial position in the melt was adjusted using a chain-fall. Off-gas was collected by the hood and exhausted using an induced raft fan. Compressed air was supplied to the CGAM as a plasma forming gas. The nominal flow rage was 5 to 8 scfm. Power was supplied using a DC Robicon AC to DC converter power supply capable of providing 1,250 amps of direct current.

The electrical circuit for the high power operation is similar to that of a direct current welder. The direct current path is isolated from earth ground. Consequently, the system is "inherently safe" and one must be electrically connected to both the positive and negative leads or directly connected to the direct current circuit path to be exposed to electric shock hazard.

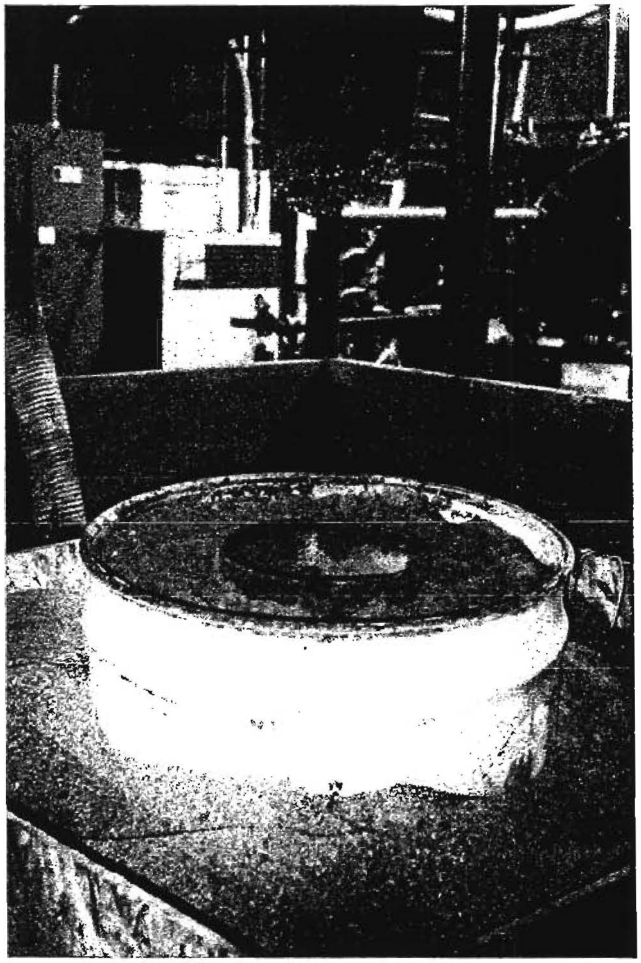

Figure 5. Photograph of barrel placed in sand box. Electrode above is being lowered into the 10 inch diameter casing.

Similar to an arc welder, the CGAM arc is quite bright and emits ultraviolet radiation, which is hazardous without vision protection. The hood that is placed over the spot to be vitrified. functions as an ultraviolet light shield, a means to collect gases and as a way to contain excess heat (radiated and convected) that results from the CGAM and the melted soil.

Test Method and Operations

Test operations were initiated by placing the CGAM into the 10" pipe and lowering it to the bottom of the pipe, resting upon the packed dirt, which is 6 inches up from the bottom of the barrel. Gas flow between the electrodes was initiated and then arc was initiated between the concentric electrodes by engaging the power supply to conduct current. Once an arc was well established and dirt at the electrode base is melted, typically in a few minutes, the CGAM was raised about one inch off of the dirt. Raising the electrode from the molten surface Raising the electrode increases the arc path length causing a voltage rise. The CGAM voltage was generally maintained in the range of 80 to 100 volts. The power supply is a constant current supply (similar to an electric welder) and the voltage adjusts to sustain the current. Consequently, both the voltage and power fluctuate proportionately as the load impedance changes. The load impedance is a function of distance of the arc from the melt, conductivity of the melt, current level and plasma-forming gas air flow.

As the process proceeds, the arc height from the melt varies as a function of height of the melt from separation of the CGAM from the melt surface (the molten liquid height increases as the soil is melted). The CGAM height changes as a function of graphite consumption during the process and by position of the electrode from adjusting its height using the chain fall.

The process variables, over which we had control, e.g., electrode height, plasma gas flow and CGAM current were adjusted to sustain a power level of approximately 100kW. However, in general the power level was allowed to vary between 75 and 125kW, and sometimes exceeded these limitations. No attempt was made to control the power lever to a tighter set of conditions, as one aspect of this project was to establish an understanding of the operating characteristics, including transient behavior, of the CGAM for this application over a relatively broad set of operating conditions.

A summary of test operations is provided in Table 2.

Table 2. Summary of test operations.

Test Number	Test Date	Barrel Number	Test Duration (minutes)	Average Power (kW)*	Total Power (kW-hr)
1	Jan 13, 1999	1	65	95	104.6
2	Jan 15, 1999	2	130	97.1	62
3	Jan 16, 1999	3	90	93	118.4
4	Jan 17, 1999	6	105	84	124.2
5	Jan 18, 1999	4	100	91	137.2
6	Jan 19, 1999	5	90	99	127.5
7	Jan 20, 1999	7	110	89	120.7
8	Jan 21, 1999	8	80	106	122.2
9	Jan 22, 1999	9	85	104	124.4
10	Jan 23, 1999	10	80	114	129.8

* Excluding time power off to record temperatures.

A view looking into a barrel as the CGAM is being withdrawn is shown in Figure 6. The off gas box cover has been removed. Figures 7 and 8 provide a sequence of photographs showing a view of the barrel top surface and access hole during cool-down.

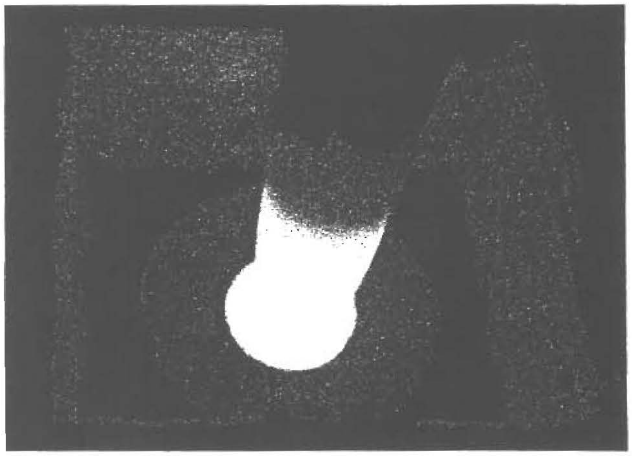

Figure 6, View from over the off gas box into a barrel as the CGAM is being withdrawn subsequent to completion of a test. The off gas box cover has been removed.

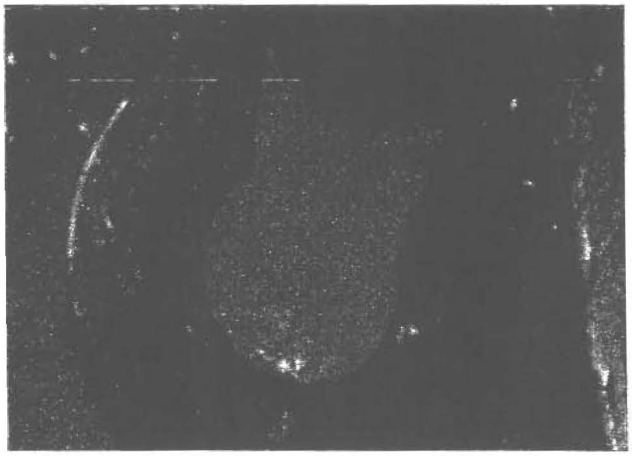

Figure 7. Photograph of treated soil shown in Figure 6 above during cool-down.

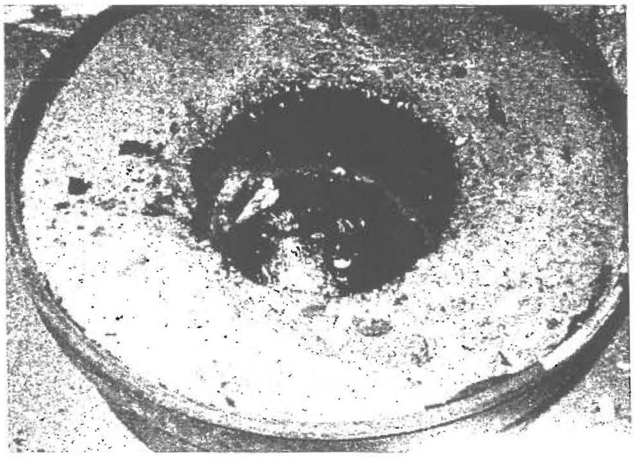

Figure 8. Photograph of treated soil shown in Figure 6 above during cool-down.

Data Recorded

Table 2 provides a summary of the data recorded during the experimentation, which includes post-test measurements of salient parameters such as electrode wear and photographs of the melt morphology. These visual data provide insight into the melt response both as a function of time and dimensionally during the test operations. Amount of power used and graphite consumption as a function of material vitrified for each test was also recorded. (These are two important economic factors relative to implementation of the process.)

Table 3. Summary listing of instrumentation and measurements.

Type	**Purpose**	**Number**	**Recorded on DAS**
Thermocouples	Soil temperature, melt growth and cool-down.	Matrix of 60 thermocouples distributed throughout barrel and sand box.	Yes
Power (DC voltage and current)	Measure power and energy.	One current, one voltage.	Yes
Pressure	Measure pressure of gas in electrode annulus.	One pressure transducer.	Yes
Flow	Measure plasma forming gas flow.	One flow meter.	No (recorded in test log)
Temperature Probe	Evaluate as method for evaluating melt profile during process operations.	Two separate probes, three temperatures each.	Yes
Resistance Ladder	Evaluate as method for evaluating melt profile during process operations.	Three resistance ladders.	Yes
Electrode Position	Measure electrode relative height in barrel.	One (position of electrode holder measured relative to fixed position.	No (recorded in test log)

Resistance Ladders and Thermocouple Probes

Two in-ground probe melt-growth detection devices were used in experimentation to aid in identifying the melt growth regions. Such devices may be used in field service to aid operators in determining the rate of melt growth during subgrade treatment. The devices used in this program included a resistance ladder and a thermocouple-containing probe. Their configuration with respect to the imbedded thermocouples in the soil-containing barrels is shown in Figure 9. Figure 10 shows installation of resistance ladders in a barrel.

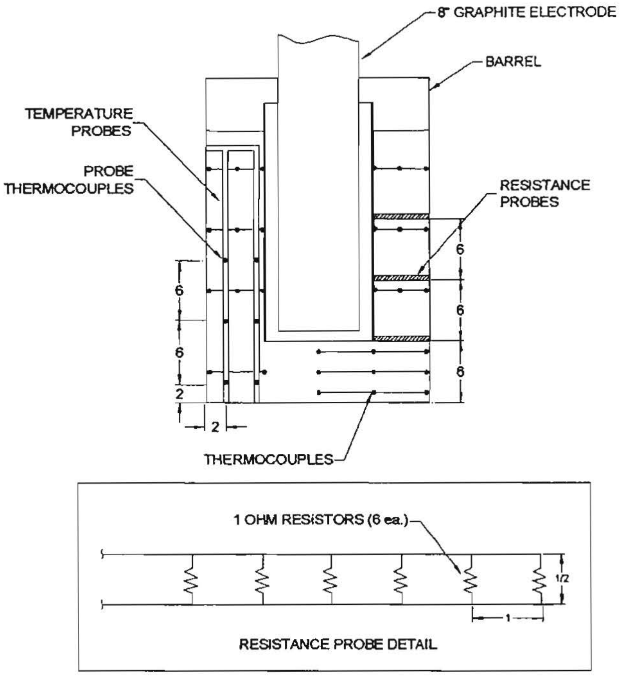

Figure 9. Schematic diagram of thermocouple and resistance ladder probe placement in experiments.

The resistance ladder consisted of six 1 Ω resistors assembled in a parallel configuration. Current from a constant voltage power source was supplied to the resistance ladder, and was monitored during experimentation through the measurement of the voltage drop across a series resistor. The resistance probes were inserted radially into the barrel at locations shown in Figure10. The orintation was such that the last resistor in the chain was closest to the electrode, and so burns out first. As the melt progresses radially, additional resistors in the chain burn out sequentially, yielding a changing current according to the equation

$$I = nV/R$$

where all resistors in the chain are of equal value, V is the applied constant voltage, and n is the number of remaining resistors in the chain. As n is reduced, the current drops and yields a detectable signal representative of melt growth.

Figure 10. Resistance ladder being installed in a barrel. Thermocouples were installed in a similar manner.

The thermocouple probe consisted of a 1/8" buried steel pipe, containing three thermocouples separated by 6" in height, and positioned radially 1" and

3" from the outside dimension of the central steel casing. Thermocouple signals represent local thermal conditions until a burnout point is reached. At the point of burnout, thermocouples at and beneath the burnout location will yield burnout signals, while those above will continue to indicate local temperature. As melt growth progresses, additional thermocouples will burnout, indicating melt propagation. The use of a finer array of thermocouples in the probes will yield greater accuracy in determining melt location in real-time.

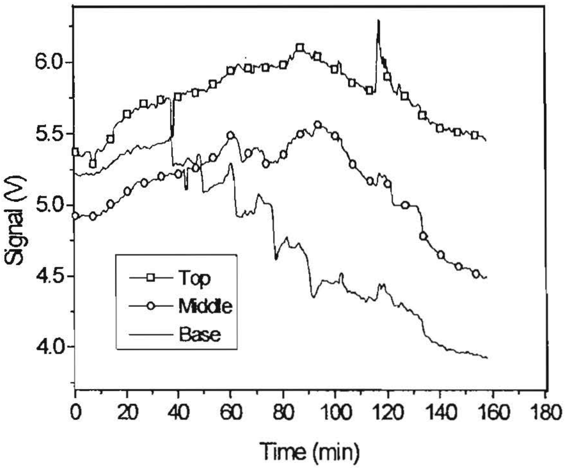

Figure 11. Real-time data of resistance ladders from Barrel #5 experiments, showing response due to loss of resistors due to melt growth.

Results of the investigations showed adequate signal determination in some experiments. Signal acquisition was often hampered by the significant electrical noise induced onto signal wires. However, reasonable probe signals were obtained from experimentation that are sufficient to present the utility of the techniques, and their potential with continued refinement. Figure 11 shows the resistor bridge measurements for the three axial locations. Significant signal drift is seen to occur in these measurements, and is thought to be due to voltage supply drift and changing soil conditions as the test progresses. The base resistance bridge, located one inch above the electrode starting point, shows the greatest response. In this figure the base resistance bridge is seen to respond strongly with melt growth and resistor burnout. Five distinct signal changes can be seen in this figure, the first of which corresponds closely with the time of burnout of thermocouple #17 in this run (separated by one inch in height), indicating a close association of signal change with melt presence. The method appears to be a suitable way to monitor melt growth provided that adequate signal stability and isolation from the conductive melt can be provided. In addition, signal resolution of the method is not good during the first few resistor destructions (when n is large, the ratio $(n-1)/n$ is small). The method may be improved by providing larger overall resistance to enhance stability, and providing a resistance-graded ladder (use of resistors of differing value from one end to the other), where more significant current changes occur with the loss of the first few resistors. Signal filtering and isolation will also aid in detecting resistor losses. The method, with a small amount of additional development, can be a reliable means of melt proximity detection.

The results of the thermocouple probes for melt growth detection was also successful in determining melt presence. With this method, local temperatures may be monitored to monitor local regions heating. Thermocouple burnout will determine melt presence. This method of melt detection was undertaken on four of the ten experiments. Representative signal response is shown in Figures 12 and 13 for Barrel #8 for the two probe rods inserted at radial locations of 1" and 3" from the

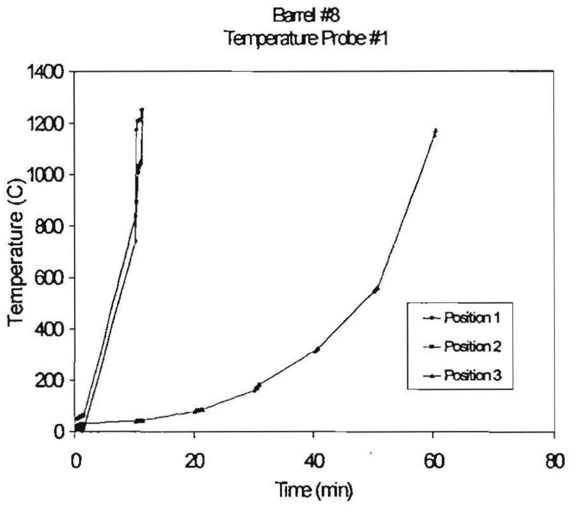

Figure 12. Temperature probe response during melt growth. Probe positioned axially, one inch away from central steel casing.

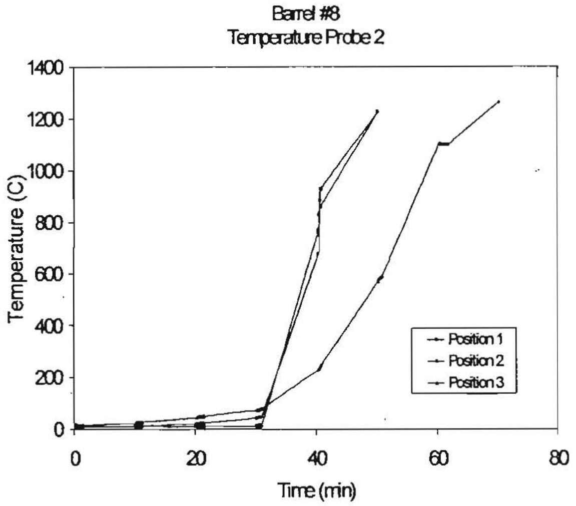

Figure 13. Temperature probe response during melt growth. Probe positioned axially, three inches away from central steel casing.

central steel casing respectively. As may be seen in these figures (data taken over a 1 minute interval every 10 minutes) the lower two thermocouples (positions 1 and 2) were found to respond and burn out simultaneously. Response of this type represents thermocouple burnout in a region residing between thermocouple positions 2 and 3. The soil melt interacting with the probe in this location will burn out thermocouples at positions 1 and 2 simultaneously. Position 3, between the melt and signal wires, will be safe to transmit temperature information until the melt progresses to its position. In the experiments, the time of probe thermocouple burnout corresponded accurately with melt growth data as indicated by the thermocouple detection array for this experiment. An improvement to the technique includes the use of a finer array of thermocouples to identify melt propagation with greater accuracy.

Test Results

Tests results presented in this section provide a summary of information for the vitrification of soil in Barrel #6 and a plot of the temperature at the end of each test for all ten barrels. Because of the large amount of data accumulated, only a limited amount can be effectively presented and discussed in this report. The bulk of the test results data is presented in the Appendix and on electronic media accompanying this report.

Data was collected for each experiment on a computerized data acquisition system. These data allowed visualization of the vitrification process online and provide a means for playback of the data post-test. The will primarily be used for evaluating the economic and technical viability of the process.

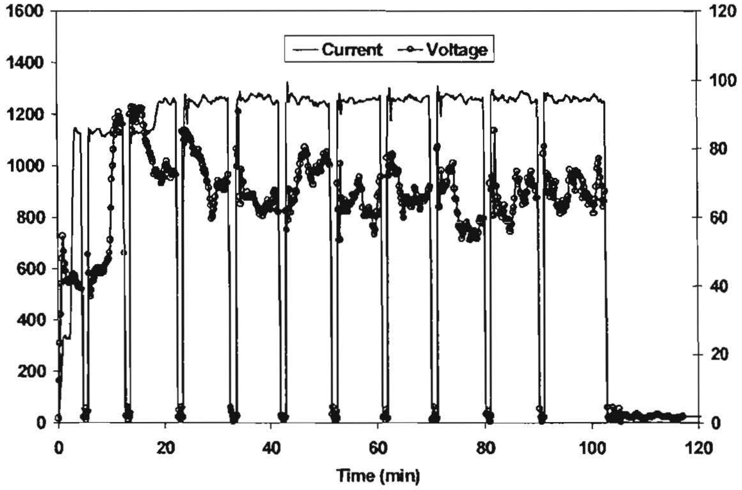

Figure 14. Plot of CGAM current and voltage during the test of Barrel #6

Figure 14 shows the CGAM voltage and current data as a function of time during the test. Figure 15 shows that the power was turned off at ten minute intervals during the test. This was to allow recording of the thermocouple output without the electrical noise that was generated when the CGAM was operating.

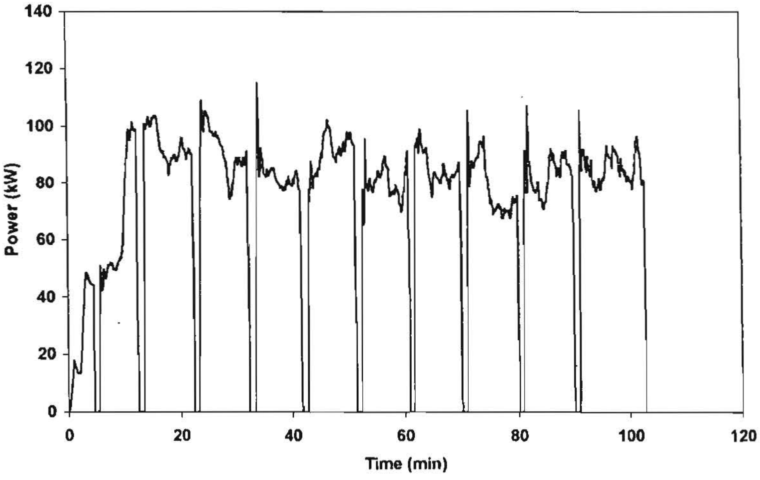

Figure 15. Plot of CGAM power during the test of Barrel #6

Figures 16 and 17 provide plots of "typical" thermocouple data during process heat-up and cool-down for a row of thermocouples in that comprise the temperature measurement matrix. (See Figure 2.) These data were used to map out a description of the temperature profile during the heat-up and cool-down process.

These data provide a clear map on the rate of cool-down for the vitrified mass. Note that sand only heats up slightly during the cool-down cycle. (Thermocouple 27 in Figure 15.)

Data from the thermocouple matrices were used in a commercial software routine (Origin) to provide a map of the thermal profile, including the molten region, as a function of time during the test. Figures 18 through 26 show a typical plot of the melt growth as a function of time. These maps provide a useful method to visualize the process growth as a function of time and process operating conditions. The thermocouple matrix (shown in Figure 2) provides a three-dimensional view of the melt soil temperature profile, providing a means to map the vitrification process as a function of time and CGAM operating conditions.

Type K thermocouples were used to make these measurements. They reach their upper limit of operation at about 1200°C. The soil melts a temperatures higher than the temperature at which the thermocouples fail. However, the thermal gradient in this region of the melt is great enough that the region defined by the failed thermocouple indication, e.g., designated as temperatures greater than 1225°C in the figures, provides a relatively accurate map of the molten soil region.

Additional photographs, showing similar views for all ten of the barrels are included in Appendix A. A VHS video was made to show the process during operations and to also record morphology of the treated soils. The video accompanies this report.

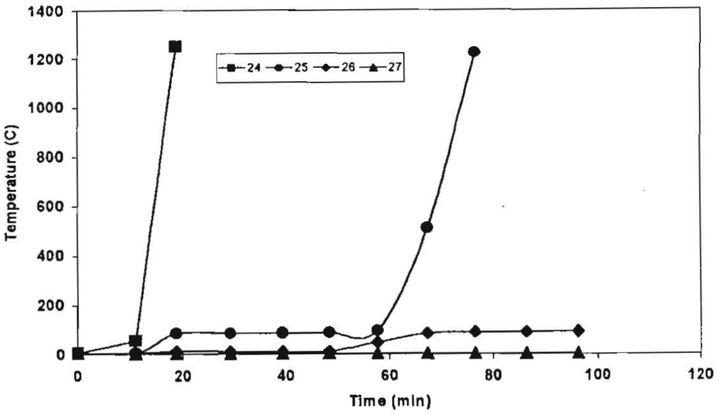

Figure 17. Plots of temperature versus time for thermocouples 24, 25, 26 and 27 during heat-up of Barrel #6. Thermocouple 24 is located adjacent to the 10 inch pipe, 25 is located midway between the pipe and the barrel , 26 is located at the barrel wall and 27 is located in the sand box. (See Figure 2 for location layout.) This thermocouple group was positioned at 12 inches elevation from the bottom of the barrel, at the lowest row adjacent to the 10 inch pipe. Thermocouple 24 failed at about 10 minutes after start of test and 25 failed at about 75 minutes due to being consumed by the melt front.

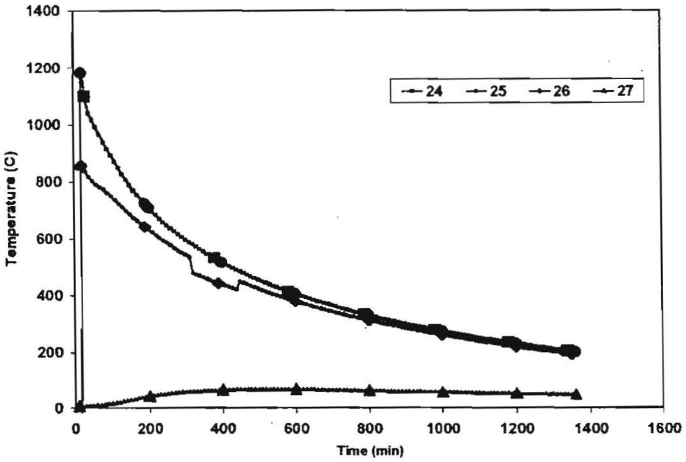

Figure 16. Plots of temperature versus time for thermocouples 24, 25, 26 and 27 during cool-down of Barrel #6. Thermocouple positions were noted in Figure 14. Thermocouples 24 and 25 provide indication during cool-down, even though they had been melted in the heat-up cycle, as shown in Figure 14. Post test inspection of thermocouples indicate that they typically from a new junction, but they have been melted back to the interface of the molten and heated soil. Consequently, although they typically provide a "reasonable" temperature indication, their position in the "matrix" is changed.

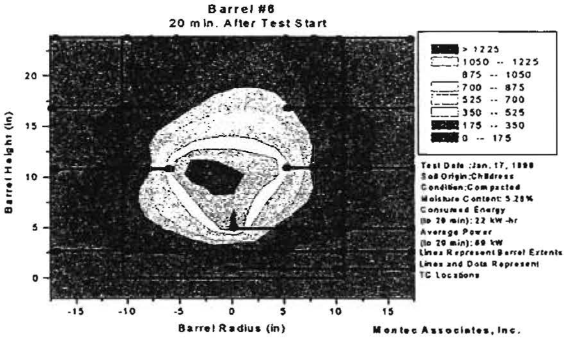

Figure 18. Measured temperature profile for Barrel 6 20 minutes after initiation of the test.

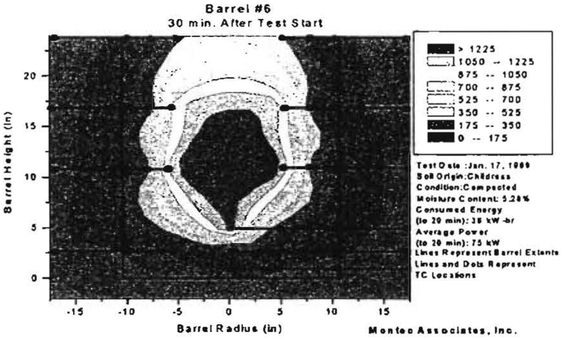

Figure 19. Measured temperature profile for Barrel 6 30 minutes after initiation of the test.

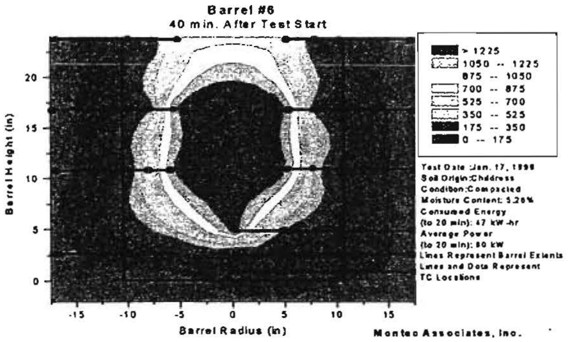

Figure 20. Measured temperature profile for Barrel 6 40 minutes after initiation of the test.

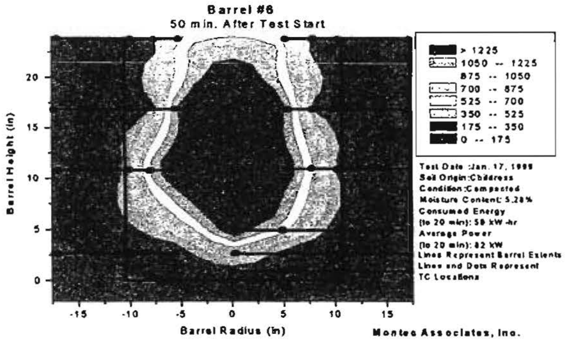

Figure 21. Measured temperature profile for Barrel 6 50 minutes after initiation of the test.

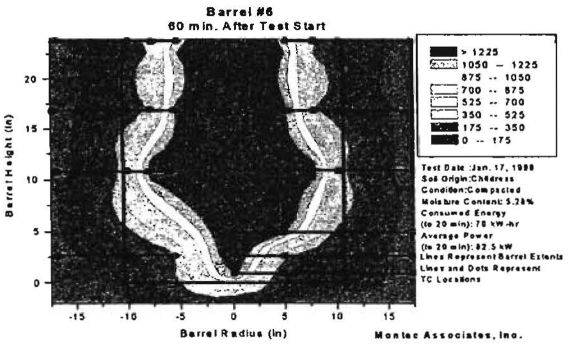

Figure 22. Measured temperature profile for Barrel 6 60 minutes after initiation of the test.

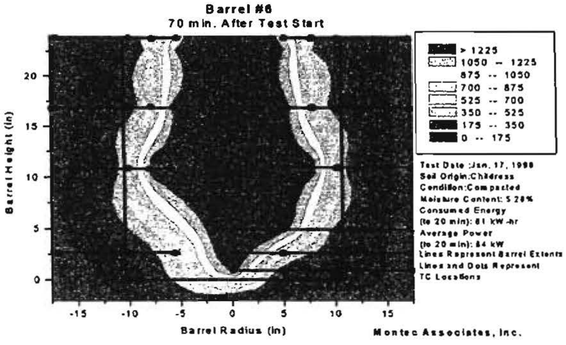

Figure 23. Measured temperature profile for Barrel 6 70 minutes after initiation of the test.

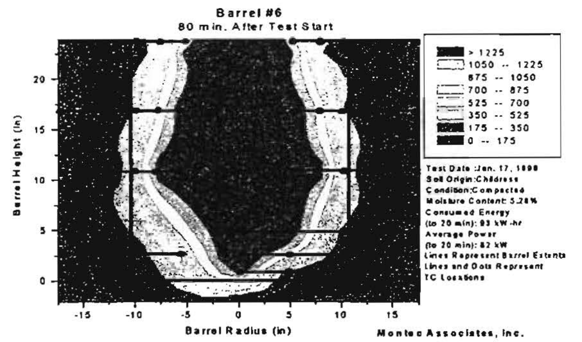

Figure 24. Measured temperature profile for Barrel 6 80 minutes after initiation of the test.

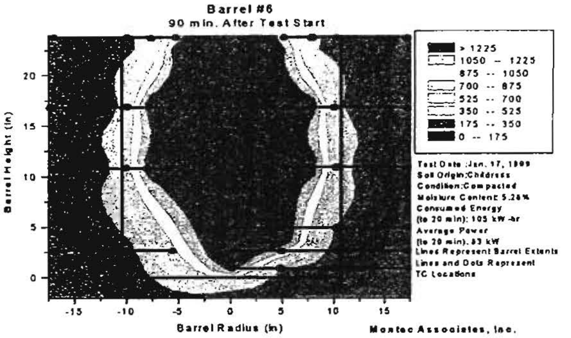

Figure 25. Measured temperature profile for Barrel 6 90 minutes after initiation of the test.

Figure 27 shows Barrel #6 with half of the side stripped away and the unvitrified soil removed exposing the extent of the vitrified region. Comparisons of the high temperature region (>1225°C) shown in Figure 26 overlays well with the actual vitrified zone exposed in Figure 27. Similar overlays are presented in the Appendix for all of the melts. The thermal maps correlate well with the melt extents. The software routine provides a concave melt profile between the thermocouple measurement grid points, where the melt shows clear evidence of the melt front being convex – more rounded and bulb-shaped. The thermocouple locations are designated on the thermal map as filled in circles on the horizontal lines.

Figures 28 through 33 show a sequence of the melt cooling subsequent to the test. Note that the interior temperature values are not a result of actual measurements, but averaging data measured by the outer thermocouples. This is because the interior thermocouples were destroyed by the advancing melt during heat-

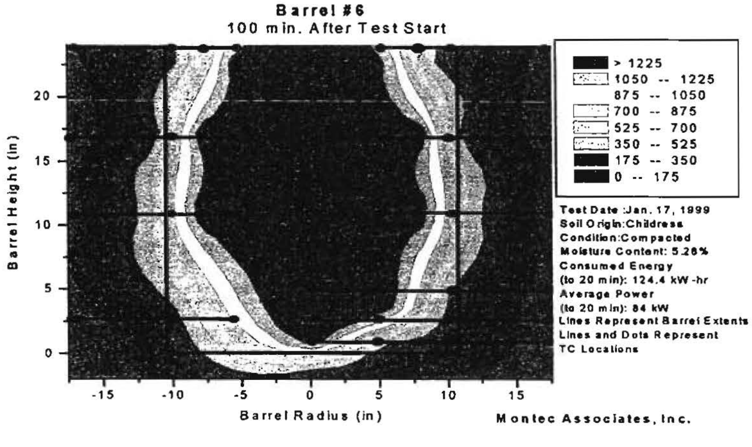

Figure 26. Measured temperature profile for Barrel 6 100 minutes after initiation of the test. The test was completed at this time.

Figure 27. Photograph of vitrified soil with unconsolidated soil removed from vitrified region.

up. However, the thermocouples in the barrel parameter and in the sand box are active. Consequently, the core temperature of the vitrified mass will be higher than indicated on these figures. These data show a clear indication of the melt cooling rate, which will provide insight into the nature and evaluation of rock-like structure formed as a result of the process and is important information for the geotechnic evaluation of the vitrified material properties.

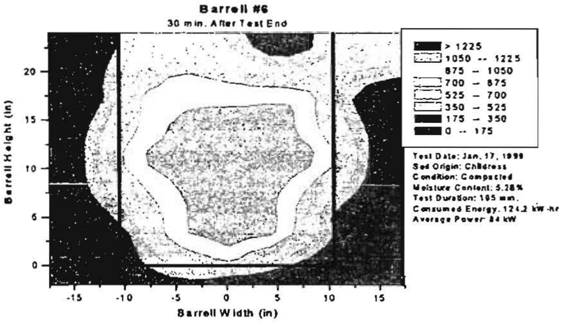

Figure 28. Measured temperature profile for Barrel 6 at 30 minutes after shutdown.

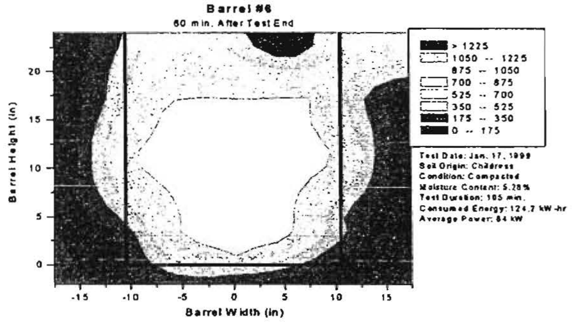

Figure 29. Measured temperature profile for Barrel 6 at 60 minutes after shutdown.

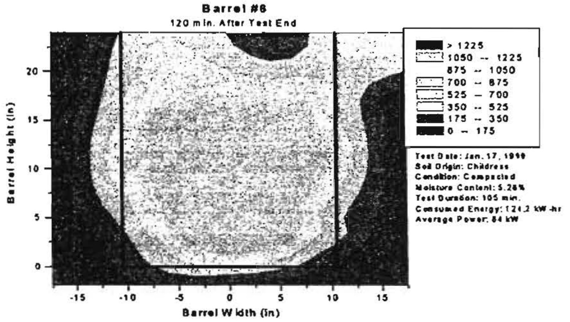

Figure 30 Measured temperature profile for Barrel 6 at 120 minutes after shutdown.

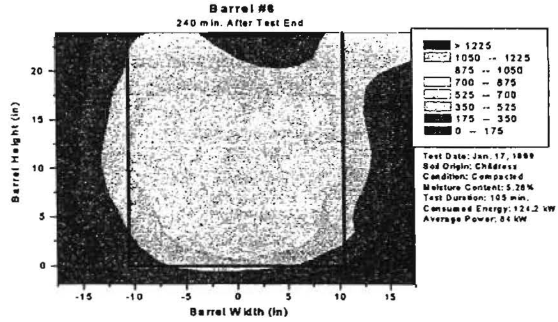

Figure 31. Measured temperature profile for Barrel 6 at 240 minutes after shutdown.

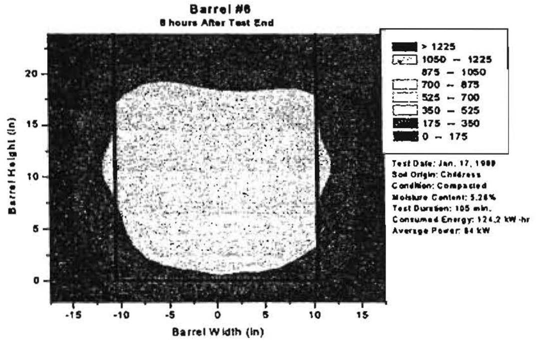

Figure 32. Measured temperature profile for Barrel 6 at 8 hours after shutdown.

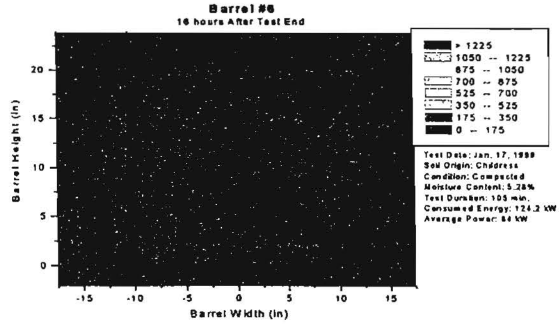

Figure 33. Measured temperature profile for Barrel 6 at 16 hours after shutdown.

Graphite Consumption Data

The CGAM electrodes are fabricated from commerical-grade graphite, which are primarily used in the steel-smelting industry. These graphite electrodes are consumed during the vitrification process, essentially converting to CO_2. One economic/operational aspect of the process is graphite consumption. The graphite consumption is a function of variables such as current level, temperature, oxidant and gas flow.

Measurements of the electrode dimensions were made subsequent to most of the tests. These data are presented in Table 4. No clear relationship between graphite loss and power, soil moisture, test duration, air flow or kW-hr was observed.

Table 4. Summary of CGAM consumption data.

Test Number(s)	Barrel Number (s)	Measured Electrode Mass Loss (lbm)	
		Cathode (outer electrode)	Anode[2] (inner electrode)
1	1	8.5	<1.4
2	2	8.1	<1.6
3	3	9.3	<1.6
4	6	8.0	<2.3
5	4	8.9	<1.8
6	5	5.6	<1.8
7 through 10	7 through 10	11.9[1]	<2.5[1]

1 Measurements were not made for each test and the loss is an average over these four tests.

[2] The anode loss during testing was less than the cathode and it's length was typically trimmed between tests to match the cathode length the mass loss shown reflects the trimmed length.

One purpose of these test was to characterize the wear as a function of CGAM operations for this application. However, the operating conditions and electrode configuration were not optimized to minimize the wear. Consequently, the wear rates are much higher than are expected during actual practice, where more attention will be paid in the design and operation of the CGAM process to minimize this variable. The electrode wear rates are high for these tests, about a factor of 3 to 5 higher than has been achieved for graphite electrodes used in this type of service, but configured differently. Montec has devised a proprietary method to reduce the wear for this type of service, which can be incorporated in subsequent testing and for the end use field applications.

Summary

The intent of this report is primary for purposes of providing a summary of the test data that can be incorporated into a global report on the process function, process economics and usefulness of the technology for application as a method for subgrade repair and stabilization, which will be authored by Texas Tech University. However, some preliminary, general observations on the test operations and results obtained are provided herein.

The tests were completed as scheduled, during a two-week window without incident. No operational or technical surprises that instill concern on the viability or safety of the process were encountered. Subsequent to the first test a day was taken to review the data to ensure all aspects were working correctly. The remaining nine tests were run, one per day for the next nine consecutive days. This aspect attests to the simplicity and operability of the process, an important factor necessary for field implementation.

Differences in operations were most dramatic with the high moisture (saturated) dirt. In particular, barrel 10, where the CGAM voltage was sustained at about 300 volts for a good part of the test. In order to keep the CGAM power level down in the 125 kW range, the current was adjusted to about 400 amps, typically 30% of the nominal operating condition for the other tests. Although an equivalent total power can be achieved by a broad range of current-voltage products, current is "more influential" on melting the dirt than is voltage.

The data transmitted in this report provides a description of the experimental work conducted and results obtained. These data, both recorded via the instrumentation and recorded photographically, will be used by Texas Tech University to correlate the vitrified material mechanical properties with the geotechnical and process operating conditions and soil characteristics.

Montec will use these data to correlate CGAM operational parameters with (voltage and current readouts) with factors such as soil temperature and melt growth, gas flow, electrode position, electrode consumption.

The evaluations by Texas Tech University and Montec will result in an assessment of the process technical and economic viability.